

**A NOVEL TYPE OF SIGNALLING FROM DNA DAMAGE UNDER
ATP STRESS IN HUNTINGTON'S DISEASE**

Ph.D. Thesis - L.E. Bowie

McMaster University - Biochemistry

**A Novel Type of Signalling from DNA Damage Under ATP Stress in Huntington's
Disease**

By: LAURA E. BOWIE, B.Sc.

A Thesis Submitted to the School of Graduate Studies in Partial Fulfilment of the
Requirements for the Degree Doctor of Philosophy

McMaster University © Copyright by Laura Bowie, September 2018

Ph.D. Thesis - L.E. Bowie

McMaster University - Biochemistry

McMaster University DOCTOR OF PHILOSOPHY (2018)
Hamilton, Ontario
(Biochemistry and Biomedical Sciences)

TITLE: A Novel Type of Signalling from DNA Damage Under ATP Stress in
Huntington's Disease

AUTHOR: Laura E. Bowie, B.Sc.

SUPERVISOR: Dr. Ray Truant

NUMBER OF PAGES: xv, 196

ABSTRACT

Huntington's disease is an autosomal dominantly inherited neurodegenerative disorder characterized by degeneration of striatal and cortical neurons. The neurons in these regions are particularly energy-demanding and need to maintain high levels of oxidative phosphorylation to support cellular activities. Reactive oxygen species are generated as a byproduct of oxidative phosphorylation and can damage DNA and other biomolecules if not properly metabolized. In HD, there is elevated oxidative DNA damage and impaired DNA damage repair, likely due to impaired function of the mutant huntingtin protein in base excision repair (BER). Previous studies have shown that mutant huntingtin is hypo-phosphorylated at serines 13 and 16 in the N17 domain, and that restoring phosphorylation can reestablish normal protein function and is protective in HD.

In this thesis, we show that a metabolite of the DNA damage product N6-furfuryladenine (N6FFA), kinetin triphosphate (KTP) increases N17 phosphorylation through casein kinase 2 (CK2) by acting as an ATP analog, with protective effects in cell and animal models of disease. We additionally show N6FFA increases the activity of CK2 on other substrates, specifically p53. We hypothesize that in times of ATP stress CK2 can utilize KTP as an alternate energy source, promoting DNA repair and cell viability. In HD, inefficient BER inhibits generation of KTP and promotes hypo-phosphorylation of CK2 substrates, which can be overcome by exogenous addition of N6FFA. Additionally, we show that another DNA-responsive kinase, PKC ζ , can also phosphorylate N17, potentially priming this domain for CK2 phosphorylation. Finally, we propose that the protective effects of N6FFA may be via a two-pronged pathway, involving both CK2 and the mitochondrial quality control kinase, PINK1. Thus, this thesis presents a novel mechanism where a product of DNA damage acts as a phosphate source for critical kinases in DNA repair and mitochondrial maintenance in conditions where ATP levels are low.

ACKNOWLEDGEMENTS

Thank-you to everyone who made this work possible, it was a long time coming.

To my supervisor, Dr. Ray Truant, I can't thank you enough for your support and guidance. Your excitement for science was a constant source of encouragement for me as I made my way through graduate school.

Thank you to my committee members, Dr. Kristin Hope and Dr. Bernardo Trigatti. Your advice, hard questions, and guidance made this project possible.

To the Truant lab members, past and present, thank you all so much for your ideas, your love of science, and for making the day-to-day lab work fun. I would like to especially thank Tam Maiuri, your advice on this project was invaluable, and your enthusiasm for knowledge was inspiring. Jianrun Xia, you were both instrumental ensuring that the lab, and my project, kept running along smoothly. Mina Falcone, not only were you a constant source of lab-related wisdom, but also of life-related wisdom and kind words, thank you for all of your help. Shreya Patel (Rajput), you kept me sane during the early years, I don't know if I would have made it without you. Claudia Hung, thank-you so much for consistently being an amazing friend, scientist, and sounding-board for my problems and ideas, both in the lab and in life. Laura DiGiovanni, Celeste Stuart, Andrew Mocle, Glenn Walpole, Sid Nath, Nick Caron, Tanya Woloshansky, Jenny Williamson, you made every success more exciting, and every failure more bearable, again, thank you all for these past 6 years.

To my roommates throughout the years, Sheila, Luc, Dean, and Kailey, thank you for filling my spare hours with fun, laughter, debates, and dance parties.

To my family, there aren't enough words to thank you all for your love and constant encouragement. Mom and Dad, everything you ever taught me got me here. Your belief in me was a constant source of comfort and motivation, thank you for your support and for teaching how to have the strength to support myself. Stephen, thank you for always bringing the good times, fun, and adventures, and, more than that, for being a constant friend and source of interesting chats.

To Jake, thank-you for sticking with me as I made my way through the ups-and-downs of graduate school. Your humour, support, and love made this journey easier. Thank you for teaching me to not take myself too seriously, to keep things in perspective, and to celebrate the small victories.

TABLE OF CONTENTS

CHAPTER 1: Introduction	1
1.1 Huntington's Disease	2
1.1.1 History of Huntington's Disease	2
1.1.2 Huntington's Disease Symptoms	3
1.1.3 Huntington's Disease Neuropathology	4
1.1.4 Genetics of Huntington's Disease	6
1.1.5 Other CAG Triplet Repeat Disorders	8
1.2 The Huntingtin Protein	10
1.2.1 The Structure of the Huntingtin Protein	10
1.2.2 The Localization of the Huntingtin Protein	13
1.2.3 Functions of the Huntingtin Protein	16
1.2.3.1 Huntingtin in development	16
1.2.3.2 Huntingtin at the synapse	17
1.2.3.3 Huntingtin in vesicular and axonal transport	18
1.2.3.4 Huntingtin in cell division	20
1.2.3.5 Huntingtin at the mitochondria	21
1.2.3.6 Huntingtin and autophagy	23
1.2.3.7 Huntingtin in the stress response	24
1.2.3.8 Huntingtin in the DNA damage response	25
1.3 Huntingtin in Disease	28
1.3.1 Polyglutamine Expansion and the Pathogenic Threshold	28
1.3.2 Proposed Mechanisms of Disease	29
1.3.2.1 Aggregation/toxic sequestration	30
1.3.2.2 Mitochondrial dysfunction	32
1.3.2.3 DNA damage	35
1.4 Huntington's Disease Therapeutic Efforts	37
1.4.1 Biomarkers of Disease	37
1.4.2 Symptom Management	39
1.4.3 Previous Efforts in Disease-Modifying Therapies	40
1.4.4 Targeting Huntingtin as a Therapeutic Strategy	42
1.4.5 Modulating Phosphorylation of the N17 Domain as a Therapeutic Strategy	44
1.5 Thesis Rationale	46
 CHAPTER 2: N6-Furfuryladenine is Protective in Huntington's Disease Models by Signaling Huntingtin Phosphorylation	 48

2.1 Abstract	49
2.2 Introduction	50
2.3 Results	53
2.4 Discussion	69
2.5 Materials and Methods	74
2.6 Supplemental Figures	88
CHAPTER 3: PKCζ: A Candidate Priming Kinase for N17	91
3.1 Overview	92
3.2 Abstract	92
3.2 Introduction	93
3.3 Results	95
3.4 Discussion	104
3.5 Materials and Methods	107
CHAPTER 4: Further Exploration of N6-Furfuryladenine in Disease	113
4.1 Overview	114
4.2 Abstract	114
4.3 Introduction	114
4.4 Further experimentation with N6FFA derivatives	116
4.5 Increased inclusion of IKBKAP exon 20 by N6FFA treatment occurs through a mechanism unrelated to huntingtin phosphorylation by CK2	119
4.6 N6FFA causes a consistent, but not significant, change in the ratio of globular to fibrillar type mutant huntingtin aggregates	125
4.7 N6FFA increases phosphorylation of p53 S392, which co-localizes with huntingtin at nuclear puncta and at sites of DNA damage	127
4.8 N6FFA riboside is elevated in cells expressing polyglutamine expanded huntingtin	132
4.9 N6-Furfuryladenine reduces DNA damage in <i>STHdh</i> ^{Q111/Q111} cells upon MMS-induced stress	133
4.10 Materials and Methods	135
CHAPTER 5: Discussion and Future Directions	141
5.1 Overview of major findings	142
5.2 DNA damage, p53, and the energy crisis in Huntington's Disease	145
5.2.1 N6FFA riboside is a biomarker for Huntington's Disease	148
5.3 The role of N6FFA and PINK1 in mitochondrial health and bioenergetics: Implications for Huntington's disease	149
5.4 Implications for other neurodegenerative diseases	154
5.5 Conclusions	155
REFERENCES	157

Figure List

Figure 1.1. Schematic of the huntingtin protein

Figure 1.2. Subcellular localization of the huntingtin protein

Figure 1.3. Exon1 conformation change at the pathogenic threshold of Huntington's disease.

Figure 2.1. Identification and validation of N6-furfuryladenine as a modulator of N17 phosphorylation

Figure 2.2. Effects of N6FFA administration on motor performance, anxiety-like behaviour, and huntingtin inclusions in YAC128 mice

Figure 2.3. CK2 uses KTP as a phospho-donor to phosphorylate huntingtin N17 when primed by phosphorylation

Figure 2.4. Components of the N6FFA-APRT-KTP-CK2-huntingtin pathway co-localize at sites of DNA damage

Figure 2.5. A product of oxidative DNA repair is used by CK2 to phosphorylate huntingtin at sites of DNA damage

Supplemental Figure 2.1. Hit compound list and additional validation of N6FFA

Supplemental Figure 2.2. CK2 can use KTP to phosphorylate substrates

Supplemental Figure 2.3. Effects of kinetin administration on body weight

Figure 3.1. Identification of PKC ζ as a modulator of huntingtin N17 phosphorylation

Figure 3.2. PKC ζ can phosphorylate N17 in vitro.

Figure 3.3. CK2 can phosphorylate N17 at either S13 or S16.

Figure 3.4. Modulation of PKC ζ results in corresponding changes in N17 phosphorylation

Figure 3.5. Colocalization of N17P and PKC ζ at nuclear puncta

Figure 4.1. The effect of N6FFA derivatives on huntingtin N17 phosphorylation

Figure 4.2. IKAP levels are modulated by huntingtin, but this effect does not seem to occur via N17 phosphorylation following N6FFA treatment

Figure 4.3. Treatment with N6FFA increases proper splicing of IKBKAP but there is no difference in this response between *STHdh*^{Q7/Q7} and *STHdh*^{Q111/Q111}

Figure 4.4. N6FFA influences inclusions formation

Figure 4.5. p53 S392 can be phosphorylated by CK2 using KTP and co-localizes with CK2 and phospho-huntingtin at nuclear puncta

Figure 4.6. p53 S392p co-localizes with N6FFA/APRT/KTP/CK2/htt pathway at sites of DNA damage

Figure 4.7. N6FFA riboside is increased in the genomic DNA of cells expressing mutant huntingtin.

Figure 4.8. N6FFA decreases tail moment in STHdh^{Q111/Q111} cells with MMS-induced DNA damage.

Figure 5.1. A metabolite of N6FFA increases N17 and p53 S392 phosphorylation in response to DNA damage.

Figure 5.2. An expanded mechanism of action for DNA damage product N6FFA in DNA damage and mitochondrial turnover.

ABBREVIATIONS

8-oxo-dG	8-oxo-7,8-dihydro-2'-deoxyguanosine
9DK	9-deaza-kinetin
9MK	9-methyl-kinetin
Aβ	Amyloid β
AD	Alzheimer's disease
ADP	Adenosine diphosphate
ALS	Amyotrophic lateral sclerosis
APP	Amyloid precursor protein
APRT	Adenine phosphoribosyltransferase
ASO	Antisense oligonucleotide
ATM	Ataxia-telangiectasia mutated
ATP	Adenosine triphosphate
BBB	Blood-brain barrier
BER	Base excision repair
BDNF	Brain-derived neurotrophic factor
BSA	Bovine serum antigen
CAG	Cytosine-adenine-guanine
CAZ	Cytomatrix proteins at active zone
CD	Circular dichroism
Cdk5	Cyclin dependent kinase 5
CK2	Casein kinase 2
CoQ10	Coenzyme Q10
CNS	Central Nervous System
CRM1	Chromosome regional maintenance 1
CSF	Cerebrospinal fluid
DG	Diacylglycerol
DMEM	Dulbecco's modified Eagle's medium
DNA	Deoxyribonucleic acid

DNA-PK	Deoxyribonucleic acid-dependent protein kinase
DSB	Double strand break
DRPLA	Dentatorubro-pallidoluyision atrophy
EDTA	Ethylenediaminetetraacetic acid
ER	Endoplasmic reticulum
ETC	Electron transport chain
FBS	Fetal bovine serum
FD	Familial dysautonomia
FLIM	Fluorescence lifetime microscopy
FRET	Förster resonance energy transfer
gDNA	Genomic DNA
GEF	Guanine nucleotide exchange factor
γH2AX	Phosphorylated histone H2A family X
GTP	Guanosine triphosphate
GWAS	Genome-wide association study
HAT	Histone acetyltransferase
HEAT	Huntingtin, elongation factor 3, subunit of protein phosphatase 2A, TOR 1
HEK293	Immortalized cell line from human embryonic kidney cells
HER	Human epidermal growth factor receptor
HD	Huntington's Disease
<i>Hdh</i>	mouse huntingtin homolog
<i>HTT</i>	Huntingtin gene
HR	Homologous recombination
hTERT	Human telomerase reverse transcriptase
IP	Intraperitoneal
IVS	Intervening sequence
IGF-1	Insulin-like growth factor receptor 1
IKAP	IKK-complex-associated protein

IKBKAP	Inhibitor of kappa light polypeptide gene enhancer in B-cells, kinase complex-associated protein
KAB	Kinase assay buffer
KTP	Kinetin triphosphate
MEM	Minimum essential medium
MMP	Mitochondrial membrane potential
MMR	Mismatch repair
MMS	Methylmethanesulphonate
MRI	Magnetic resonance imaging
MRN	MRE11/RAD50/NBS1
MSN	Medium Spiny Neuron
N17	Huntingtin amino-terminal 17 amino acids
N6FFA	N6-furfuryladenine
NAD	Nicotinamide adenine dinucleotide
NER	Nucleotide excision repair
NES	Nuclear export signal
NHEJ	Non-homologous end-joining
NFL	Neurofilament light protein
NLS	Nuclear localization signal
NMDA	N-methyl-D-aspartate
Nrf1/2	Nuclear respiratory factor 1/2
NuMA	Nuclear mitotic apparatus
OGG1	8-oxoguanine glycosylase
PAC1N1	Protein kinase C and casein kinase substrate in neurons 1
PARIS	Parkin interacting substrate
PARP	Poly(ADP-ribose)polymerase
PB1	Phox/Bem 1p
PCA	Principal component analysis
PD	Parkinson's disease

PDE10A	Phosphodiesterase 10A
PDGFR	Platelet-derived growth factor receptor
PET	Positron emission tomography
PGC-1α	Peroxisome proliferator-activated receptor gamma coactivator-1-alpha
PINK1	PTEN-induced putative kinase 1
PIP₃	Phosphatidylinositol (3,4,5)-triphosphate
PKC	Protein kinase C
PKCζ	Protein kinase C ζ
PKMζ	Protein kinase M ζ
PNBM	P-nitrobenzylmesylate
PP2A	Protein phosphatase 2A
PPAR	Peroxisome proliferator-activated receptors
PSD-95	Post-synaptic density-95
PTM	Post-translational modification
PVDF	Polyvinylidene difluoride
PY-NLS	Proline-tyrosine nuclear localization signal
Rac 1	Ras-related C3 botulinum toxin substrate 1
RBP	RNA-binding protein
RCT	Randomized control trial
RNA	Ribonucleic acid
RNAi	RNA interference
ROS	Reactive oxygen species
RPE1	Retinal pigment epithelial 1
S	Serine
SBMA	Spinal-bulbar muscular atrophy
SCA	Spinocerebellar ataxia
SDS-PAGE	Sodium dodecyl sulphate polyacrylamide gel electrophoresis
SH3	Src homology 3
siRNA	Small interfering RNA

shRNA	Short hairpin RNA
SNP	Single nucleotide polymorphism
SR-SIM	Super resolution-structured illumination microscopy
SSB	Single-strand break
SSRI	Selective serotonin reuptake inhibitors
STHdh	ST14 cells from mouse striatum, <i>Hdh</i> is the mouse huntingtin homolog
TrkA	Tropomyosin receptor kinase A
TruHD	hTERT immortalized human skin fibroblasts
UPR	Unfolded protein response
VEGFR	Vascular endothelial growth factor receptor
VMAT-2	Vesicular monoamine transporter-2
WT	Wild-type
WT:MU	Wild-type:mutant transcript
YAC	Yeast artificial chromosome

DECLARATION OF ACADEMIC ACHIEVEMENT

All writing and experimental content in the following chapters is the work of the author, Laura Bowie, unless otherwise stated.

CHAPTER 1
INTRODUCTION

1.1 Huntington's Disease

1.1.1 History of Huntington's Disease

Huntington's Disease (HD) is a dominantly inherited genetic disorder that is characterized clinically by a triad of motor, cognitive, and psychiatric symptoms (1). This disease is also known as "Huntington's chorea", reflecting the most obvious disease symptom, the involuntary jerking or twitching movements that have been described as "dance-like". It was Paracelsus, in the 1500s, who first used the term chorea to describe this condition, and even suggested that its origin might be in the central nervous system (CNS)(2). However, in spite of this insight, the disease remained misunderstood, and was often feared as demon possession for much of the following two centuries. In fact, there is evidence that some individuals suffering from HD-like symptoms were burned as witches during the infamous Salem Witch Trials (3, 4).

Although a number of attempts were made at devising a medical description for "chronic hereditary chorea", the first accurate characterization of HD was made in 1872 by a third-generation physician, George Huntington, in his manuscript "*On Chorea*"(5). Hereditary chorea made up a rather small portion of his report, with most of it being focused on Sydenham's chorea, nonetheless, his short description managed to capture the key features of this disease: it's hereditary nature and adult onset; the associated, progressive physical and mental disability (chorea and dementia); a tendency towards

suicide; and a lack of response to treatment (5, 6). Thus the disease became known as “Huntington’s Disease”, although it was originally called “Huntington’s Chorea”.

1.1.2 Huntington’s Disease Symptoms

“Chorea” is a latin word meaning “dance-like motions”, and, indeed, the most obvious symptoms of HD are the involuntary motor movements displayed by affected individuals. However, this overt symptom may be mild or absent, and is usually preceded by several years by cognitive impairment and emotional disturbances (7). HD typically manifests between the ages of 35 to 50, although onset can vary from childhood to old age, with patients experiencing progressive dementia and deterioration of overall health and motor function (1). Death usually occurs about 15-20 years following symptom onset and is commonly a result of secondary complications since affected individuals have great difficulty in performing even simple tasks, such as swallowing (dysphagia). This particular deficit is likely responsible for a number of HD deaths due to choking, nutritional deficiencies, and aspirational pneumonia (8). In fact, the most common cause of death amongst HD patients is pneumonia (8, 9). Other common motor symptoms include dystonia, bradykinesia, and dysarthria (10). Traditionally, clinical diagnosis of HD is made based on confirmation of an unexplained movement disorder in a patient with a family history of HD or who has tested positive for the gene mutation. While presence of the motor phenotype - generally assessed using the Unified Huntington Disease Rating

Scale (UHDRS-99) - is necessary for clinical diagnosis of HD, the cognitive and psychiatric symptoms are not (11).

Cognitive symptoms, which often manifest before motor symptoms, can include slowness of thought (bradyphrenia), defective visuospatial, auditory, and procedural memory, and impaired executive function (11–13). The most common psychiatric or behavioural symptoms include apathy, depression, obsessive-compulsive behaviour, psychosis, and aggression - more often verbal than physical (11, 14, 15). Due to the mental disorder, particularly depression, and the decrease in quality of life experienced by affected individuals, another common cause of HD-associated death is suicide, the rates of which are significantly higher than the general population after symptom onset (8, 9, 16).

Currently, no treatment exists to either halt or attenuate the progression of this disease, leaving only symptomatic treatments such as neuroleptics and anticonvulsants (17).

1.1.3 Huntington's Disease Neuropathology

The most notable feature of HD pathogenesis is progressive degeneration of the striatum, the largest structure of the basal ganglia, which includes the caudate nucleus and the putamen (18). Striatal atrophy in HD can be entirely attributed to the selective loss of the GABA-ergic medium spiny neurons (MSNs) that account for 95% of the striatal population. The other striatal neuronal subtype, the aspiny cholinergic interneurons, are

relatively spared by comparison (19–22). This striatal loss forms the basis of the Vonsattel score, which classifies pathological burden in HD post-mortem tissue into five classes of severity (0-4)(18), although this score does not always correlate with functional disability prior to death (23). This discrepancy is potentially due to the fact that changes in other brain regions do not factor into the Vonsattel score (24).

Though striatal degeneration is the most notable neuropathological change in the HD brain, the diverse presentation of cognitive and psychiatric symptoms point to a more wide-spread degeneration and involvement of other brain structures. In addition to neuronal loss in the striatum, there is also clear loss of volume in the cerebral cortex, thalamus, hippocampus, cerebellum, substantia nigra, and globus pallidus (25–27). Magnetic resonance imaging (MRI)-based morphometric analysis has revealed that, in HD brains, there is a significant reduction in volume in almost all brain structures (28). An analysis of longitudinal MRI data from the TRACK-HD study identified previously uncharacterized atrophy of the white-matter in premanifest HD patients, which, along with striatal atrophy, were the earliest detectable changes by this modality (29).

Prior to the massive neuronal death and structural atrophy seen in HD, it is believed that there is early neuronal dysfunction that may contribute to the early, subtle symptoms noted in prodromal HD. Impairment in emotion recognition, working memory, psychomotor processing, and visuomotor integration, as well as in a variety of motor tests have been noted in observational studies in premanifest patients (30–33). Although the cause of these changes cannot be verified in humans, early neuronal dysfunction has been

noted in knock-in mouse models of HD (34). Many of these models do not display overt cell death but do present with typical hallmarks of HD, such as the presence of mutant huntingtin inclusions, defective synaptic transmission, energy deficits, and abnormal transcription profiles (35–38). The presence of these early changes, both symptomatically and neuropathologically, highlight two important points. The first is the need to target future HD therapeutics to the premanifest stages of disease, where neuronal changes have already occurred, with potentially long-lasting consequences. The second is that the mechanism, or, more likely, mechanisms of neuronal dysfunction need to be elucidated to inform these therapeutics.

1.1.4 Genetics of Huntington's Disease

While the pattern of HD inheritance was originally described back in 1872 by George Huntington (5), it wasn't until over a hundred years later, in 1983, that this disease was molecularly mapped to a human chromosome, specifically the short arm of chromosome 4. This was the first time this had been done without any prior indication of gene location (39). Using Restriction Length Polymorphism (RFLP) screening, Gusella *et al.* screened thousands of samples to identify genetic markers that track with disease (39). Many of those samples came from communities in Lake Maracaibo, Venezuela, where the founder effect has led to a population with in the highest incidence of HD in the world (40). With the advent of new genomic technologies, ten years later the causal mutation was identified as an expansion of a cytosine-adenine-guanine (CAG) trinucleotide repeat

tract in the *IT15* (interesting transcript 15) gene (41), later renamed the huntingtin (*HTT*) gene. This expansion translates to a polyglutamine expansion in the *HTT* gene product, the huntingtin protein. As HD is autosomal dominant, only one copy of the mutated gene is required for an individual to present with the disease. Although rare, there are some individuals that are homozygous for the HD mutation, which is associated with a more severe clinical course (42). A recent study has found that, in some areas of the world, the incidence of HD is as high as 1:5500 (43).

In unaffected individuals, the length of the CAG repeat is 35 or less (44), while those with 40 or more repeats have full penetrance of the disease and will develop symptoms. Those with repeats between 36-39 exhibit incomplete penetrance, and may or may not develop HD symptoms within their lifetime (45). Individuals with repeats falling just below the pathogenic threshold are not in danger of developing HD, but their offspring may be at risk of disease due to a phenomenon called “genetic anticipation” (46, 47). As the CAG tract is genetically unstable, there is a risk, especially at longer repeat lengths, that germ-line expansion of the tract may occur. This more commonly happens in spermatogenesis than oogenesis (48).

Beyond the pathogenic threshold, the length of the CAG tract affects both age of disease onset as well as disease severity. Age of onset is inversely correlated with CAG tract length, with individuals who have longer repeat lengths experiencing earlier disease onset and faster disease progression (40, 49). Repeat lengths greater than 60 result in juvenile-onset HD, which manifests before the age of 20 with a more severe progression

of symptoms (50). Although repeat length is the primary modifier of disease onset, there is a great amount of variability in age of onset and disease progression between individuals with the same repeat length, suggesting other modifiers of disease progression (40). A recent genome-wide association study (GWAS), the largest in HD history, has identified a number of these gene modifiers, which fall into three mechanistic categories: those involved in deoxyribonucleic acid (DNA) damage repair pathways, those involved in redox signalling, and those involved in mitochondrial function (51).

1.1.5 Other CAG Triplet Repeat Disorders

CAG tract expansion is by no means a phenomenon that is unique to HD. HD belongs to a family of nine CAG triplet repeat disorders, each caused by a CAG expansion in the coding region of a different gene above a certain threshold (52). Since this mutation results in expansion of the polyglutamine tract in the protein product of these genes, this family is also known as the “polyglutamine diseases” and includes, spinocerebellar ataxia (SCA) types 1, 2, 3, 6, 7, and 17, as well as spinal-bulbar muscular atrophy (SBMA), dentatorubro-pallidoluysion atrophy (DRPLA) and HD. It is hypothesized that these expansions occur due to the ability of the CAG tract to form hairpin structures, leading to strand slippage and expansion of the repeat during DNA replication or repair (resulting in germline or somatic expansion, respectively) (47, 53, 54). Generally speaking, these diseases are all inherited in an autosomal dominant

fashion, and all present as neurodegeneration with midlife onset that is inversely correlated with the length of the CAG repeat expansion (55).

These similarities have led to speculation that there might be a common, gain-of-function of the expanded polyglutamine domain, such as the promotion of protein aggregation (the “amyloid hypothesis”) (56). While each of these diseases present as neurodegeneration, this degeneration takes place in different regions of the brain, with different neuronal subtypes affected, and with different motor, cognitive, and psychological outcomes (55). For instance, while HD primarily affects the striatum, with additional degeneration noted in other regions of the brain, SCA1 primarily affects the cerebellum (57). This variability indicates the protein context of the expansion is important and, therefore, each of these diseases needs to be understood in the context of the protein where the mutation takes place, and not simply as “polyglutamine diseases” as a whole. Taken together, the marked similarities and differences between these diseases implies that there is indeed a common pathogenic mechanism of these diseases, but it is likely more complex than the amyloid hypothesis suggests.

1.2 The Huntingtin Protein

1.2.1 The Structure of the Huntingtin Protein

Huntingtin is a large, 3144 amino acid protein, with a molecular weight of almost 350 kDa. For many years following the identification of the causal mutation, the high molecular weight, as well as the flexibility of the huntingtin protein made determination of a high resolution structure difficult. Although early computational and biochemical studies suggested that huntingtin was primarily composed of HEAT (huntingtin, elongation factor 3, subunit of protein Phosphatase 2A (PP2A), and TOR 1) repeats (58, 59), most structural studies have focused on amino-terminal (N-terminal) fragments. Recently, advancements cryo-electron microscopy (cryo-EM) have led to the very first high resolution structure of full-length huntingtin with an overall resolution of 4 Å (60).

The earliest studies of huntingtin structure suggested that the majority of the huntingtin protein is composed of approximately 36 HEAT repeat domains (58, 59). These motifs, named for the first 4 proteins they were identified in, are composed of approximately 40 amino acids that normally appear as tandem helical domains separated by a non-helical domain (helix-turn-helix) (59). These motifs confer an overall α -helical solenoid structure on their respective proteins and mediate a number of protein-protein interactions (61–63). Additionally, these motifs give their host proteins an incredible amount of conformational flexibility as well as the ability to store and release energy (64). The ability to stretch and compress may give HEAT repeat proteins the flexibility

required to mechanically transduce signals along their length and alter the epitopes available for interaction allosterically. So, while huntingtin lacks any enzymatic activity, the presence of these repeats suggests that huntingtin may act as a scaffold to facilitate complex formation.

Arguably, the most well studied domain of huntingtin is exon1, due in no small part to the fact that this domain contains the region of pathogenic expansion, the polyglutamine tract. Flanking the polyglutamine tract on the N-terminal side is a 17-residue, amphipathic α -helix, also called N17, and on the carboxy-terminal side is a proline-rich region. All of these domains have been shown to serve as protein-interaction domains (56, 65–67), again pointing to the potential function of huntingtin as a scaffolding protein.

The N17 domain has been shown by sequence analysis and circular dichroism (CD) spectroscopy, later confirmed by x-ray crystallography, to form an amphipathic α -helix (68, 69). This helix targets huntingtin to membranes in a structure-dependent manner (69). This region also is responsible for modulating huntingtin localization between the cytoplasm, nucleus, and primary cilium, and has been shown to contain a chromosome regional maintenance 1 (CRM1)-dependent nuclear export signal (NES) (70, 71). Post-translational modifications (PTMs) of the N17 domain are important regulators of localization (71), mutant protein toxicity (72, 73), and inclusion formation (74).

The polyglutamine tract begins at amino acid 18 of exon1 and is expanded in HD. In its unexpanded form, this region has been shown to adopt multiple structures, including

α -helical, random coil, extended loop (68). Thus, at normal polyglutamine lengths, this polyglutamine tract adopts structures more amenable to flexibility of exon1. When this region is expanded beyond the pathogenic threshold of HD, it is generally agreed that this domain becomes more structured, forming β -sheets (56, 75, 76), which may promote aggregation due to the formation of “polar zippers” (56). Caron *et al.* used Fluorescence lifetime microscopy combined with Förster resonance energy transfer (FLIM-FRET) to show that there is a change in exon1 conformation right at the pathogenic threshold of 37 glutamine repeats (77). While it is hypothesized by some that the propensity of polyglutamine expanded mutant huntingtin to aggregate due to interactions between intermolecular β -sheets explains polyglutamine toxicity, it is also possible that this loss of flexibility in exon1 impairs the function of the huntingtin protein.

Immediately distal to the polyglutamine domain is the polyproline region. This domain is only found in higher mammals, and, in humans, is comprised of 2 pure poly-proline tracts separated by an intervening sequence (IVS). In addition to its role as a protein-interaction domain, the proline-rich region has been shown to affect protein solubility and inclusion formation (78, 79).

Further downstream of the proline-rich region lie two regulators of huntingtin localization. The first is a proline-tyrosine nuclear localization signal (PY-NLS) found at amino acids 174-207 (80). The PY-NLS mediates huntingtin localization to the nucleus through both the karyopherin β 1 and β 2 pathways, and is unique among known PY-NLSs as it contains an unusually long IVS between its motifs (80). This IVS gives the PY-NLS

a β -sheet structure that is critical to huntingtin nuclear import (80). Finally, at the extreme carboxyl-terminus of huntingtin lies another CRM1-dependent NES (81). The presence of two NESs, as well as the unusual PY-NLS inform on the importance of nuclear-cytoplasmic shuttling of huntingtin, suggesting important roles for the protein in both cellular compartments.

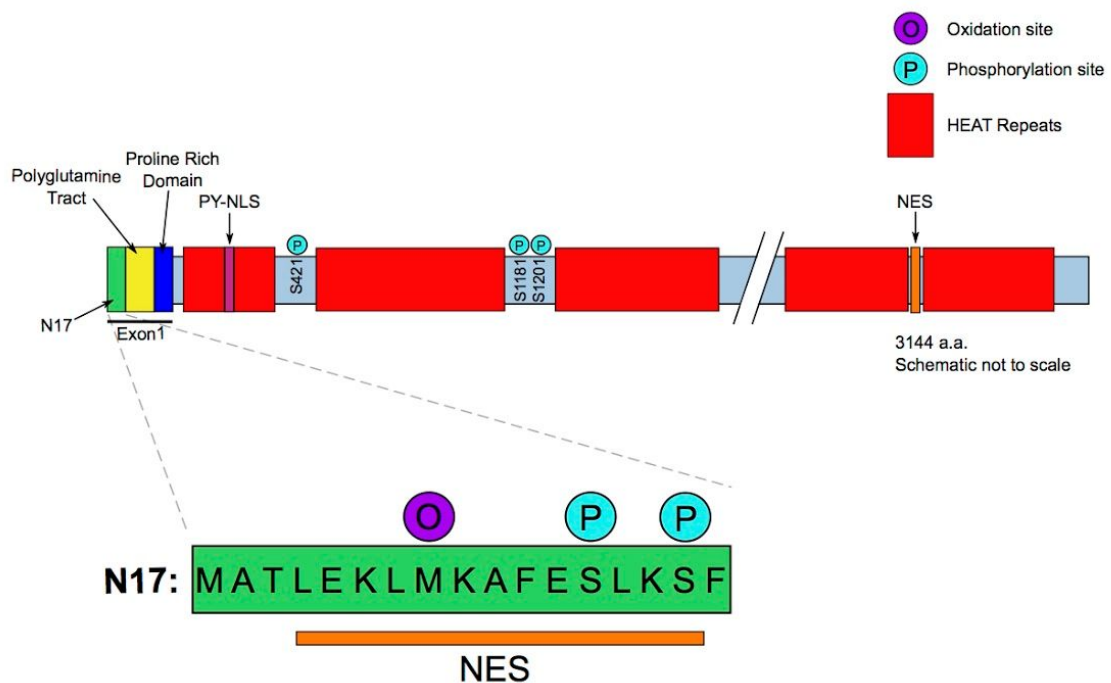


Figure 1.1. Schematic of the the huntingtin protein. Important domains, phosphorylation sites, oxidation sites, as well as nuclear export signals (NES) and the proline-tyrosine nuclear localization signal (PY-NLS) are shown. Below is an enlargement of the amino-terminal (N17) domain, again showing important PTMs, as well as the amino acid (a.a.) sequence.

1.2.2 The Localization of the Huntingtin Protein

Huntingtin is ubiquitously expressed in every cell in the body, but has particularly high expression in the brain and testes (82). In spite of this generalized expression, HD manifest as a primarily CNS disease. Within the cell, huntingtin is localized primarily in

the cytoplasm and is associated with a variety of organelles, such as the Golgi complex, mitochondria, endosomal compartments, and endoplasmic reticulum (ER) (83–85). It has also been shown to interact directly with actin, microtubules, and lipids (71, 86–91). Huntingtin has also been visualized in the nucleus and perinuclear region (92–94) and, additionally, has been shown to interact with DNA and ribonucleic acid (RNA) (95–97). Under normal conditions, huntingtin is generally found associated with the ER via the N17 domain, but this interaction is transient, and, under conditions of stress, the protein is released to shuttle between the cytoplasmic and nuclear compartments (69, 98). Shuttling is mediated by the previously described NLS, between amino acids 174-207, and two CRM1-mediated NESs, one near the carboxy-terminus and one on the hydrophobic face of the N17 α -helix (70, 80, 81).

The N17 region is an important modulator of huntingtin localization. This region can be modified by a number of different PTMs such as phosphorylation, acetylation, and ubiquitination (99). Serines 13 and 16 (S13 and S16) have been identified as critical regulators of huntingtin biology. In addition to acting as regulators of huntingtin localization to the nucleus under conditions of stress, phosphorylation of these residues targets wild type protein to mitotic structures, as well as the primary cilium (70, 71).

In HD, localization of the huntingtin protein is perturbed, and there is accumulation of mutant huntingtin in the nucleus (37). Neuronal aggregates of mutant huntingtin in the nucleus and the cytoplasm have been noted both in animal models of HD (34, 100–102) and in post-mortem HD tissues (103); however, though initially thought to be toxic, these

aggregates have not been found to correlate with increased susceptibility of neurons to death (104). In fact, some studies have found that these aggregate-containing cells may be less susceptible to neurodegeneration (105), suggesting that aggregates are not the toxic species but are, instead, a protective mechanism to sequester the toxic build-up of soluble mutant huntingtin protein.

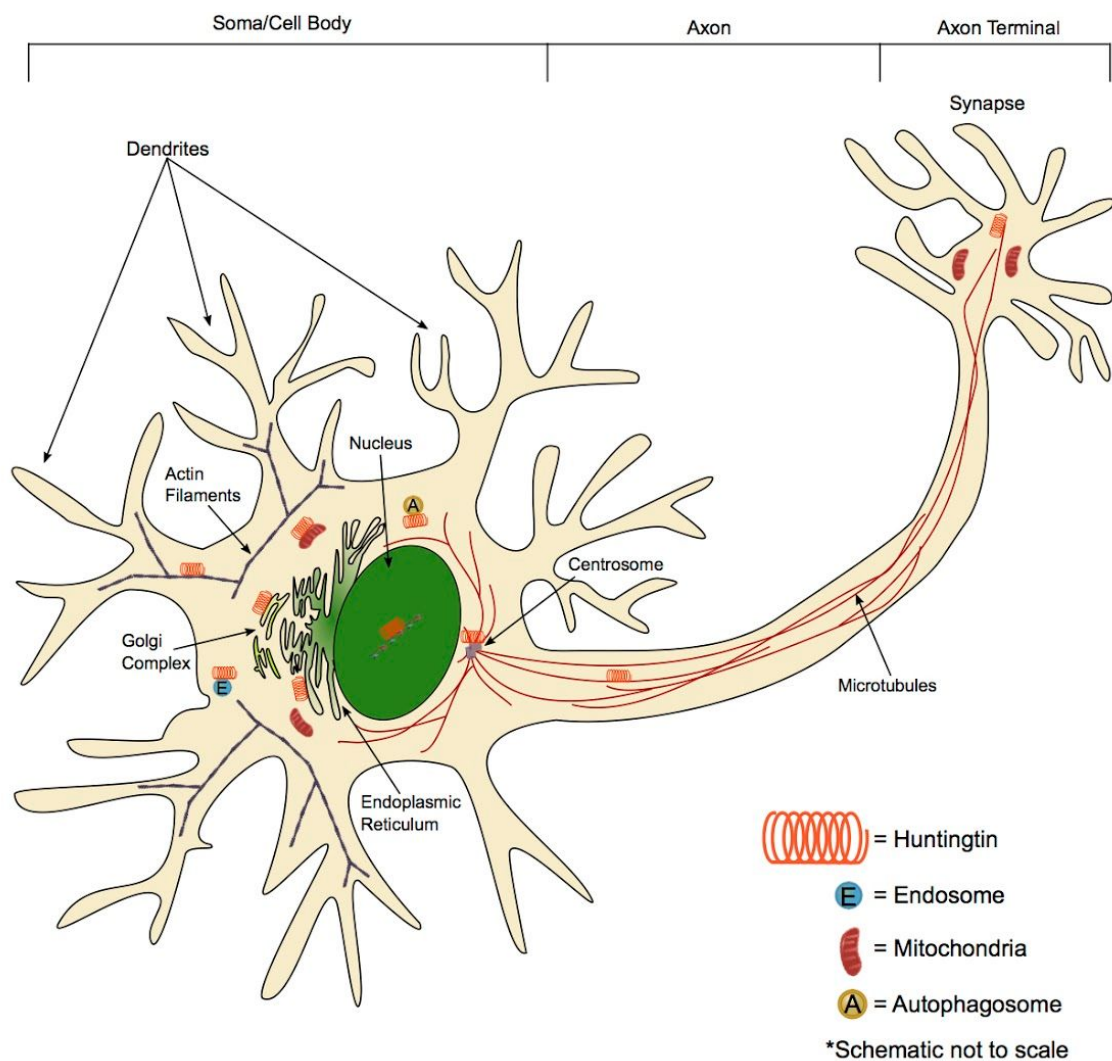


Figure 1.2. Subcellular localization of the huntingtin protein.

1.2.3 Functions of the Huntingtin Protein

Ever since the discovery of the *HTT* gene in 1993, there has been intense effort dedicated to determining the functions of the huntingtin protein. In some cases, structure has informed function, such as the role of huntingtin as a scaffold protein (106). The apparent involvement of huntingtin in so many cellular processes has led to intense debate as to whether HD is a “gain-of-function” disease, with the mutant huntingtin protein acting as a toxic entity, or a “loss-of-function” disease, with impaired mutant huntingtin function leading to disruption of cellular processes and cell death (99). With current HD therapeutic strategies focusing on “huntingtin-lowering” of both the mutant and wild type protein, it is important that the normal functions of huntingtin be considered as they may be impaired by this strategy.

1.2.3.1 *Huntingtin in development*

The importance of the huntingtin protein in development is underscored by its absolute necessity. Constitutive knockout of huntingtin expression is embryonic lethal between embryonic day 7.5 to 8.5 (107, 108). Inactivation of the mouse *HTT* homolog, *Hdh*, results in abnormal gastrulation at day 7.5, with resorption beginning at day 8.5 (107). It is at this point that development of the nervous system has just begun. Specifically, knockout embryonic stem cells display increased cell death of the ectoderm, the germ layer from which the CNS develops (109, 110). Embryonic stem cells homozygous for mutant huntingtin also show some stage specific changes in lineage

development and maturation (109). It is of note that, in these models, mice heterozygous for huntingtin knockout develop normally, suggesting that wild-type huntingtin expression that is 50% of normal is sufficient for development (107).

To further elucidate the role of huntingtin in development, *Cre/loxP* conditional huntingtin knockout mice, which have loss of huntingtin expression in embryogenesis after the critical threshold of 7.5-8.5 days or soon after birth, were used (111). These mice are born at normal Mendelian ratio but develop motor and neurological abnormalities, including cortical degeneration, degeneration of axon fibre tracts, and DNA breaks in the cortex and striatum (112). When huntingtin levels were restored to 50 % after neural development (post-natal day 20), deficits in motor coordination and progressive neurological abnormalities, such as striatal degeneration and abnormalities in the germative zone, were noted (113). These studies demonstrate the importance of the presence of a certain level of the huntingtin protein during development of the nervous system.

1.2.3.2 Huntingtin at the synapse

Huntingtin is found at the synapse at both pre- and postsynaptic terminals. At the presynaptic terminal, it has been shown to be associated with synaptic vesicles and with the major proteins that comprise the cytomatrix proteins at active zone (CAZ) complex (83, 114). The CAZ complex provides a structural platform at the presynaptic terminal to

facilitate neurotransmitter exocytosis. Interaction of huntingtin with this complex, as well as synaptic vesicles, suggests a role for huntingtin in neurotransmitter release.

At the postsynaptic terminal, huntingtin associates with *N*-methyl-D-aspartate (NMDA) and kainate receptors via postsynaptic density 95 (PSD-95) (115). This interaction is mediated by the Src homology 3 (SH3) domain of PSD-95, which binds to the polyproline domain of the huntingtin protein (115). PSD-95 is a scaffold protein that binds to NMDA and kainate receptor GluR6 and causes clustering of these receptors at the postsynaptic membrane (116). Suppression of PSD-95 expression impairs NMDA-dependent long term potentiation, activation of nitric oxide synthase, and excitotoxicity (117, 118). Huntingtin binding to PSD-95 sequesters and prevents it from interacting with NMDA receptors and GluR6 (115). Polyglutamine expansion interferes with the ability of huntingtin to interact with PSD-95, leading to sensitization of NMDA receptors and subsequent glutamate-mediated apoptosis (115).

Protein kinase C and casein kinase substrate in neurons 1 (PACSIN1) also interacts with the polyproline region of huntingtin via its SH3 domain (119). PACSIN1 is responsible for endocytosis and synaptic removal of NMDA receptors (120), and, unlike PSD-95, PACSIN1 is sequestered by mutant huntingtin (119), inhibiting receptor recycling. This, in combination with the increased activity of NMDA receptors, may be responsible for the glutamate-mediated excitotoxicity seen in HD (121).

1.2.3.3 Huntingtin in vesicular and axonal transport

Axonal transport in neurons is a highly regulated process as the proper localization of vesicles and other cargo is critically important in cells with such long processes. Transport can occur in both the anterograde direction, generally mediated by kinesins, and the retrograde direction, generally mediated by dynein. Huntingtin has been found to be associated with proteins that play roles in vesicular trafficking as well as vesicles and microtubules, implicating huntingtin in this process (65, 83, 122). In 1997, Block-Galarza *et al.* observed that huntingtin and huntingtin associated protein 1 (HAP1) are rapidly transported in axons, in both the anterograde and retrograde direction, at a rate that was consistent with vesicle transport (123). Since then, huntingtin has been shown to mediate vesicular transport through a direct interaction with dynein (124) as well as HAP1, which interacts directly with the p150^{Glued} subunit of dynactin and kinesin (125, 126). In the context of mutant huntingtin, axonal transport is slowed, as the interaction of polyglutamine expanded huntingtin with p150^{Glued} and HAP1 is increased but their association with microtubules is decreased (127, 128). Expression of wild-type huntingtin or phosphorylation of serine 421 (S421) of huntingtin can rescue this deficit (128, 129).

Phosphorylation of this residue has also been shown to act as a molecular switch for retrograde/anterograde transport (130). When S421 is phosphorylated, huntingtin recruits kinesin-1 to the dynactin complex, resulting in anterograde transport, but when

this residue is not phosphorylated, kinesin-1 dissociates from this complex and retrograde transport is resumed (130).

Of particular interest in HD is how aberrant vesicular trafficking affects transport of brain derived neurotrophic factor (BDNF). BDNF is a neurotrophic factor that is produced by cortical neurons and is then transported to the striatum where it acts as a prosurvival factor (131, 132). There are reduced BDNF levels in the brains of HD patients, and it is hypothesized that this deficit is due to inefficient transport of BDNF-containing vesicles (128, 133). Restoration of proper transport by enhancing phosphorylation of S421 increases BDNF release, and may play a role in the protective mechanism of this PTM (129, 134).

1.2.3.4 Huntingtin in cell division

During eukaryotic cell division, cytoskeletal microtubules are reorganized into bipolar mitotic spindles. The orientation of these spindles is critical for proper segregation of chromosomes, and, as a result, is tightly regulated. Spindle assembly and movement is controlled by the astral microtubule, the nuclear mitotic apparatus (NuMA) protein (135), and associated plus- and minus-end directed motor proteins (136–139). Huntingtin is found at high levels in dividing cells in association with some of these components, forming a complex with dynein/dynactin and also with HAP1 (128, 140), which localizes to spindle poles during mitosis. Consistent with a role of huntingtin in regulating spindle orientation, Godin *et al.* found that depletion of huntingtin by RNA interference (RNAi)

resulted in smaller spindles and mislocalization of the spindle components, dynein, dynactin, and NuMA (89). Mutant huntingtin alters the localization of dynein, NuMA, and the p150^{Glued} subunit of dynactin, causing misorientation of the mitotic spindle in cultured cells and dividing mouse cortical progenitors (141). This phenotype can be rescued by phosphorylation of S421 by Akt (141). Taken together, these results suggest a role for huntingtin in spindle orientation through scaffolding spindle components (142). Although HD is a disease that primarily affects non-dividing cells in the CNS, improper spindle orientation caused by expression of mutant huntingtin has implications in neurogenesis that should not be overlooked.

1.2.3.5 Huntingtin at the mitochondria

While it is clear that there are mitochondrial-related issues that arise in HD, the role of huntingtin at the mitochondria is less well characterized than its roles in other areas of the cell. Neurons are high-energy utilizers, consuming adenosine triphosphate (ATP) to maintain activities such as neurotransmission (143). As the primary generators of ATP by oxidative phosphorylation, as well as regulators of calcium homeostasis, and a major source of endogenous reactive oxygen species (ROS) (144), mitochondria are crucial for normal neuronal function. There is abundant evidence of mitochondrial dysfunction in HD. There is a marked decrease in the level of glucose metabolism and increased lactate in affected brain regions of HD patients (145). Additionally, striatal cells from HD mouse model brains have impaired mitochondrial respiration and ATP synthesis

(146). One of the earliest mouse models of HD was generated by injection of the mitochondrial toxin 3-nitropropionic acid (3-NP), resulting in selective striatal degeneration, depressed ATP levels, and elevated lactate levels (147, 148). Mutant huntingtin disrupts mitochondria homeostasis and dynamics, impairing proper fission and fusion, resulting in improper turnover of damaged mitochondria (149, 150). Furthermore, Trushina *et al.* observed significantly slower mitochondria transport in striatal neurons taken from transgenic mice expressing polyglutamine expanded mutant huntingtin (151). The results of these studies indicate that mutant huntingtin is interfering with mitochondrial transport in one of two ways; either mutant huntingtin is sequestering factors involved in mitochondrial transport, or wild-type huntingtin has a role at the mitochondria that is being impaired by expansion of the polyglutamine domain.

To determine if wild-type huntingtin plays a role at the mitochondria, several studies have examined the effects of huntingtin knockdown and knockout on mitochondrial transport. *Hdh^{ex4/5}/Hdh^{ex4/5}* knockout embryonic stem cells show abnormal perinuclear mitochondrial clustering, as shown by staining with mitochondrial marker Grp75, but no change in the surrounding cytoskeletal organization. This implies a direct role for huntingtin in mitochondrial localization (94). Neurons have unique mitochondrial localization compared to other cell types due to different metabolic demands in different cellular regions. Therefore, effective transport and proper localization of mitochondria are critical to cell health. HAP1 associates with mitochondria (152), and, through association

with HAP1, and the motor proteins kinesin and dynein, huntingtin may be a key integrator of mitochondrial transport (153).

In addition to the observed abnormalities in mitochondrial localization, huntingtin knockout in mouse embryonic stem cells results in loss of mitochondrial structural integrity (154). Although there was no change in mitochondrial membrane potential (MMP), a total failure of ATP production as well as maximal glycolysis was observed in this study, suggesting a critical role for huntingtin in normal mitochondrial function (154). Wild-type and mutant huntingtin have been found in purified mitochondrial fractions, and have further been localized to the cytosolic surface of the outer mitochondrial membrane (155). In this study, an N-terminal fragment of mutant huntingtin was found to induce mitochondrial permeability transition pore opening, sensitizing cells to calcium (Ca²⁺)-mediated depolarization. The role of wild-type huntingtin at the membrane was not investigated (155). In spite of this, it is clear that wild-type huntingtin plays an important role in both the proper localization and function of mitochondria, which are impaired by loss of huntingtin or expansion of the polyglutamine domain.

1.2.3.6 Huntingtin and autophagy

In addition to its interaction with proteins involved in vesicular and mitochondrial transport, huntingtin has also been shown to associate with several proteins involved in selective autophagy (156). Selective autophagy is process by which damaged cellular

components, such as damaged membranes, peroxisomes, and mitochondria, as well as protein aggregates, are recognized and targeted to the lysosome for degradation. Loss of autophagy results in premature aging and neurodegeneration (157). In *Drosophila*, loss of huntingtin has been shown to result in inhibition of starvation-induced stress-related autophagy (156). Conditional knockout of huntingtin in mice resulted in dysregulation of autophagy, as shown by increased levels of the autophagic adaptor p62, as well as accumulation of lipofuscin and ubiquitin in the thalamus and striatum (156). These findings have led to the hypothesis that huntingtin may function as a scaffold for selective macroautophagy (156).

The role of huntingtin in microtubule-based transport is important in autophagy as loss of huntingtin or HAP1 in mouse neurons disrupts transport of autophagosomes to lysosomes resulting in defective degradation of damaged cellular components (158).

1.2.3.7 Huntingtin in the stress response

In spite of the fact that the expansion of the polyglutamine domain is present in all cells since birth, HD is an age-onset disease that presents primarily in the CNS. A common hypothesis for this discrepancy is that there is an accumulation of cellular damage due to aging-related, ROS-induced stress that neurons expressing the mutant protein are no longer able to compensate for. The huntingtin protein has been shown to participate in the cell stress response in several different capacities. Heat shock stress causes a global unfolding of proteins, activation of the unfolded protein response (UPR),

a spike in calcium signaling, and drop in cellular ATP levels (159, 160). Upon induction of heat shock stress, huntingtin has been shown to dissociate from the ER and associate with nuclear cofilin-actin rods (88). These rods halt actin remodelling, increasing the available pool of ATP during times of stress. The resolution of these rods is impaired in the presence polyglutamine-expanded huntingtin (88). In another heat shock stress response, this time in the cytoplasm, huntingtin rapidly accumulates at RabC positive early endosomes, halting early-to-recycling and early-to-late endosome fusion (161). Although distinct from canonical cell stress structures, like cofilin-actin rods, the purpose of this stress response is likely to increase available ATP quickly. Also like cofilin-actin rods, there is defective resolution of this response when mutant huntingtin is expressed (161).

The N17 domain of huntingtin is a critical regulator of the response of huntingtin to stress. Within this domain, S13 and S16 are phosphorylated upon stress (71), mediating huntingtin translocation and retention in the nucleus by inhibiting CRM-1 binding to the N17 NES (70). Within this domain lies another critical residue, methionine 8 (M8), which becomes sulphoxidated under conditions of oxidative stress, facilitating release of huntingtin from the ER and subsequent phosphorylation (98). In this way, the N17 domain of huntingtin acts as a ROS sensor, translocating to chromatin-dependent nuclear puncta following an oxidative insult (71, 98).

1.2.3.8 Huntingtin in the DNA damage response

Oxidative stress and ROS, both endogenously and exogenously generated, are common DNA damage-inducing agents. There have been extensive reports of damage to nuclear and mitochondrial DNA in HD patient samples and mouse models (162–165), implying a potential role for huntingtin in the DNA damage response that is impaired in disease (166). Consistent with this idea, a recent HD GWAS with almost 4000 participants identified genes involved in DNA repair pathway as modifiers of HD age of onset.

A central regulator of the cellular response to DNA damage is ataxia-telangiectasia mutated (ATM) kinase. ATM is HEAT repeat-rich, serine/threonine kinase that signals DNA damage to a variety of proteins, including the tumor-suppressor protein p53. ATM is classically known to signal double-stranded DNA breaks, but can also be activated by single-stranded breaks (167), oxidative stress (168), and chromatin reorganization (169). Elevated ATM signalling, as measured by the levels of phosphorylated H2A histone family X (γ H2AX), has been noted in the BACHD mouse model (170), and inhibition of this signalling by knockdown was protective in mammalian cells and transgenic *Drosophila* models (170). A more direct connection between huntingtin and ATM has recently been shown in human telomerase reverse transcriptase (hTERT) immortalized patient derived human fibroblasts with clinically relevant allele lengths (TruHD cells), where N17-phosphorylated huntingtin localizes to

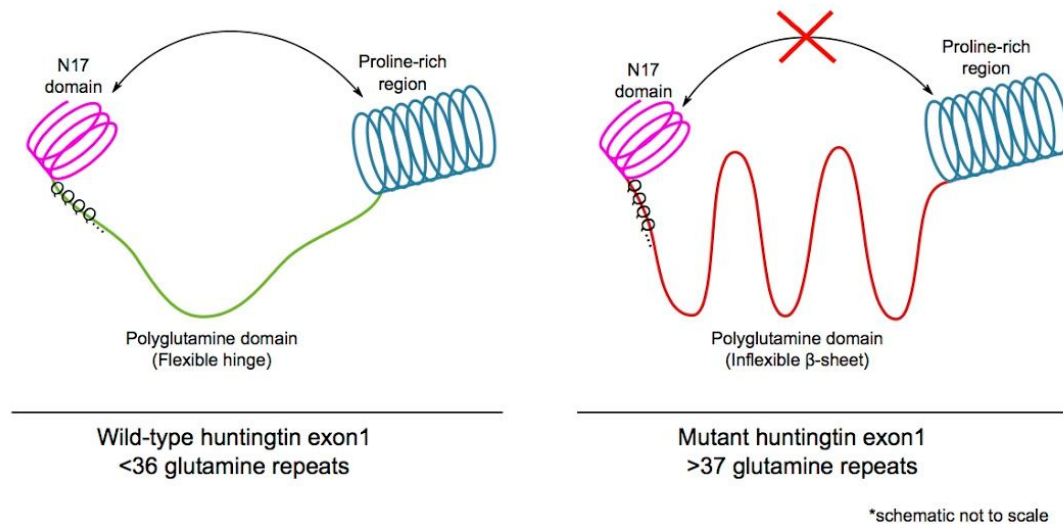
sites of DNA damage in an ATM-dependent manner (171). Additionally, huntingtin interacts with DNA repair proteins X-ray repair cross-complementing protein 1 (XRCC1), Flap structure-specific endonuclease 1 (FEN1), and apurinic/aprimidinic endonuclease (APE1) in an oxidative stress-dependent manner, implying a role for huntingtin as a scaffold in base excision repair (BER) as a part of the ATM complex (171).

This is not the first time that a role for huntingtin in the DNA damage response has been suggested. In 2006, Anne *et al.* demonstrated that upon induction of DNA damage, cyclin-dependent kinase 5 (Cdk5) phosphorylates huntingtin at serines 1181 and 1201, and there is a subsequent increase of huntingtin in the nuclear compartment at “nuclear dots” (172). Additionally, phosphorylation of these residues was shown to be protective, modulating neuronal death in a p53-dependent manner (172). Interestingly, the huntingtin promoter contains a number of p53-responsive sites, thus allowing modulation of huntingtin expression levels by p53 activity (173, 174). A brain region-specific increase in huntingtin levels in response to γ -irradiation has been shown in mice expressing normal levels of p53 that is absent in p53 knockout mice (173).

1.3 Huntingtin in Disease

1.3.1 Polyglutamine Expansion and the Pathogenic Threshold

Since the identification of the causal mutation in HD, a major question has been why there is a sudden toxicity at a certain number of CAG, or glutamine repeats. In HD, this threshold is around 36 polyglutamine repeats, and a similar threshold can be seen in other polyglutamine diseases, specifically SBMA, SCA2, and SCA7 (55). A comparison of crystal structures of wild-type and polyglutamine expanded huntingtin have revealed a change in structure right around this threshold of 36 repeats (68, 175). FLIM-FRET studies of exon1 indicate that at the pathogenic threshold, there is a decrease in the flexibility of the polyglutamine domain and a change in the conformation of exon1 (77). This structural change has been attributed to the propensity of polyglutamine expanded huntingtin to take on a β -sheet conformation (75). Not only might this gain of structure impair the usual protein-protein interactions of exon1, important for a scaffolding protein such as huntingtin, but it might also increase aberrant interactions (56), mediating cellular dysfunction on several levels.



1.3. Exon1 conformation change at the pathogenic threshold of Huntington's disease. Exon1 of wild-type huntingtin has a dynamic conformation due to the flexibility of the polyglutamine domain (left). Exon1 of mutant huntingtin loses this flexibility due to the expansion of the polyglutamine domain and the formation of a β -sheet structure.

1.3.2 Proposed Mechanisms of Disease

Histopathological and biochemical evidence has led to the proposal of a variety of potential mechanisms for HD pathogenesis. These mechanisms include loss of BDNF, either through defective vesicle transport or reduced transcription (128, 176); excitotoxicity and corticostriatal dysfunction (177, 178); proteolysis (179); toxic protein misfolding and aggregation (180–182); defective autophagy (156, 183); dysregulation of transcription; mitochondrial dysfunction (165, 184); and, most recently, DNA damage and defects in DNA damage repair (170, 171, 185). These processes are not mutually exclusive, and it is more than likely that more than one of these mechanisms are responsible for HD pathogenesis. In the next section, a few of these mechanisms that are common between HD and other neurodegenerative diseases will be discussed.

1.3.2.1 Aggregation/toxic sequestration

One of the most common hallmarks of neurodegenerative disease is the formation of aggregates of mutated/misfolded proteins, found in over half of the defined neurodegenerative diseases. These aggregates typically consist of fibres of misfolded protein with a β -sheet conformation. In HD, these aggregates are composed of mutant huntingtin; in Alzheimer's disease (AD), amyloid β -peptides ($A\beta$) form intracellular plaques and tau protein aggregates into neurofibrillary tangles; in Parkinson's disease (PD), misfolded α -synuclein forms insoluble fibrils called Lewy bodies; in SCA1, these aggregates are composed of mutant ataxin-1 protein; and in amyotrophic lateral sclerosis (ALS), these aggregates are composed of a variety of ubiquitinated, RNA-binding proteins and superoxide dismutase 1 (SOD1) (186). The presence of aggregates in all of these diseases led to the hypothesis that aggregates were a cytotoxic entity and that protein aggregation may be common pathogenic mechanism in all of these diseases.

The presence of aggregates in HD post-mortem brains was first described by Roizin *et al.* using electron microscopy (187). Subsequently, aggregates composed of amino-terminal fragments of huntingtin were found in transgenic R6/2 mice expressing a polyglutamine expanded copy of huntingtin exon1 (181). DiFiglia *et al.* analysed post mortem brain tissue from HD patients, also by electron microscopy, observing that these aggregates were found in all cortical layers, as well as in the MSNs of the striatum (180). Interestingly, these aggregates were not seen in the cerebellum or globus pallidus, which

are both relatively unaffected in HD. Aggregates have been identified in both the nucleus and the cytoplasm of HD patient neurons. These observations led to the hypothesis that these aggregates are toxic, and, indeed, inclusion formation in cultured cells has been shown to correlate with susceptibility to cell death in some cases, and aggregate load tracks with disease progression in some mouse models (188, 189). The mechanism of aggregate-induced toxicity has been attributed to a number of processes, including sequestration of other polyQ containing proteins, such as transcription factors and transcriptional regulators, impairment of the the ubiquitin-proteasome system and a failure of mutant huntingtin degradation, and inhibition of axonal transport (127, 190, 191).

However, there is also a great body of evidence to suggest that aggregates themselves are not toxic, and may, in fact be benign or even protective. In 1998, Saudou *et al.* found that while nuclear mutant huntingtin does induce apoptosis, the presence of aggregates themselves does not correlate with neuronal death (104). A later study from the lab of Dr. Steve Finkbeiner showed that primary neurons expressing an exon1 fragment of huntingtin survived significantly longer if they formed aggregates than if they did not, suggesting that these aggregates are likely a protective mechanism (192). Consistent with this finding, compounds that promote the formation of mutant huntingtin aggregates by inhibiting downstream degradation were protective in cell models of disease (193). These same compounds also promoted aggregation of α -synuclein in PD model cells with similar protective effects, suggesting that in PD, Lewy body formation

may be a protective mechanism as well (193). In Alzheimer's disease (AD), the pathogenic nature of A β aggregates is also being questioned due to the failure of anti-amyloid drugs to meet endpoints in clinical trials (194, 195).

In HD, evidence of the protective effects of mutant huntingtin aggregation has led to an alternative theory wherein the soluble form of mutant huntingtin, either in its monomeric or oligomeric form, is cytotoxic, while the aggregated form is protective as it sequesters away the toxic entity (99). It is possible that this theory could translate to other neurodegenerative diseases where aggregation is a hallmark.

1.3.2.2. Mitochondrial dysfunction

The brain only accounts for 2 % of the body's overall weight, yet consumes 20 % of total basal oxygen (196). This high oxygen consumption can be attributed to the high energy demands of neurons (197). As a result of this high energy requirement, the CNS is incredibly sensitive to energetic stress, making proper energy metabolism critical for neuronal health. Mitochondria are the major source of cellular ATP through the process of oxidative phosphorylation. The first evidence of mitochondrial dysfunction in HD came from ultrastructural studies of cortical biopsies of HD patient brains, which revealed abnormal mitochondria (198). Consistent with impaired mitochondrial function, there is altered glucose metabolism in early HD, and elevated lactate levels have been reported in the basal ganglia and cerebral cortex of HD patient brains (199–201). Additionally, in these same brain regions, ¹H-magnetic resonance spectroscopy (¹H-MRS) revealed that

there is depletion of *N*-acetylaspartate, the production of which is reflective of mitochondrial metabolic function (201). Impaired mitochondrial calcium handling has been reported in lymphoblasts from HD patients and a transgenic mouse model expressing mutant huntingtin with 72 CAG repeats (YAC72) (202).

Early animal models of HD also pointed to mitochondrial dysfunction as a pathogenic mechanism, where, as previously mentioned, injection of the mitochondrial toxin 3-NP recapitulated both the striatal degeneration and some of the physical symptoms associated with HD (203). Another mitochondrial toxin, 1-methyl-4-phenyl-1,2,3,6-tetrahydropyridine (MPTP), induced PD-like symptoms and degeneration in mice and primates, suggesting that mitochondrial dysfunction plays a role in this disease as well (204, 205). In fact, there is abundant evidence that mitochondrial dysfunction plays a role in PD and AD, as well as HD.

From a genetics perspective, both familial PD and familial AD have a clear pathological link to dysfunctional bioenergetics. There are 6 known, inherited, monogenetic forms of PD, 3 of which are caused by mutations in proteins associated with mitochondrial function (206). The *PARK6* PD variant is caused by mutations in PTEN-induced-kinase 1 (PINK1), a kinase involved in mitochondrial turnover (207, 208). When mitochondrial membrane potential (MMP) decreases, indicative of mitochondrial dysfunction, PINK1 is stabilized on the outer mitochondrial membrane and can phosphorylate and recruit the E3 ubiquitin ligase, parkin, which targets the damaged mitochondria for degradation. Parkin is another protein that is mutated in familial PD,

specifically the *PARK2* variant, again implicating mitochondrial dysfunction in this disease (209). Finally, DJ-1, an oxidative stress sensor that localizes to mitochondria, is mutated in the *PARK7* variant of PD (210–212). All of these variants are inherited in an autosomal recessive manner and present as early-onset PD with identical phenotypes (206). Familial AD is caused by inherited mutations in either amyloid precursor protein (APP) or presenilin, causing increased intracellular calcium and A β production, which is associated with decreased mitochondrial function (213).

The effects of mitochondrial dysfunction in these diseases is multifold. There is evidence of decreased cellular ATP levels in AD, PD, and HD, consistent with mitochondrial dysfunction and decreased ATP synthesis, making these cells very susceptible to energetic stressors, such as DNA damage (36, 214–216). Improper function of the mitochondrial electron transport chain (ETC) leads to generation of excessive superoxide, a very reactive type of ROS, which in turn causes damage to mitochondrial and nuclear DNA. Consistent with this, there is evidence of increased oxidative DNA damage in the form of 8-oxo-7,8-dihydro-2'-deoxyguanosine (8-oxo-dG), either as DNA adducts in disease-affected brain regions or in patient cerebrospinal fluid (CSF), in all of these diseases (165, 217, 218). These two processes, working in concert, cause a progressive cycle of mitochondrial impairment, DNA damage, and ROS stress that results in energy depletion and neuronal death.

1.3.2.3. DNA damage

In mammalian cells there are multiple overlapping pathways of DNA repair, including BER, nucleotide excision repair (NER), mismatch repair (MMR), homologous recombination (HR), and non-homologous end-joining (NHEJ) (219, 220). Loss of function of proteins involved in these pathways can lead to a variety of disorders, including developmental defects, cancer, neurodegeneration, and aging (221, 222). There is increasing evidence that DNA damage and defective DNA damage repair may play a role in the pathogenesis of HD as well as other neurodegenerative diseases. HD, AD, and PD are all age-onset disorders affecting different subsets of neurons. The major DNA repair pathway in these post-mitotic cells is BER (223). As cells age, BER becomes less efficient (224), and, in combination with age- and disease-associated mitochondrial dysfunction and ROS stress, oxidative damage to nucleotides becomes more prevalent (225–227). Elevated levels of oxidative damage is an early change in AD as well as in PD, and has been extensively documented in cell and animal models of HD and HD post-mortem brains (162, 164, 228, 229).

While this increased oxidative damage load is certainly sufficient to contribute to the pathogenesis of HD and other neurodegenerative disorders, in many cases, there are, also defects in the DNA damage repair process that could also contribute to disease. Recently, in HD, studies have supported the involvement of DNA damage repair pathways in HD pathogenesis (185, 230). In a 2015 GWAS, pathway analysis identified

genes associated with DNA damage repair pathways as the most common modifiers of HD age of onset (51), and a later study found significant association between gene variants involved in DNA repair pathways and the age of onset of HD and several SCAs, suggesting that this mechanism may be common amongst polyglutamine diseases (230). Around the same time, Dr. William Yang's lab found that there was abnormal ATM activity in HD model mice, and when this activity was corrected by small molecule ATM inhibitors, there was reduced mutant huntingtin-induced cell death (170). Huntingtin has recently been shown to scaffold the ATM complex, implicating this protein directly in disease pathogenesis (171). ATM is DNA damage "first responder", and is activated in response to a variety of types of DNA damage as well as oxidative stress (168), although it is canonically activated by DNA double strand breaks (DSBs). This protein is mutated in ataxia-telangiectasia, resulting in radiosensitivity, immunodeficiency, and degeneration of the cerebellum that is likely reflective of the loss of ATM-mediated signalling of DSBs (231, 232).

Defective response to DSBs has also been hypothesized to be involved in AD pathogenesis (233) with increased levels of γ H2AX, a downstream target of ATM, being noted in AD mouse models (234). Dysregulation of DNA repair associated proteins, including DNA-dependent protein kinase (DNA-PK), 8-oxoguanine glycosylase (OGG1), and the MRN complex (MRE11/RAD50/NBS1), has also been noted in AD (235–237), again suggesting that there is defective DNA damage repair. In PD, experiments with patient fibroblasts have shown NER to be inefficient (238). NER is responsible for

removal of damage that causes structural deformations in the DNA, including pyrimidine dimers, chemical adducts, intra-strand cross links, and some forms of oxidative damage (239).

Taken together, this evidence suggest that hyperactive, but insufficient, DNA repair may be involved in the pathogenesis of these neurodegenerative diseases. As DNA repair is a high-energy process, it is likely that this high level of repair, in combination with mitochondrial dysfunction, is leading to a lack of cellular energy, resulting in neuronal death. In AD and PD, hyperactivation of DNA damage response protein poly(ADP-ribose)polymerase-1 (PARP-1) due to increased oxidative stress, and the resulting depletion of cellular nicotinamide adenine dinucleotide (NAD⁺), induces a cellular energy crisis and cell death (240). Based on the presence of both elevated oxidative stress-related DNA damage and mitochondrial dysfunction, it is likely that this pathogenic mechanism is also at play in HD.

1.4 Huntington's Disease Therapeutic Efforts

1.4.1 Biomarkers of Disease

In order to assess HD patient progress and monitor efficacy of new potential therapeutics, biomarkers that correlate with disease progression are necessary. In the HD field, these biomarkers can be divided into three categories: clinical biomarkers, biofluid biomarkers, and imaging biomarkers (241).

Clinical biomarkers are themselves divided into three categories based on the three prominent clinical features of HD: cognitive, psychiatric, and motor symptoms. Assessment of cognitive symptoms, through measures such as the Stroop colour and word test and circle tracing, are sensitive to longitudinal changes in manifest HD patients but not in pre-manifest (242). In contrast, assessment of motor symptoms, as measured by tests such as grip force and speed tapping, are sensitive to changes in pre-manifest and manifest individuals (29). Longitudinal psychiatric changes are more variable than these other measures and, thus, with the exception of apathy, are not easily used as biomarkers (243).

Biofluid markers are molecules in either the blood or CSF that have been found to correlate with disease progression. At present, only a few of these markers have been identified. Neurofilament light (NFL) protein levels in the plasma have been shown to correlate with both CSF levels of the same protein and, more importantly, with brain atrophy and motor and cognitive changes (244). Other proposed plasma biomarkers include immune protein levels, which are increased in HD, and mutant huntingtin levels in blood-derived monocytes (245, 246). Recently, mutant huntingtin levels in the CSF have been shown to correlate with disease burden and be associated with motor and cognitive performance (247). Based on this research, decreased mutant huntingtin in the CSF is being used as a primary endpoint for clinical trials with antisense oligonucleotides (ASOs) (248), which will be discussed later.

Changes in white and grey matter have also been used as biomarkers of disease. Generally, magnetic MRI has been used to visualize these changes, and, as technology has improved, so has the resolution at which researchers are able to look at these changes (29, 249, 250). Additionally, other modalities, such as positron emission tomography (PET) have been able to detect changes in pre-manifest individuals years before disease onset (251).

1.4.2 Symptom Management

To date, there are no effective disease-modifying treatments for HD, and, as a result, current treatment focuses on managing symptoms and improving quality of life. Symptom management can be pharmacological or non-pharmacological and requires a multi-disciplinary approach. The most pronounced motor symptom of HD is chorea, for which there is only one licensed drug, tetrabenazine (252). Tetrabenazine inhibits monoamine uptake by binding to, and inhibiting the action of, vesicular monoamine transporter-2 (VMAT-2). Inhibition of VMAT-2 depletes monoamines, such as serotonin, norepinephrine, and histamine, but has a greater effect on dopamine (253). Another drug, deutetabenazine, deuterated tetrabenazine, is also effective in reducing hyperkinetic movements, but its effectiveness has not been compared to that of tetrabenazine, so it is unclear if this treatment is relatively more effective or not (254).

There are no well-established pharmacological means of treating cognitive symptoms. Two randomized control trials (RCT) of anti-cholinesterase inhibitors yielded

conflicting results (255), and the selective serotonin reuptake inhibitor (SSRI) citalopram showed no effect on cognitive function (256). Non-pharmacological management is restricted to development of coping mechanisms, such as adjusting job-related duties to match current capabilities and levels of focus (241).

Treatment of psychiatric symptoms varies depending on clinical presentation. Some symptoms, such as depression, obsessive compulsive disorder, and anxiety can be treated by cognitive behavioural therapy, but this becomes more difficult with worsening cognition. Pharmacological management of symptoms generally involves SSRIs to deal with depression and anxiety symptoms, neuroleptics to mitigate aggression and psychosis, and other medications, such as the norepinephrine reuptake inhibitor atomoxetine, have been used to treat apathy (241).

While these strategies can mitigate symptoms of disease and improve the quality of life of HD patients, they do not affect overall disease progression. In the next section, previous efforts at disease-modifying therapies as well as current strategies will be discussed.

1.4.3 Previous Efforts in Disease-Modifying Therapies

In the past two decades of HD therapeutics research, there have been 99 different clinical trials, with 41 different drugs tested, but the success of these trials, as measured by progression to the next trial phase, was only around 3.5 % (257). Indeed, of the drugs tested, the only ones that made it to the market were those aimed at symptom

management rather than modifying disease progression. While the list of potential disease modifying drugs that have failed to make it through clinical trials is long, a few of the more recent drugs to have failed to achieve clinical endpoints will be discussed here.

Pridopidine is a dopamine stabilizer that had previously been shown to normalize dysregulated psychomotor function, strengthen corticostriatal glutamate function, and improve motor phenotypes in HD mouse models (258–260). Unfortunately, these findings did not translate to clinic and pridopidine did not meet primary outcomes in 3 different phase 3 clinical trials (241, 261, 262). A phosphodiesterase 10A (PDE10A) inhibitor was the subject of a phase 2 clinical trial, “Amaryllis”, run by Pfizer (263). PDE10A is a dual substrate enzyme, highly expressed in MSNs, that regulates signaling cascades controlling phosphorylation and activity of various transcription factors, neurotransmitter receptors, and voltage-gated ion channels (264–266). Levels of PDE10A are altered early in HD pathogenesis and experimental evidence suggested that inhibition of this enzyme might be beneficial in disease (251, 267, 268). Unfortunately, the Amaryllis trial did not show significant improvement in motor, cognitive, or behavioural outcomes as a result of PDE10A inhibition (263).

Coenzyme Q10 (CoQ10) and creatine are both compounds that have been tested for efficacy in HD with the goal of correcting impairments in energy metabolism. Creatine was postulated to correct this defect by buffering intracellular energy levels (269), while CoQ10 was hypothesized to correct this dysfunction at the level of the mitochondria by increasing intracellular levels of this essential electron transport chain

(ETC) cofactor (270–272). Although both of these drugs had neuroprotective effects in HD mouse models generated by injection of mitochondrial toxins, as well as in the transgenic R6/2 model (200, 273–275), neither was able to significantly increase total functional capacity compared to placebo in clinical trials (276, 277).

The failure of these trials in humans suggests that there is a more complicated disease process at play and that these drugs are either not being administered in time to prevent neuronal failure and death, or that the target of these drugs is not the appropriate one. Currently, there are 25 HD clinical trials recruiting or active listed on *clinicaltrials.gov*, ranging from cognitive training, to deep brain stimulation, to dietary supplementation. Of the drugs being tested, many focus on treating the downstream effects of mutant huntingtin, and, while these trials may yet yield promising results for HD patients, lately, the focus of HD therapeutics has shifted towards those drugs targeting processes closer to the root cause of disease, expression of the mutant huntingtin protein itself.

1.4.4 Targeting Huntingtin as a Therapeutic Strategy

The monogenetic nature of HD makes it an appealing candidate for strategies targeting the huntingtin protein itself, or, more accurately, reducing mutant huntingtin levels by targeting the *HTT* DNA or RNA. Currently, there are two clinical trials targeting *HTT* RNA by intrathecal injection of ASOs. ASOs are single stranded DNA molecules that bind pre-mRNA in the nucleus and target it for degradation by RNase H (278). The

more advanced of these trials is that of an ASO designed by Ionis Pharmaceuticals in partnership with Roche, which targets both mutant and wild-type huntingtin mRNA, leading to a universal reduction in huntingtin levels (279). While this drug has just completed phase 1b, showing safety of the ASO as well as efficacy in lowering htt levels in the CSF, the effects of this drug on HD symptoms have not yet been tested and there are some concerns regarding the long-term consequences of universal lowering of huntingtin levels. Another ASO, designed by Wave Pharmaceuticals, currently beginning clinical trials, presents a potentially safer option in that it selectively targets only mutant huntingtin RNA using associated single nucleotide polymorphisms (SNPs) (280, 281). The only downfall of this particular drug is that these mutant huntingtin-associated SNPs are not present in the entirety of the HD population and therefore these drugs will not be useful for all patients.

Other potential therapies targeting RNA include: RNAi by short interfering RNA (siRNA), short hairpin RNA (shRNA), or microRNA, promoting degradation by argonaut 2; and small molecule splicing modulators (282). Both of these strategies run the risk of generating toxic RNA, making ASOs the more attractive strategy.

Strategies for targeting huntingtin at the DNA level are comparatively less developed than those targeting huntingtin at the RNA level. There are two approaches currently being pursued, the first of which is the use of a zinc finger transcription repressor that targets the expanded polyglutamine tract of huntingtin and reduces expression of the mutant protein (283). The second strategy uses a CRISPR/Cas9

cleavage system that has been adapted to excise the promoter regions, transcription start site, and CAG mutation of the mutant huntingtin gene in human fibroblasts (284). While both of these strategies have been successfully tested in mouse models, with decreased levels of mutant huntingtin and correction of HD phenotypes noted, more research into potential off-target side effects are needed before a clinical trial is considered (283, 285).

1.4.5 Modulating Phosphorylation of the N17 Domain as a Therapeutic Strategy

The variety of cell processes in which huntingtin is involved requires strict regulation of protein levels and localization. A common means of protein regulation is via PTMs, and, indeed, there is a large body of evidence that huntingtin is modified in a variety of manners, including: SUMOylation, ubiquitination, phosphorylation, acetylation, palmitoylation, and proteolysis (286). Of these modifications, the best characterized, and arguably most critical, with obvious effects on huntingtin function and mutant huntingtin toxicity, is phosphorylation (71, 129, 287). Mutant huntingtin has been shown to be hypo-phosphorylated at several residues, including S13, S16, and S421 (71, 134). Moreover, increasing phosphorylation of these residues through phospho-mimetics or exogenous compounds restores several known functions of the mutant huntingtin protein that are impaired by polyglutamine expansion (72, 77, 128, 129, 288). In the case of S13 and S16, increased phosphorylation of these domains restores conformational flexibility of huntingtin exon1, mediates proper protein degradation, and rescues HD mouse model phenotypes (72, 77, 288). Phosphorylation of S421 restores proper vesicular

trafficking of BDNF (128). Furthermore, increasing phosphorylation at this residue by administration of insulin-like growth factor-1 (IGF-1) is protective in HD cells models (128, 129, 134). In all cases, increased phosphorylation promotes an overall protective effect in cell and/or animal models of disease and suggests an important role for phosphorylation in mitigating mutant huntingtin-related toxicity. These data show that targeting post-translational modifications of huntingtin may be another promising therapeutic strategy, one that does not pose the same potential risks that huntingtin-lowering strategies do.

1.5 Thesis Rationale

The effects of phosphorylation of S13 and S16 in the N17 domain have been well established by our own lab and others, finding that modification of these residues is critical for modulating huntingtin localization, function, and toxicity (71, 72, 74, 287). Although the protective effects of phosphorylation of mutant huntingtin N17 have been well studied, there has been little progress in development of disease-modifying therapies targeting this domain. As such, the purpose of my project was to establish that modulating phosphorylation of the N17 domain is a valid therapeutic target, characterize the pathways involved in phosphorylation, and, finally, to identify molecules with the potential to modify this domain.

In Chapter 2, I describe the use of high content screening to identify modulators of N17 phosphorylation as well as a follow-up investigation of one of those hits, N6-furfuryladenine (N6FFA). I also describe a potential mechanism of action for this compound, specifically, upregulation of the activity of casein kinase 2 (CK2) on N17, and, finally, the protective effects of N6FFA against mutant huntingtin-induced toxicity are validated in a mouse model of HD. In Chapter 3, I provide preliminary evidence of another kinase that may be responsible for phosphorylating N17, priming it for phosphorylation by CK2, and, in Chapter 4, I show data from additional experiments that provide further insight into the effects of N6FFA. Finally, in Chapter 5, the biological and

therapeutic implications of the presented data will be discussed in the context of HD and other neurodegenerative diseases.

CHAPTER 2

N6-FURFURYLADENINE IS PROTECTIVE IN HUNTINGTON'S DISEASE MODELS BY SIGNALING HUNTINGTIN PHOSPHORYLATION

The contents of this chapter are a representation of the following publication:

Bowie LE, Maiuri T, Alpaugh M, Gabriel M, Arbez N, Galleguillos D, Hung CLK, Patel S, Xia J, Hertz NT, Ross CA, Litchfield DW, Sipione S, Truant R (2018)
N6-Furfuryladenine is protective in Huntington's disease models by signaling huntingtin phosphorylation. Proceedings of the National Academy of Science. 115(30):E7081-E7090

Most experiments and writing were done by the author, L.E. Bowie.

Images presented in Figure 4 were the work of T. Maiuri.

Mouse dosing and characterization were by M. Alpaugh and D. Galleguillos.

Cortical neuron assays were conducted by N. Arbez.

Kinase assays were conducted with the assistance of M. Gabriel

The work presented in this chapter has led to a new hypothesis regarding the role of huntingtin as a DNA damage response protein. In addition, it has led to identification of a new lead compound for the treatment of HD, the derivatives of which are currently being investigated in conjunction with an industry partner. Finally, this study laid a platform for small molecule investigation in HD using high content analysis that is currently being used in our lab.

2.1 Abstract

The huntingtin N17 domain is a modulator of mutant huntingtin toxicity and is hypo-phosphorylated in Huntington's disease (HD). We conducted high content analysis to find compounds that could restore N17 phosphorylation. One lead compound from this screen was N6-furfuryladenine (N6FFA). N6FFA was protective in HD model neurons, and N6FFA treatment of an HD mouse model corrects HD phenotypes and eliminates cortical mutant huntingtin inclusions. We show that N6FFA restores N17 phosphorylation levels by being salvaged to triphosphate form by adenine phosphoribosyltransferase (APRT) and used as a phosphate donor by casein kinase 2 (CK2). N6FFA is a naturally occurring product of oxidative DNA damage. Phosphorylated huntingtin functionally re-distributes and colocalizes with CK2, APRT, and N6FFA DNA adducts at sites of induced DNA damage. We present a model in which this natural product compound is salvaged to provide a triphosphate substrate to signal huntingtin phosphorylation via CK2 during low ATP stress under conditions of DNA damage, with protective effects in HD model systems.

2.2 Introduction

Huntington's disease (HD) is a dominantly-inherited neurodegenerative disorder characterized by late age-onset loss of cognition, emotional disorder, and loss of motor control. The disease is caused by a CAG expansion within the first exon of the *HTT* gene, which translates to a polyglutamine expansion in the huntingtin protein (41). Although CAG expansion length is correlated with age of disease onset, individuals with the same number of CAG repeats may vary in their disease onset by forty years or more (289). Genome-wide association studies (GWAS) performed on large cohorts of HD patients to identify genetic modifiers of disease onset highlighted DNA repair pathways, redox control proteins, and mitochondrial energy metabolism as the major modifiers of the onset of HD (290, 291). We have since defined huntingtin as a component of the ataxia telangiectasia mutated (ATM) DNA damage response complex that accumulates at sites of DNA oxidative damage, and as a scaffold for DNA repair factors (292). Along with these newly defined functions, huntingtin has also previously been implicated in vesicular and axonal trafficking, cell division, synaptic transmission, and the cell stress response (99, 106, 142, 293–295). Reflecting this variety of functions, the huntingtin protein localizes to several subcellular compartments. Localization is largely regulated by the first 17 amino acids of the protein, the N17 domain, which is phosphorylated at two key residues: serines S13 and S16 (296, 297).

The N17 domain, directly adjacent to the polyglutamine tract, forms an amphipathic alpha-helix that reversibly tethers huntingtin to membranes (298, 299), regulating intracellular localization between vesicles, the ER, the primary cilium, and the nucleus (300). Huntingtin nuclear localization is primarily affected by cell stress (301), and the N17 domain is a ROS sensor, whereby sulfoxidation of the methionine M8 residue promotes release of huntingtin from membranes, S13/S16 phosphorylation, and translocation to the nucleus (295). Deletion of the N17 domain accelerates disease in mouse and zebrafish models of HD (302, 303), implicating the domain in disease progression. In HD mouse models, serine phospho-mimetics (296) or induced serine phosphorylation (304) can prevent, or fully reverse, the toxicity of mutant huntingtin, defining restoration of N17 phosphorylation as a valid sub-target for HD therapeutic development.

We therefore set out to identify compounds that could modulate N17 phosphorylation in an attempt to restore the phosphorylation of N17 seen in HD cells (297, 305). Using an extensively validated antibody against phosphorylated S13 and S16 (297), we conducted a high content screen for the effects of diverse small molecule natural products on N17 phosphorylation. In order to minimize investigator bias, we used both blind, automated microscopy image acquisition and non-supervised machine sorting of the images. We identified a number of compounds with known activities in the context of HD, as well as one unique compound, N6-furfuryladenine (N6FFA), also known as kinetin.

N6FFA has been extensively studied (306) and annotated as a plant cytokine with biological effects in mammalian cells, including protection against oxidative stress (307), and delay of age-related phenotypes in human fibroblasts (308). N6FFA is also a product of DNA oxidation by ROS (309), and occurs as a normal excreted human metabolite (310). N6FFA/kinetin was found to be the precursor to N6FFA/kinetin triphosphate (KTP), an ATP analog produced upon salvaging of N6FFA by adenine phosphoribosyltransferase (APRT) (311). This nucleotide salvaging is important in the context of HD, where ATP levels are significantly reduced (214), particularly in neurons which rely heavily on nucleotide salvage as opposed to *de novo* nucleotide biosynthetic pathways (312, 313). Further, ATP production can halt during DNA damage repair (314), and free ATP levels drop significantly during ER stress response (294). Here, we show casein kinase 2 (CK2) can use KTP to phosphorylate N17, and that treatment with the N6FFA precursor molecule is protective in cell neuronal and animal models of HD.

We propose a model in which this natural product, upon being salvaged, potentiates the enzymatic phosphorylation reaction on polyglutamine-expanded huntingtin, allowing proper mutant protein degradation (315). *In vivo* administration of N6FFA, a blood-brain barrier (BBB) permeable molecule (316), in HD model mice resulted in reduced cortical brain inclusions in YAC128 mice, as well as HD phenotypic reversal.

2.3 Results

High content analysis identifies N6-furfuryladenine as a modulator of N17 phosphorylation

Phosphorylation of huntingtin N17 at S13 and S16 has been shown to be a beneficial modification in the context of HD in both cell and animal models (296, 304). To identify modulators of N17 phosphorylation of huntingtin, we used high content analysis to screen a library of 133 natural compounds (Selleckchem) for their potential effects on the fluorescent signal pattern of anti-N17-S13pS16p, an antibody recognizing N17 phosphorylated on S13 and S16. This antibody was raised to the phospho-S13/phospho-S16 epitope and cross purified by peptide affinity chromatography both to the phospho-peptide and against the unmodified peptide. Specificity and selectivity of this antibody was validated by: peptide dot blot titrations; western blots to whole cell extracts of wild-type, heterozygous, and homozygous mutant huntingtin cells; immunofluorescence with peptide competition; and lack of signal in huntingtin knockout mouse embryo fibroblasts by western blot (297). Huntingtin recruitment to DNA damage adducts, which was visualized by multiple independent huntingtin monoclonal antibodies, was also demonstrated using this antibody (292). The antibody was also used to define the phospho-dependent switch in huntingtin conformation (317), the increased phosphorylation of huntingtin by ganglioside GM1 treatment of mice (304), and the role of methionine M8 sulfoxidation as a precursor to N17 phosphorylation (295).

The anti-N17-S13pS16p antibody was directly labelled, and direct immunofluorescence was performed on *STHdh^{Q7/Q7}* cells (318) treated with a library of 133 compounds. Images were taken in an unbiased manner with a 40X objective at 5 software-randomized locations per well, with hardware autofocus. There was no investigator observation beyond the first well to set exposure levels to within the camera dynamic range.

The 12-bit depth images were analyzed by Phenoripper software (319) in a single channel, by assaying image textures. These are a set of pixel level and space metrics calculated in image processing, designed to quantify the perceived texture of an image. Phenoripper measures multiple bitmap texture elements in each image, defines the three most variant textures, and uses these three variances to plot a vector in unitless 3D space such that the points farthest from one another represent the most dissimilar images within that dataset, without any predetermined parameters. The plot is generated by principal component analysis (PCA) within the dataset, thus has no units on the axes. Hits were chosen based on which compounds plotted furthest from the vehicle control, 0.01% DMSO (**Figure 2.1a**). A summary of these of hits, shown in **Supplemental Figure 2.1a**, includes several anti-inflammatory, antioxidant and apoptosis-inducing compounds, as well as several compounds that did not fall into any specific category (summarized in **Figure 2.1b**).

Antioxidant compounds plotted distinctly from vehicle control, consistent with our previous study which defined methionine M8 sulfoxidation as a trigger of S13/S16

phosphorylation by affecting N17 helicity (295). Another distinct group of compounds was annotated as anti-inflammatories. This is consistent with our results from another previous study implicating the IKK β pathway in regulating huntingtin phosphorylation (297), which has been previously defined by Thompson *et al.*, as the trigger for huntingtin degradation (320). One of the most distant hit compounds from the control that did not plot near any anti-inflammatories nor antioxidants, had the most effect in the system: N6-furfuryladenine (N6FFA) (**Figure 2.1c**). N6FFA is a blood-brain barrier-permeable compound (321, 322) with a potent effect on phospho-N17 signal. We therefore pursued N6FFA for further investigation.

N6-furfuryladenine increases phosphorylation of N17 in cells expressing mutant huntingtin and is protective in cell models of HD

To further understand the effects of N6FFA, we directly examined the phosphorylation state of N17 by immunoblot in mouse striatal-derived cells expressing either wild-type or humanized mutant huntingtin: *STHdh*^{Q7/Q7} and *STHdh*^{Q111/Q111}, respectively (318) with increasing doses. In wild-type cells treated with N6FFA, we observed a modest increase in N17 phosphorylation that did not reach significance (**Figure 2.1d**). This modest increase was amplified by the more sensitive immunofluorescence technique used in the initial screen, accounting for the identification of N6FFA as a hit. In contrast, when we tested the effect of N6FFA on HD knock-in homozygote model cells expressing expanded huntingtin (*STHdh*^{Q111/Q111}), we observed a

robust and statistically significant increase in N17 phosphorylation (**Figure 2.1e**).

Optimal treatment concentration was between 0.5 - 1 μM for a time of 24 hours. These results validated N6FFA as a hit from the high content analysis screen and a modulator of N17 phosphorylation.

As phosphorylation of mutant huntingtin is a protective modification (304, 323), we next asked whether N6FFA affected cell viability. We found that N6FFA was protective in *STHdh*^{Q111/Q111} cells against serum starvation-induced stress, with a significant reduction in Annexin V staining noted at a concentration of 10 μM as shown in **Supplementary Figure 2.1b**. This effect was not seen in *STHdh*^{Q7/Q7}. Previous studies have reported substantially different thresholds for N6FFA cytotoxicity, with some groups reporting decreased cell viability at doses as low as 500 nM (324), while others seeing decrease in viability at doses as high as 100 μM (325). As this difference in N6FFA toxicity threshold may be due to cell type differences, we sought to test the protective effects of this compound against mutant huntingtin-induced toxicity in a more disease-relevant cell type: mouse primary cortical neurons. We transfected mouse embryonic cortical neurons with a fragment of huntingtin (amino acids 1-586) containing either a wild-type polyglutamine length of 22 aa (N586-HttQ22) or mutant polyglutamine length of 82 aa (N586-HttQ82) to assay apoptotic cell death (326), and treated these cells with increasing concentrations of N6FFA. There was a significant protective effect in cells expressing polyglutamine expanded huntingtin at 1 μM and 10 μM N6FFA (**Figure 2.1f**), consistent with the dose-response curves assaying mutant huntingtin

phosphorylation in mouse striatal-derived cells (**Figure 2.1e**). We saw no significant effect of N6FFA in the neurons expressing wild-type huntingtin at any of the concentrations tested (**Figure 2.1f**).

Thus, we have identified N6FFA as a compound that affects N17 phosphorylation and promotes cell viability in a dose-dependent manner, in mutant huntingtin-expressing cells.

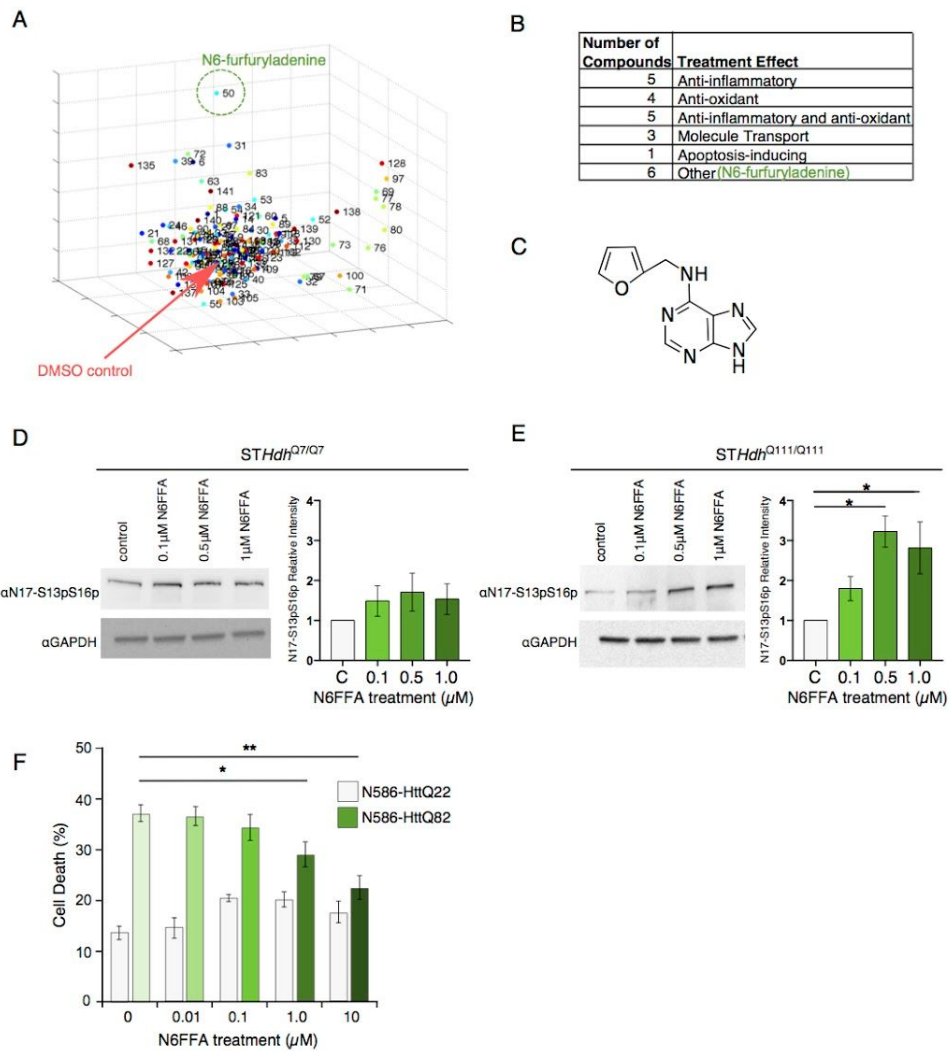


Figure 2.1. Identification and validation of N6-furfuryladenine as a modulator of N17 phosphorylation. Cells were methanol fixed and stained with a primary conjugate antibody recognizing N17 with phospho-groups at S13 and

S16 (N17-S13pS16p). Five images were taken per well with a 40x air objective. Images were analyzed by open source software, Phenoripper. Unitless PCA plot and a summary of hits are presented in (A) and (B), respectively. Compound 134, indicated with a red arrow represents vehicle control; compound 50, encircled in green, represents N6FFA. (C) Chemical structure of N6FFA. STHdhQ7/Q7 (D) and STHdhQ111/Q111 (E) cells were treated with the indicated concentrations of N6FFA for 24 h and total cell lysates were separated by SDS-PAGE followed by immunoblotting with N17-S13pS16p antibody. Pixel intensity results from n=3 independent replicates were quantified. Asterisks (*) indicate concentrations of N6FFA that significantly increased N17 phosphorylation compared to control as determined by AVOVA with multiple comparisons test. Bars represent mean values \pm SEM (* p <0.05). (F) Mouse cortical neurons were transfected with N586-HttQ22 or N586-HttQ82 and treated with various concentrations of N6FFA. A nuclear condensation assay was performed to determine percent cell death. Concentrations of N6FFA that significantly decreased cell death are indicated as determined by unpaired two-tailed t-test from n=3 independent replicates (* p <0.05; ** p <0.001).

N6FFA treatment reduces cortical mutant huntingtin inclusions and improves phenotypes in an HD mouse model

Having determined that N6FFA was protective in an HD neuronal model, we next tested the effect of N6FFA on the motor phenotypes of the YAC128 HD mouse model (327). This is a transgenic mouse model in which a full-length copy of human huntingtin bearing 128 CAG repeats is expressed on a yeast artificial chromosome (YAC). Mice were injected with N6FFA intraperitoneally (IP) daily at approximately 8 months of age. As this modality is highly stressful, with mice being handled and receiving painful injections regularly, all mice lost body weight during the course of the treatment (**Supplemental Figure 2.2a**). Motor tests, but not anxiety tests, were therefore pursued in this experiment. While YAC128 mice performed significantly worse than wild-type littermates on both the accelerating and fixed rotarod motor coordination assays as determined by two-way ANOVA, YAC128 mice that received an IP injection of N6FFA exhibited increased latency to fall for both tests (**Figures 2.2a and 2.2b**). (Accelerating rotarod: effect of genotype, $F_{1,26}=11.86$, $p=0.002$; effect of treatment, $F_{2,26}=4.974$,

$p=0.015$. Fixed rotarod: effect of genotype, $F_{1,26}=5.542$, $p=0.026$; effect of treatment, $F_{2,26}=11.94$, $p=0.0002$). The motor behavior of YAC128 mice, as measured by the narrow beam test, was also improved with N6FFA treatment (**Figure 2.2c**). There was also some improvement in motor phenotypes in wild-type control mice upon N6FFA dosing. This is consistent with effects of N6FFA on wild-type huntingtin phosphorylation (**Figure 2.1c**), and with the primary screen assaying wild-type huntingtin (**Figure 2.1a**).

To observe the effects of N6FFA in a modality that was less stressful, allowing acquisition of more reliable data related to anxiety-like behaviour, as well as being more amenable to patient treatment, we dosed the animals orally at approximately 9 months of age with N6FFA added to chow for 49 days. At this lower dose and oral modality, no motor-correction effects were noted. We then assessed the effect of N6FFA oral dosing on YAC128 anxiety phenotypes, given that this modality did not affect a pain stress on the mice. While YAC128 mice spent more time in the closed arms of the elevated plus maze than wild-type mice (effect of genotype, $F_{1,30}=5.670$, $p=0.02$), indicating increased anxiety, N6FFA treatment did not correct this behaviour (**Figure 2.2d**). On the other hand, N6FFA decreased anxiety behavior and restored exploratory activity in the first 5 minutes of the open field arena test (**Figure 2.2e**) (effect of treatment, $F_{1,33}=11.26$, $p=0.002$). We next measured fecal boli dropped in conditions that elicit anxiety. In the forced swim test, YAC128 mice released more fecal pellets compared to wild-type littermates, an indication of increased anxiety, which was reversed by administration of N6FFA (**Figure 2.2f**) (effect of genotype, $F_{1,34}=5.773$, $p=0.02$; effect of treatment,

$F_{1,34}=3.896, p=0.05$). In summary, N6FFA improved YAC128 motor phenotypes by intraperitoneal administration, and anxiety-like phenotypes by oral administration.

We next asked whether the effect of N6FFA on YAC128 phenotypes is due to a direct effect on the huntingtin protein. We measured the levels of insoluble mutant huntingtin inclusions in the brains of control-treated and N6FFA-treated YAC128 mice. As shown in **Figure 2.2g**, the levels of insoluble mutant huntingtin protein were dramatically decreased upon N6FFA treatment in the cortex, but not in the striatum (**Figure 2.2h**). While we hypothesize that this difference may be due to incomplete delivery of N6FFA to the striatum, with most of the compound metabolized in the cortex, as directed by cerebrospinal fluid flow, we have not investigated this phenomenon further. We also investigated levels of insoluble mutant huntingtin in the striatum and cortex of the mice who received IP injections of N6FFA. In the cortex, we again see significantly decreased levels of insoluble huntingtin, and in the striatum, while there is a trend towards decreased levels of insoluble mutant huntingtin, this trend did not reach significance (**Supplementary Figure 2.2b and 2.2c**). Thus, we observed protective effects of N6FFA in HD cell and mouse models, with direct effects on huntingtin protein levels.

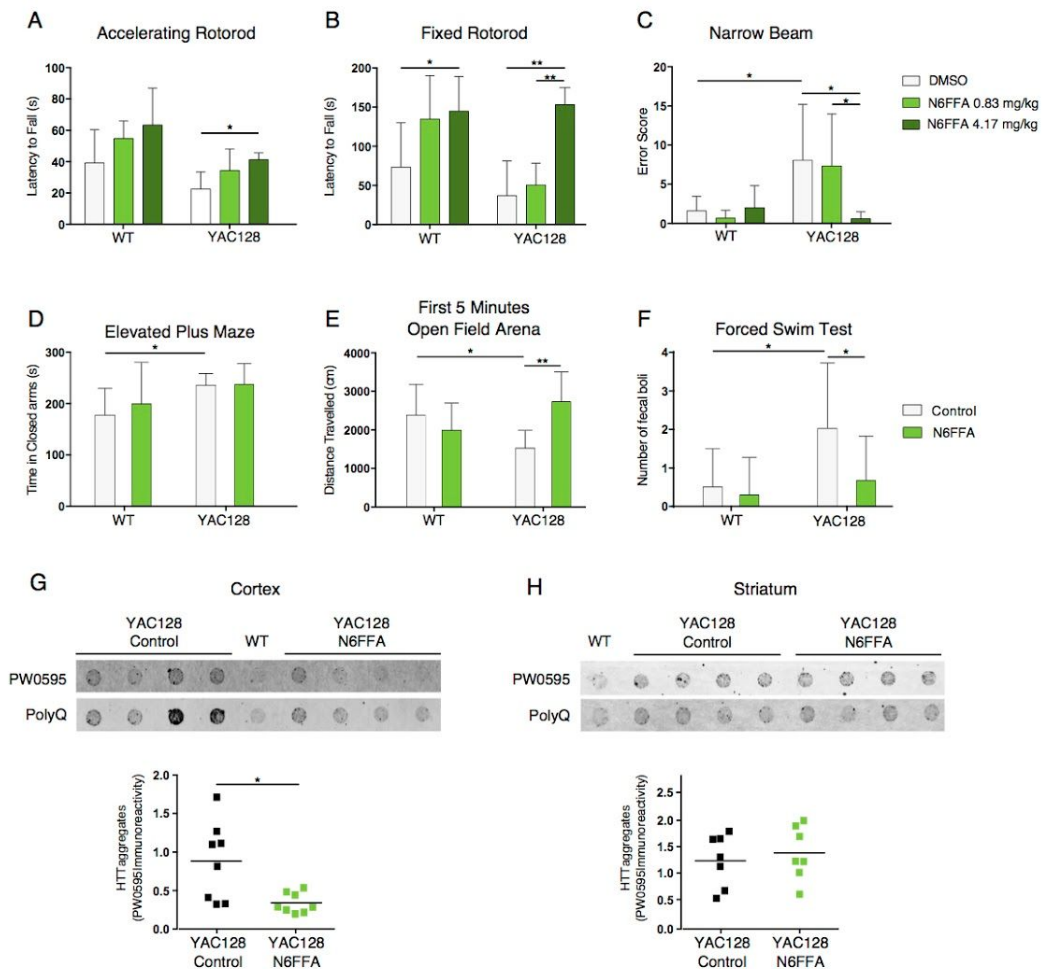


Figure 2.2. Effects of N6FFA administration on motor performance, anxiety-like behaviour, and huntingtin inclusions in YAC128 mice. (A) Mice were tested on accelerating rotarod (4-40 RPM in 2 min) after 42 days daily intraperitoneal injection (IP) N6FFA or vehicle (1.5% DMSO). (B) Mice were tested on fixed rotarod (12 RPM) after 42 days IP N6FFA or vehicle. For (A) and (B) N = 7 for WT DMSO, and N = 5 for WT N6FFA (0.83 mg/kg and 4.17 mg/kg), YAC128 DMSO, and YAC128 N6FFA (0.83 mg/kg and 4.17 mg/kg). (C) Mice were tested in the narrow beam test. N = 6 for WT DMSO, WT N6FFA 4.17 mg/kg, and YAC128 N6FFA 4.17 mg/kg; N = 5 for WT N6FFA 0.83 mg/kg, YAC128 DMSO, and YAC128 N6FFA 0.83 mg/kg. (D) Time in the closed arms of the elevated plus maze was tested. N = 10 for WT control, 10 for WT N6FFA, 7 for YAC128 control, and 7 for YAC128 N6FFA. (E) Exploratory activity in the first 5 min spent in an open field arena is shown N = 10 for WT control, 10 for WT N6FFA, 8 for YAC128 control, and 9 for YAC128 N6FFA. (F) The number of fecal pellets released in the forced swim test was measured. N = 10 for WT control, 10 for WT N6FFA, 9 for YAC128 control, and 9 for YAC128 N6FFA. SDS-insoluble aggregates of mutant huntingtin were measured in YAC128 cortex (G), or striatum (H), after treatment with control or N6FFA-containing diet (N=8 YAC128 control, 7-9 YAC128 N6FFA). Representative membranes and pixel intensity analysis are shown (*p<0.05). Statistical analysis was performed using two-way ANOVA and Bonferonni post-test for mouse performance, and by the Student's t-test for insoluble mutant huntingtin data. For all figures, bars represent mean \pm SEM.

The metabolic product of N6FFA/kinetin, kinetin triphosphate, can be used as a phospho-donor by CK2 to phosphorylate N17

We next evaluated possible mechanisms of N6FFA action. Cells can metabolize exogenously applied N6FFA/kinetin to kinetin triphosphate (KTP) by means of the nucleotide salvaging enzyme, adenine phosphoribosyltransferase (APRT) (311). The resulting ATP analogue, KTP (**Supplemental Figure 2.3a**), can be used by PTEN-induced putative kinase 1 (PINK1) for the transfer of its gamma-phosphoryl group to the PINK1 substrate (311). The kinase CK2 can utilize multiple substrates as phospho-donors, including GTP and ATP (328). We have previously reported that CK2 was a putative N17 kinase, based on results of a kinase inhibitor screen with multiple CK2 inhibitors as hits (297). More precise effects were achieved by treatment with nanomolar levels of the CK2 inhibitor, DMAT (329), with inhibition of CK2 specifically decreasing phosphorylation of N17 (297). We therefore hypothesized that the mechanism by which N6FFA increases N17 phosphorylation is through its metabolism to KTP and use by CK2 as a phospho-donor for huntingtin N17.

To test whether CK2 can use KTP to phosphorylate its canonical substrates, we performed a peptide array assay comparing CK2 kinase activity with either ATP or KTP as phospho-donors. A full table of these peptides is presented in **Supplemental Figure**

2.3. As shown in **Supplemental Figure 2.3b**, CK2 phosphorylates numerous substrates to similar degrees using either ATP or KTP.

We next asked whether CK2 can directly phosphorylate the N17 domain *in vitro*. We found that CK2 can use either ATP or KTP to phosphorylate N17, provided that serine 13 is already primed by phosphorylation (**Figure 2.3a** and **2.3b**). This is consistent with the description of CK2 as a ubiquitous acidophilic kinase, where its activity is typically regulated by the substrate, and priming adds a negative charge to the site (330). To confirm that the effect we are seeing is mediated by CK2, we treated cells with N6FFA in the presence of DMAT (331). DMAT prevented N6FFA from modulating N17 phosphorylation levels (**Figure 2.3c**), consistent with previous work that defined CK2 as a N17 kinase (297). Thus, the restoration of N17 phosphorylation by N6FFA can be blocked by inhibition of CK2.

To form KTP for CK2 to utilize, N6FFA must be salvaged to the triphosphate form. To test if N6FFA salvaging to KTP is critical for the observed increase in N17 phosphorylation, we treated cells with 9-deaza-kinetin (9DK), a derivative of N6FFA that cannot be salvaged due to the lack of a nitrogen at position 9 (structures in **Figure 2.3d**). In contrast to N6FFA, 9DK did not cause an increase in huntingtin phosphorylation in *STHdh^{Q111/Q111}* cells (**Figure 2.3d**), indicating that the increase in N17 phosphorylation upon N6FFA treatment occurs through its conversion to KTP by nucleotide salvaging.

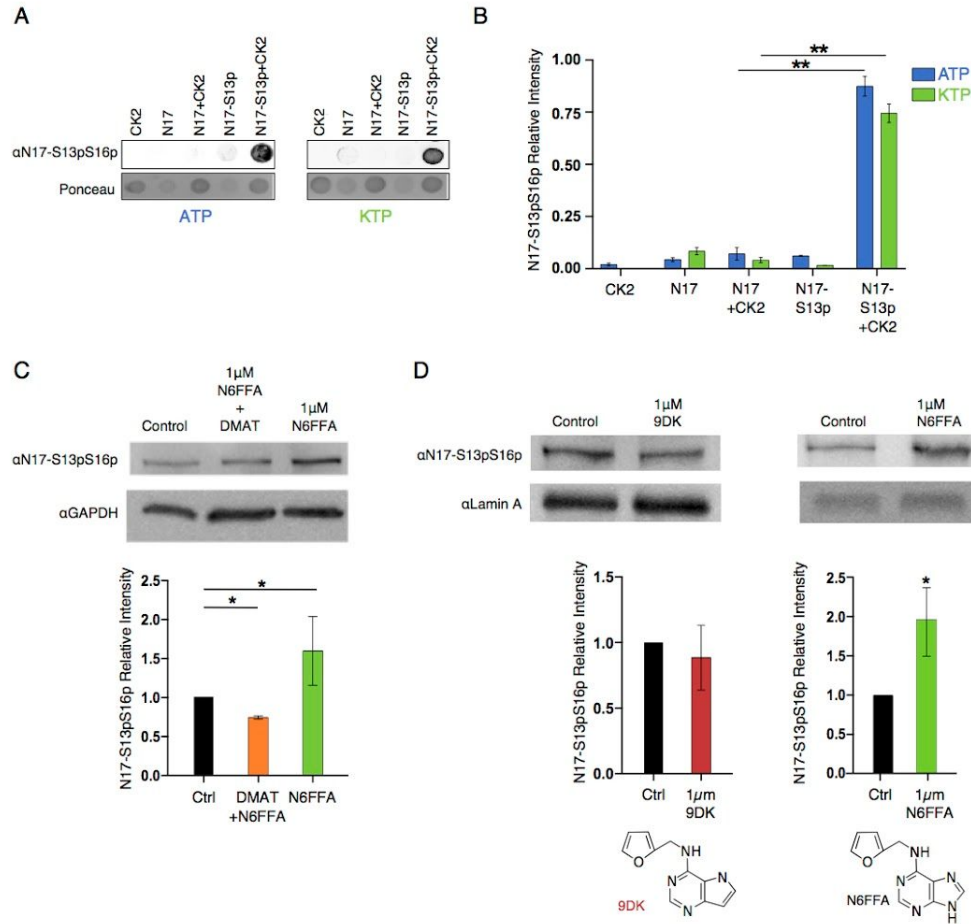


Figure 2.3. CK2 uses KTP as a phospho-donor to phosphorylate huntingtin N17 when primed by phosphorylation. Representative blot (A) and quantification (B) of an in vitro N17 phosphorylation assay using CK2 with either ATP or KTP as phospho-donor. Analysis by Mann-Whitney test (n=3 independent replicates, **p<0.001). (C) Representative blot (top) and quantification (bottom) of N17-S13pS16p levels in STHdh^{Q111/Q111} cells upon treatment with N6FFA either with or without the addition of the CK2 inhibitor DMAT (4.5 μ M). Analysis by Mann-Whitney test (n=4 independent replicates, *p<0.05). (D) Representative blot (top) and quantification (bottom) of N17-S13pS16p levels in STHdh^{Q111/Q111} cells upon treatment with N6FFA derivative 9-deaza-kinetin (9DK) (left), analysis by Mann-Whitney, and N6FFA (right), analysis by unpaired t-test (n=3 independent replicates for both experiments, *p<0.05). For all data, bars show mean \pm SEM.

Components of the N6FFA salvaging and signaling pathway functionally colocalize at sites of DNA damage

CK2 is a constitutively active kinase regulated, in part, by subcellular localization and proximity to its substrates (332). CK2 is well characterized to phosphorylate DNA repair factors (333), and we previously defined huntingtin at sites of ATM-mediated DNA repair (292). We therefore asked whether CK2 and huntingtin colocalize within the cell at both resting states and during active DNA damage repair. We have previously reported that the anti-N17-S13pS16p antibody highlights insoluble, chromatin-dependent nuclear puncta (292, 295, 297), which we recently identified as nuclear speckles (305). Using antibodies against CK2 and N17-S13pS16p, and super-resolution structured illumination microscopy (SR-SIM), we observed colocalization of these endogenous proteins at nuclear speckles (**Figure 2.4a**), suggesting that CK2 kinase activity on N17 may take place in the nucleus, similar to CK2 activity on DNA repair proteins (334), such as XRCC1 (335) or P53BP1 (336).

N6FFA is an endogenous byproduct of oxidative DNA damage, whereby addition of a furfuryl group to an adenosine base within the DNA backbone under Fenton reaction-oxidizing conditions generates N6FFA riboside (337). The generation of this adduct is followed by excision of N6FFA from the DNA backbone (338). We have shown that the huntingtin protein acts as a scaffold for DNA repair proteins in response to oxidative stress (292). The importance of this role was given context when the results of a large GWAS study revealed a high number of DNA repair genes as modifiers of age of disease onset (290). Similar to the protective effects we observed in HD model mice (**Figure 2.2**), a recent study showed neuroprotective effects of N6FFA against

radiation-induced behavioural changes in a Swiss albino mouse model (339). Together, these findings prompted us to investigate a connection between N6FFA and huntingtin in the context of DNA damage.

We first asked whether we could directly detect N6FFA riboside and the nucleotide salvaging protein, APRT, at sites of DNA damage where huntingtin is known to accumulate (292). Using a 405nm laser, we induced DNA damage in a line across chromatin. After a 20-minute incubation, endogenous CK2 and huntingtin phosphorylated at N17 were enriched at the irradiated regions of DNA damage (**Figure 2.4b**). Unlike steady state imaging at nuclear puncta, this functional relocation with colocalization was triggered by induced DNA damage. While protein colocalization alone is not definitive of interactions, the functional colocalization of these proteins supports the concept that they are functioning as part of a complex relevant to functions in DNA damage repair. Furthermore, both the oxidative DNA damage product, N6FFA riboside (**Figure 2.4c**), and the salvaging enzyme responsible for converting this product to KTP, APRT (311) (**Figure 2.4d**), concentrated at the same DNA damage sites. Thus, components of the N6FFA salvaging pathway functionally colocalize to sites of DNA damage.

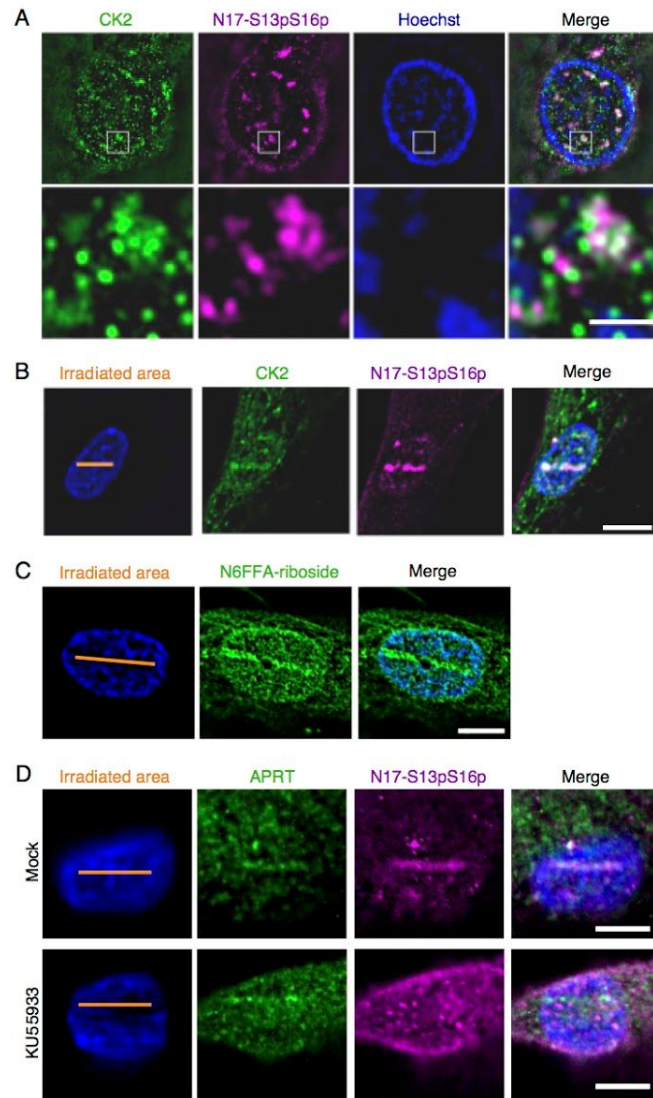


Figure 2.4. Components of the N6FFA-APRT-KTP-CK2-huntingtin pathway co-localize at sites of DNA damage. (A) Human fibroblasts were stained with anti-CK2 (green) and anti-N17-S13pS16p (magenta) and imaged using super resolution-structured illumination microscopy (SR-SIM). Bottom panel depicts magnified regions outlined by white boxes in the top panel. Scale bar is 1 μ m. (B) Human fibroblasts were irradiated with a 405 nm laser in the indicated region to induce DNA damage. After a 20-min incubation period, immunofluorescence was performed against CK2 (green) and N17-S13pS16p (magenta), and XY coordinates were revisited to image the irradiated cells by Z-stacked wide-field microscopy and deconvolution. We observed a 100% correlation between CK2 and N17-S13pS16p localization to irradiated regions in 20-30 cells per experiment for two experiments. (C) Human fibroblasts were irradiated as in (B), stained with anti-N6FFA riboside (green), and imaged by Z-stacked wide-field microscopy and deconvolution. (D) Human fibroblasts were treated with vehicle control (mock) or 10 μ M KU55933 for 25 min then irradiated as in (B), stained with anti-APRT (green) and anti-N17S13pS16p (magenta), and imaged by Z-stacked wide-field microscopy and deconvolution. Scale bar is 10 μ m in panels B-D.

We previously found that huntingtin localization to sites of DNA damage is dependent on ATM kinase activity (292). We therefore asked whether APRT recruitment is regulated in a similar fashion. As shown in **Figure 2.4d**, APRT could still localize to UV irradiation sites in the presence of ATM inhibitor KU55933 (340), under conditions that inhibit huntingtin recruitment. This suggests that recruitment of the nucleotide salvager APRT to DNA damage sites and KTP generation does not require ATM activation, and hence do not require huntingtin recruitment. CK2 is required for P53BP1 accumulation at sites of DNA damage, which is a prerequisite for efficient activation of the ATM-mediated signaling pathway (341). Huntingtin makes up part of the ATM complex and its recruitment to DNA damage is blocked by ATM kinase inhibition (292). These results allow us to hypothesize a mechanism in which KTP, produced proximal to DNA damage via APRT activity, is used by CK2 to phosphorylate substrates in the ATM DNA damage repair response, including the huntingtin N17 domain. Thus, this salvaged product of oxidative DNA damage may act as a signalling molecule to potentiate DNA repair (**Figure 2.5**), under the repair-associated conditions of low ATP “energy crisis” (342).

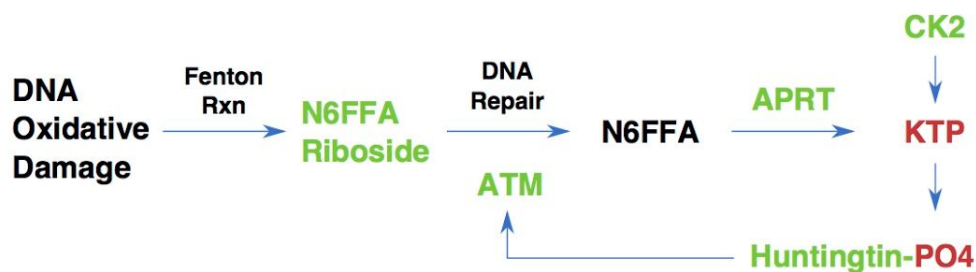


Figure 2.5. A product of oxidative DNA repair is used by CK2 to phosphorylate huntingtin at sites of DNA damage. DNA is oxidized via the Fenton reaction by age-onset reactive oxygen stress. N6-furfuryladenine riboside

results, and is excised by the DNA damage repair machinery. APRT salvages the excision product, N6-furfuryladenine, to yield kinetin triphosphate (KTP). KTP is used as a phosphate donor by CK2 to modify huntingtin N17, and potentially other DNA repair proteins, in a positive feedback mechanism. We hypothesize that exogenous administration of N6FFA potentiates the reaction. All components of the model seen to functionally co-localize proximal to DNA damage regions are highlighted in green.

2.4 Discussion

Many current drug discovery efforts are limited to high throughput analysis with low-resolution endpoints (343). As an alternative, we used high content analysis to screen a small natural compounds library encompassing a wide breadth of biologically active chemical space to define modulators of N17 phosphorylation. We show that high content analysis of endogenous, phosphorylated huntingtin is extremely effective for identifying potential disease-modifying compounds. The use of principal component analysis (PCA) and image textures allowed us to visualize the degree to which compounds affected N17-S13pS16p signal properties without bias, in that we did not predefine any parameters for sorting. We found that the two predominant types of compounds affecting our assay were anti-inflammatory agents and antioxidants. Consistent with this, we and others have previously shown that inhibition of IKK β within the NF-kB inflammation pathway affects huntingtin phosphorylation (297, 344).

The identification of antioxidants as modulators of N17 phosphorylation is also compelling, given the implication of ROS in HD pathology (345). The antioxidant XJB-5-131 is known to modify toxicity in an HD model, by either preventing onset, or improving pathophysiology in a mouse that has developed disease (346). Our group has recently shown that huntingtin acts as a ROS sensor, elucidating a mechanism by which

sulfoxidation of methionine eight within N17 leads to increased huntingtin solubility from lipid membranes of the endoplasmic reticulum, enhancing S13/S16 phosphorylation and translocation of huntingtin to the nucleus (295). The identification of several antioxidant compounds in our screen supports these findings, as these compounds reduced the phospho-N17 signal. In the context of ROS, increased N17 phosphorylation upon IKK β inhibition may be due to prevention of the NF- κ B pathway ROS signaling response and the resulting elevated intracellular ROS levels (347).

N6FFA compound was selected for further experimentation as it has been demonstrated in animal models to be both blood-brain barrier permeable (348) and neuroprotective (339). We show a protective effect of N6FFA in a cell line expressing a severe toxic mutant huntingtin fragment in cortical neuronal culture. This is consistent with other studies showing protective effects of N6FFA under conditions of stress (324, 339, 349–351). N6FFA has been broadly categorized as an antioxidant (352); however, we note N6FFA increasing huntingtin phosphorylation, whereas antioxidants decrease phosphorylation (295). More recent studies have shown that N6FFA is not effective at scavenging free radicals (349), but instead activates other antioxidant defense mechanisms (324, 325, 349, 350). Our results support an alternative mechanism in which huntingtin is directly modified by N6FFA.

We observed reduced cortical mutant huntingtin aggregate load upon N6FFA treatment in YAC128 mice. Previous findings have shown that mutant huntingtin is not properly degraded, leading to toxic accumulation (104). Studies have shown that

phosphorylation of huntingtin mediates clearance (353–355), and that mutant huntingtin is hypo-phosphorylated at many sites of proteolytic activity (356). Huntingtin N17 phosphorylation enhances protein clearance by the proteasome and lysosome (357). Our results are consistent with increased mutant huntingtin phosphorylation, via administration of N6FFA, mediating protein clearance. With the efficacy of N6FFA established, we next sought to determine the mechanism.

The report that the metabolic product of N6FFA, KTP, is an ATP analog that can be utilized by PINK1 as a phospho-donor (311), prompted us to investigate a similar mechanism for CK2, which we previously identified as a regulator of N17 phosphorylation (297). CK2 exhibits unusual catalytic site flexibility and is one of the few known kinases that can use both ATP and GTP as phosphate donors (358). We found that CK2 can also use KTP to phosphorylate its substrates, including N17. Furthermore, N17 phosphorylation was not achieved with an N6FFA derivative that could not be metabolized by nucleotide salvagers, nor in the presence of a CK2 inhibitor, implicating nucleotide salvaging activity and CK2 activity as crucial elements of the N6FFA effect. As KTP is also used by PINK1 to regulate mitochondrial proteostasis, and enhanced mitochondrial proteostasis is protective against beta amyloid proteotoxicity (359), some pleiotropy of KTP-mediated signaling could be beneficial beyond just phospho-huntingtin correction.

We found that CK2 colocalizes with N17-phosphorylated huntingtin at nuclear speckles. CK2 is a ubiquitous kinase known to modify proteins involved in DNA repair

(360, 361), and huntingtin is part of the ATM oxidative DNA damage response complex (292). The influence of DNA repair pathways on HD disease onset, revealed by GWAS (185, 290, 291), suggests that ROS and DNA damage repair are critical modifiers for HD age of onset. CK2 may be phosphorylating huntingtin N17 at these nuclear puncta in response to oxidative DNA damage. This is similar to the way CK2 phosphorylates the deubiquitinating enzyme OTUB1, mediating its nuclear entry, and the formation of P53BP1 DNA repair foci (362).

N6FFA riboside is a known product of oxidative DNA damage via the Fenton reaction, causing perturbation of DNA structure (338, 363). Upon induction of DNA damage via 405 nm laser, we detected N6FFA riboside generated within the DNA. We propose that following excision from the DNA, N6FFA is salvaged to KTP via the same mechanism proposed by Hertz *et al.* (311). The accumulation of huntingtin, CK2, N6FFA, and the nucleotide salvager APRT at DNA damage sites suggests that the effective local concentration of these pathway factors, in proximity to DNA damage, facilitates phosphorylation of N17.

In HD, KTP-mediated signaling immediately proximal to DNA damage may be important in the context of low ATP. Aging cells demonstrate significantly decreased ATP levels (364), a condition that is exacerbated in HD (214, 365). The role of huntingtin as a stress response protein (161, 295, 297) also suggests that a signaling pathway utilizing an alternate source of phosphates may be critical under stress conditions, where most ATP is utilized at the ER lumen for the unfolded protein response (UPR) (366),

which is chronically active in HD (367). The energy deficits seen classically in HD may also be the result of chronic DNA damage repair, triggered by age-onset ROS stress: the first step of DNA single strand break (SSB) damage repair is identification of the lesion by the Poly (ADP-ribose) polymerase proteins, or PARPs. PARP hyperactivation during DNA damage can result in a cellular energy crisis in which polyADP-ribose inhibits ATP production (368). Finally, salvaged purines may be the only potential source of triphosphate in proximity to DNA damage complexes. Neurons rely heavily on salvaging of nucleotides rather than *de novo* synthesis (312, 369), and a recent GWAS identified RRM2B/P53R2, a ribonucleotide salvaging enzyme, as a modifier of HD age of onset. This highlights a potential important role of salvage pathways in HD (290).

The large number of neurodegenerative disorders for which a DNA repair protein is defective, suggests DNA repair may be a critical node for neuronal health, particularly at the ATM complex (370). Given the role of huntingtin as a scaffold for the ATM complex (292), dominant mutant huntingtin effects coupled with age-related ROS increase could lead to the age-onset accumulation of DNA damage. As mutant huntingtin is hypo-phosphorylated at the N17 domain (297, 305) and phosphorylation is beneficial in HD models (296, 304), the effects we observed with N6FFA treatment connect DNA damage repair, altered bioenergetics, and mutant huntingtin phosphorylation and inclusion load.

2.5 Materials and Methods

Reagents and antibodies

All reagents were from Sigma-Aldrich unless otherwise stated. Polyclonal antibody against huntingtin phosphorylated at S13 and S16 of the N17 domain (anti-N17-S13pS16p) was previously characterized and validated (297). To directly conjugate the anti-N17-S13pS16p antibody to Alexa Fluor 488 succinimidyl ester dye (Molecular Probes/Life Technologies), 1 μ L dye per 10 μ L antibody and 5% NaHCO₃ was incubated overnight at 4°C with rotation. The conjugate antibody was then run through a Sephadex G-25 bead (Amersham Pharmacia Biotech AB) column and collected by elution with PBS until the visible dye front reached the base of the column. Additional antibodies used in this study: anti-N17-S13pS16p (New England Peptides), anti-CK2 alpha (Abcam), anti-N6FFA/kinetin riboside (Agrisera) for immunofluorescence. For westerns: anti-thiophosphate ester (Abcam), anti-GAPDH (Abcam), rabbit anti-huntingtin (PW0595, Enzo Life Sciences), mouse anti-polyglutamine (mAB1574, Chand mouse anti-huntingtin). Secondary antibodies against rabbit, mouse, and goat IgG, conjugated to Alexa Fluor 488, 555, 594, or Cy5, were from Invitrogen. Secondary HRP conjugates were from Abcam. Goat anti-rabbit IRDye 800CW, goat anti-rabbit IRDye 680CW and goat anti-mouse IRDye 800 were from Li-COR Biosciences.

Cells

Cells derived from mouse striatum, *STHdh*^{Q7/Q7} and *STHdh*^{Q111/Q111} (a kind gift from M.E. MacDonald, Center for Genomic Medicine, Massachusetts General Hospital), were grown in Dulbecco's modified Eagle's medium (DMEM) with 10% fetal bovine serum (FBS) at 33°C in a 5% CO₂ incubator. Human hTERT-immortalized foreskin fibroblast BJ-5ta cells (ATCC) and primary human fibroblasts from Coriell Institute for Medical Research Biorepositories (ND30014 wild-type fibroblasts bearing 21/18 CAG repeats in *HTT* gene alleles) were grown in minimal essential medium (MEM) with 15% FBS and 1% Glutamax at 37°C with 5% CO₂. All media and supplements were from Gibco Life Technologies. Primary cortical primary neurons were prepared from CD1 mice as described (326). In brief, cortices of E15 DC1 embryos are dissected, quickly dissociated and plated at 1.10⁵ cells/mm². Cells were kept in Neurobasal medium supplemented with B27 and 2 mM GlutaMAX (GIBCO) in 5% CO₂ at 37°C throughout the experiment.

High content screen and analysis

STHdh^{Q7/Q7} cells were seeded into 96-well ibiTreat dishes (Ibidi) and grown for 24 hours before treatment with a 133-compound natural compound library (Selleckchem) for 6 h at 33°C. Immunofluorescence was performed as described below with Alexa Fluor 488-conjugated anti-N17-S13pS16p antibody at 1:15 dilution. Images taken with 40X objective were analyzed using Phenoripper (319) in which 5 images per well were thresholded by random sampling and analysis was carried out using a block size of 15.

Hits were scored by selecting points on the resulting PCA plot lying furthest from controls where they fell outside of an arbitrarily defined radius.

Compound administration to cells

All compounds were administered in DMEM with 0.2% FBS for 24 hours unless otherwise indicated.

Protein extraction and immunoblotting

Cells were lysed in either NP-40 lysis buffer (50 mM Tris-HCl pH 8.0, 150 mM NaCl, 1% NP-40) or RIPA lysis buffer (50 mM Tris-HCl pH 8.0, 150 mM NaCl, 1% NP-40, 0.25% sodium deoxycholate, 1 mM ethylenediaminetetraacetic acid (EDTA)) containing protease and phosphatase inhibitors (Roche). Lysates were centrifuged at 17000 x g for 12 min and the supernatant was collected for immunoblot analysis. Equal amounts of protein were separated by SDS-PAGE on pre-cast 4-20% polyacrylamide gradient gels (Biorad) and electroblotted onto Immobilon polyvinylidene difluoride (PVDF) membrane (EMD Millipore). Membranes were blocked in TBS-T (50 mM Tris-HCl, pH 7.5, 150 mM NaCl, 0.1% Tween-20) containing 5% non-fat dry milk for 1.5 h at room temperature, followed by overnight incubation with primary antibodies diluted in blocking buffer at 4°C (anti-N17-S13pS16p 1:2500; anti-GAPDH 1:7500). After 3x 15-min TBS-T washes, membranes were incubated with HRP-conjugated secondary antibodies diluted in blocking buffer (1:50000) for 45 min at room temperature, and

visualized using Immobilon enhanced chemiluminescence HRP substrate (EMD Millipore) on a MicroChemi system (DNR Bio-imaging Systems). Bands were quantified using NIH Image J software and normalized to GAPDH controls.

In vitro kinase assays

GST-CK2 α was purified from bacterial culture as previously described (371). Enzyme concentration was determined by absorbance at 595 nm, measured on a Victor3 V 1420 multilabel counter (Perkin Elmer) using bovine serum antigen (BSA) standards. The enzyme was diluted (up to 1:5000) in CK2 Dilution Buffer (5 μ M MOPS pH 7.0, 200 mM NaCl, 1 mg/mL BSA) immediately before use in kinase assays.

For CK2 phospho-donor specificity assay, peptide arrays were synthesized using SPOT technology on nitrocellulose membranes using the Auto-Spot Robot ASP 222 (Abimed) as previously described (372, 373). Filters bearing CK2 substrate sequences and controls were moistened with 95% ethanol to ensure solubilization of the peptides on the filter, then an equal volume of water was added with rocking for 15 min. Membranes were washed 5x with water and 1x with kinase assay buffer (KAB) (50 mM Tris-HCl pH 7.5, 30 mM MgCl₂, 50 mM KCl), then incubated in KAB overnight with gentle rocking, and fresh KAB was added at 30°C for 1 h with rocking. 100 μ M ATP γ S or KTP γ S (Biolog) was added followed by 100 μ M BSA, and the reaction was started by adding CK2 α holoenzyme (1:2500, 32.44 mg/ml with 665.1 nmol/min/mg specific activity) and incubated at 30°C with rocking for 20 min. 1 M NaCl was added to stop the reaction and

membranes were washed 5x with water. To alkylate the thiophosphate, the membranes were incubated in 2.5 mM p-nitrobenzylmesylate (PNBM)(Abcam) in water for 2 h at room temperature and then washed 5x with water. To decrease background noise, membranes were incubated in stripping solution (4 M Guanidine-HCl, 1% SDS, 0.5% β -mercaptoethanol) for 1 h at 40°C. Membranes were washed 10x in water and 3x in TBS-T, blocked in 5% milk in TBS-T for 1 h at room temperature, and incubated with thiophosphate ester primary antibody (1:5000, Abcam) in 5% milk in TBS-T overnight at 4°C, and then washed 3x in TBS-T. Membranes were then incubated for 45 min at room temperature with IRDye 800CW goat anti-rabbit secondary antibody (1:10000, LI-COR) in 5% BSA in TBS-T and then washed 3x in TBS-T and 1x in TBS. The LI-COR Odyssey (LI-COR) imaging system was used to visualize the array.

For *in vitro* kinase assays with unphosphorylated and S13p-primed N17 peptide, 1000 ng peptide (New England Peptides) was incubated in 1:5 KAB with 100 μ M adenosine triphosphate (Sigma-Aldrich) or N6FFA/kinetin triphosphate (Biolog) in a 10 μ L reaction. Reaction was initiated by addition of CK2 α holoenzyme (1:2500, 32.44 mg/ml with 665.1 nmol/min/mg specific activity) and was incubated at 30°C for 15 min with shaking. In each case, the reaction was stopped by placing on ice and 8 μ L kinase assay mixture was spotted onto nitrocellulose membrane (Pall Life Sciences) in 2 μ L dots (X4) and allowed to dry for 30 min. Membranes were washed once in TBS-T and blocked in 5% non-fat milk in TBS-T for 1.5 h and then incubated in anti-N17-S13pS16p (1:2500) overnight at 4°C with rocking. Membranes were then washed 3x in TBS-T and incubated

with either HRP-conjugated secondary antibody (1:50000, Abcam), and visualized using Immobilin enhanced chemiluminescence (EMD Millipore) on a MicroChemi system (DNR Bio-imaging Systems), or with IRDye 800CW goat anti-rabbit secondary antibody (1:10000, LI-COR) and visualized on a LI-COR Odyssey system (LI-COR). Signal intensity of dots was quantified using NIH Image J software.

Immunofluorescence

Cells were grown to approximately 80% confluence in 96-well ibiTreat dishes (Ibidi) for screening or in glass-bottom tissue culture dishes for irradiation experiments prior to the indicated treatments. Fixation and permeabilization by methanol at -20°C for 10 min followed by washing with wash buffer (50 mM Tris-HCl, pH 7.5, 150 mM NaCl, 0.1% Triton X-100) and blocking for 1 h at room temperature with blocking buffer (wash buffer + 2% FBS). Cells were incubated with primary antibodies diluted in blocking buffer for either 1 h at room temperature or overnight at 4°C before washing and imaging in PBS (Alexa Fluor 488-conjugated anti-N17-S13pS16p), or incubation with secondary antibodies diluted in blocking buffer for 30 min at room temperature. After washing, nuclei were stained with Hoechst (0.2 µg/ml in PBS) for 5 min at room temperature, washed, and imaged in PBS. Cells grown for SR-SIM imaging were seeded on to #1.5 coverslips, fixed and stained as above, and mounted on to glass slides using frame slide chambers (Bio-Rad). Cells stained with the anti-N6FFA antibody were fixed and permeabilized in 1:1 methanol:acetone at -20°C for 10 min, washed with PBS, then

incubated with 2M HCl for 45 min at room temperature to denature DNA. Following neutralization in 50 mM Tris-HCl pH 8.8 for 5 min and washing with PBS, cells were blocked and stained as above.

Induction of DNA damage

For micro-irradiation experiments, cells were grown overnight in glass-bottom dishes then stained with NucBlue (Molecular Probes/Life Technologies) for 15 min at 37°C in a 5% CO₂ incubator. Media was replaced with Hanks' Balanced Salt Solution (HBSS) (Gibco) immediately prior to micro-irradiation. Cells were irradiated using the Nikon C2+ confocal system, equipped with an InVivo Scientific environmental chamber held at 37°C. Regions of interest (~20 pixels each) were irradiated at a scan speed of 1/16 frames per second (512x512) using a Coherent OBIS 405nm diode laser (Coherent Inc, Santa Clara, CA, USA) set to 100% power. XY-coordinates were recorded, and cells were incubated at 37°C for the indicated periods prior to fixation and immunofluorescence. XY-coordinates were then revisited to image the irradiated cells.

Microscopy

Wide-field epifluorescence microscopy was done on a Nikon Eclipse Ti wide-field epifluorescent inverted microscope using the PLAN FLUOR 40x/0.6 air objective (for screening), or PLAN APO 60x/1.4 oil objective and Spectra X LED lamp (Lumencor, Beaverton, OR, USA). Images were captured using a Hamamatsu Orca-Flash

4.0 CMOS camera (Hamamatsu, Japan). Image acquisition and deconvolution of Z-stacks were done with NIS-Elements Advanced Research version 4.30 64-bit acquisition software (Nikon Instruments, Melville, NY, USA). Super-resolution imaging was done on the Nikon N-SIM super-resolution microscope system attached to a Nikon Eclipse Ti inverted microscope using an APO TIRF 100×/1.49 oil objective, and 405 nm, 488 nm, and 561 nm lasers (Coherent Inc). Images were captured using a Hamamatsu Orca-Flash 4.0 CMOS camera and acquired with the NIS-Elements software version 4.50.

Animal care and N6FFA trials

Male YAC128 mice overexpressing the human *HTT* gene with 128 CAG repeats (374) were originally purchased from Jackson Laboratories (Jackson Laboratories, Bar Harbor, ME, USA) and subsequently maintained on FVB background in the animal facility at the University of Alberta. All mice were maintained on a 12-12 h light-dark cycle in a temperature and humidity-controlled room. All procedures involving animals were approved by the University of Alberta's Animal Care and Use Committee and were in accordance with the guidelines of the Canadian Council on Animal Care. All YAC128 mice and wild-type (WT) littermates used in our studies were males.

Treatment started between 6 and 10 months of age and 14 days after the start of treatment motor testing began. For experiments involving intraperitoneal injection all mice were group housed for the duration of treatment. For experiments involving oral administration mice were individually housed for the duration of treatment. Animals in all

experimental groups were carefully matched for age.

Intraperitoneal administration of N6FFA

Mice were 6-9 month-old at the beginning of treatment. N6FFA (0.83 mg/kg or 4.17 mg/kg of body weight, in 1.5% DMSO in saline solution) was administered daily at 1600 h, by intraperitoneal injection, alternating side of injection. Control mice were injected with 1.5% DMSO in saline. Animals in all experimental groups were carefully matched for age (average animal age in months \pm SD, WT saline: 8.1 ± 1.08 ; WT N6FFA 6 mg/kg: 7.51 ± 1.51 ; WT N6FFA 30 mg/kg: 7.91 ± 1.31 ; YAC128 saline: 7.2 ± 1.50 ; YAC128 6 mg/kg N6FFA: 7.2 ± 1.60 ; YAC128 30 mg/kg N6FFA 7.0 ± 1.57).

Oral administration of N6FFA

Mice were 8-10 month-old at the beginning of treatment. Chow diet supplemented with 653 mg N6FFA/kg chow (OpenSource Diets) was administered for 49 days. Each mouse was provided with 10 g of chow diet and food was replaced every second day, such that food was available *ad libitum*. Food intake was measured every second day at 1700 h. Body weight was measured weekly. Animals in all experimental groups were carefully matched for age (average animal age in months \pm SD: WT control chow: 8.9 ± 0.68 ; WT N6FFA chow: 9.0 ± 0.69 ; YAC128 control chow: 9.13 ± 0.74 ; YAC128 N6FFA chow: 9.12 ± 0.69).

Behavioural tests

Behavioural testing was conducted in the light phase of the light cycle, between 0800h and 1800h. In all behavioural training and testing sessions, mice were allowed to acclimate to the testing room for 1 h. All experiments were performed by experimenters who were blind to animal genotype and treatment. All equipment was cleaned with 70% ethanol after each test and prior to testing the next animal.

For the rotarod, mice were tested in three consecutive trials of 3 min each, with 1 min rest in between trials, at fixed speed (12 RPM). The time spent on the rotarod in each of the three trials was averaged to give the overall latency to fall for each mouse. A similar training protocol was used to test mice on an accelerating rotarod (4-40 RPM in 2 min). For the narrow beam test, mice were placed at the extremity of a 100 cm-long wooden narrow beam (0.75 cm wide, suspended 30 cm above the floor) and allowed to traverse the beam from one extremity to the other three times. Mouse performance was recorded with a video camera and footfalls, body balance, and motor coordination were analyzed using an established footfall scoring system (304). For the open field test mice were placed in an open field apparatus (90 cm x 90 cm) and filmed during 30 min sessions as they explored the environment. Distance travelled was measured using EthoVision XT tracking software. At the end of each 30 min session in the open field, the number of fecal pellets dropped by each mouse was counted. For the elevated plus maze, mice were placed in the center of the maze facing the open arm and left to freely explore for 5 min. Arm crosses into and out of open and closed arms, as well as time spent in each

arm were recorded with a video camera and scored. An entry was defined as 75% of the body of the mouse, excluding the tail, entering into a compartment.

The forced swim test was performed as in (375) to assess anxiety through the number of fecal boli dropped. Mice were placed for 6 min in a 4 L beaker (25 cm tall, 16 cm wide) filled with 2.6 L of water pre-warmed to 23-25°C. After each session, fecal pellets dropped by each mouse were counted.

Tissue collection and processing

Mice were euthanized by cervical dislocation. Brain tissue was flash frozen in liquid nitrogen and immediately homogenized in ice-cold lysis buffer (20 mM Tris, pH 7.4, 1% Igepal, 1 mM EDTA, 1 mM EGTA, 50 µM MG132, 1X Roche cOmplete protease inhibitor cocktail and 1X Roche PhosStop phosphatase inhibitor cocktail) using a Wheaton homogenizer. Tissue lysates were sonicated twice for 10 sec each at power 2 using a Sonic Dismembrator Model 100. Protein concentration was measured with the bicinchoninic acid (BCA) assay.

Filter retardation assay

Filter retardation assay was performed as described (376, 377), with minor modifications. Briefly, 100 µg of protein lysates were diluted in phosphate buffered saline (PBS) containing 2% SDS and 100 mM DTT, followed by heating at 100°C for 10 min. Samples were filtered through a cellulose acetate membrane (0.2 µm pore size, Sterlitech)

in a Bio-Dot microfiltration unit (Bio-Rad). Wells were washed twice with PBS. After drying for 30 min, membranes were washed twice with 2% SDS in PBS and then blocked with 5% BSA in TBS-T followed by incubation with primary antibody. IRDye secondary antibodies (LI-COR Biotechnology) were used at 1:10000 for 1 h at RT. Infrared signal was acquired and quantified using the Odyssey Imaging System.

Nuclear condensation toxicity assay

Nuclear condensation assay to determine toxicity of the N586 fragment of Htt in neurons was performed as described (326). At 5 days in vitro (DIV), neurons were co-transfected with N586-Htt containing either Q22 or Q82 and GFP for 48 h. At the time of transfection, cells received a treatment with doses of N6FFA ranging from 0 to 100 μ M. After 48 h, the cells were fixed with paraformaldehyde and the nuclei stained with DAPI. Image acquisition was automatic on an Axiovert 200 inverted microscope (Zeiss) using Axiovision. Nuclear staining intensity of GFP positive cells was quantified automatically using Volocity (Perkin-Elmer). Any cell with intensity greater than 2 standard deviations of the control intensity of untransfected cells was considered dead. Results are presented as a percentage of the total transfected cells.

Annexin V Cell Death Assay

STHdh^{Q7/Q7} and *STHdh*^{Q111/Q111} cells were plated in 12-well plates and left to attach overnight. Cells were washed once with Dulbecco's PBS (DPBS) prior to incubation in

serum free medium (high glucose DMEM with 400µg/mL geneticin, 2 mM L-glutamine, and 1 mM sodium pyruvate) containing the indicated concentrations of N6FFA for 9 h at 39°C. At the end of the incubation period, cells were washed with PBS, trypsinized, washed in PBS and stained with annexin V PE (BD Pharmingen) in 45 µL of 1X annexin binding buffer (ABB) (BD Pharmingen) for 15 min at room temperature. Cells were then washed once with 1X ABB and fixed overnight with 2% paraformaldehyde in 1X ABB. FACS analysis of Annexin V+ cells was performed using a CANTO II cell analyzer. Ten thousand events per sample were acquired and analyzed using either CellQuestPro or FlowJo analysis software.

Statistical analysis

For mouse data, all statistical analyses were performed using two-way ANOVA followed by Bonferroni post-test, except for the analysis of body weight where repeated measures two-way ANOVA followed by Bonferroni post-tests was used, and for changes in mutant huntingtin expression where an unpaired t-test was performed. All comparisons were performed using a statistical significance level of 0.05. For *in vitro* and cell-based assays, treatments were compared to control using unpaired two-tailed t-test or ANOVA with multiple comparisons test unless data data did not pass Shapiro-Wilk normality test, then Mann-Whitney analysis (two-tailed) was used.

Acknowledgements:

Funding: This study was supported by the Canadian Institutes of Health Research, MOP-119391 Project Grant, The Krembil Foundation, and the Huntington Society of Canada.

Author Contributions: L.E.B., T.M., M.A., M.G., N.A., S.S., and R.T. designed research; L.E.B., T.M., M.A., M.G., N.A., D.G., C.L.K.H., S.P., and J.X. performed research; T.M., M.A., M.G., N.A., D.G., C.L.K.H., S.P., J.X., and N.T.H. contributed new reagents/analytic tools; L.E.B., T.M., M.A., M.G., N.A., N.T.H., C.A.R., D.L., and R.T. analyzed data; and L.E.B., T.M., S.S., and R.T. wrote the paper.

Competing Interests: N.T.H. is CSO and Shareholder, Mitokinin LLC. R.T. is on SAB and shareholder, Mitokinin LLC.

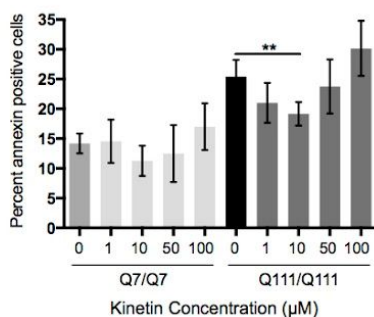
Data and Materials Availability: All reagents and cell lines in this study are available upon request.

2.6 Supplemental Figures

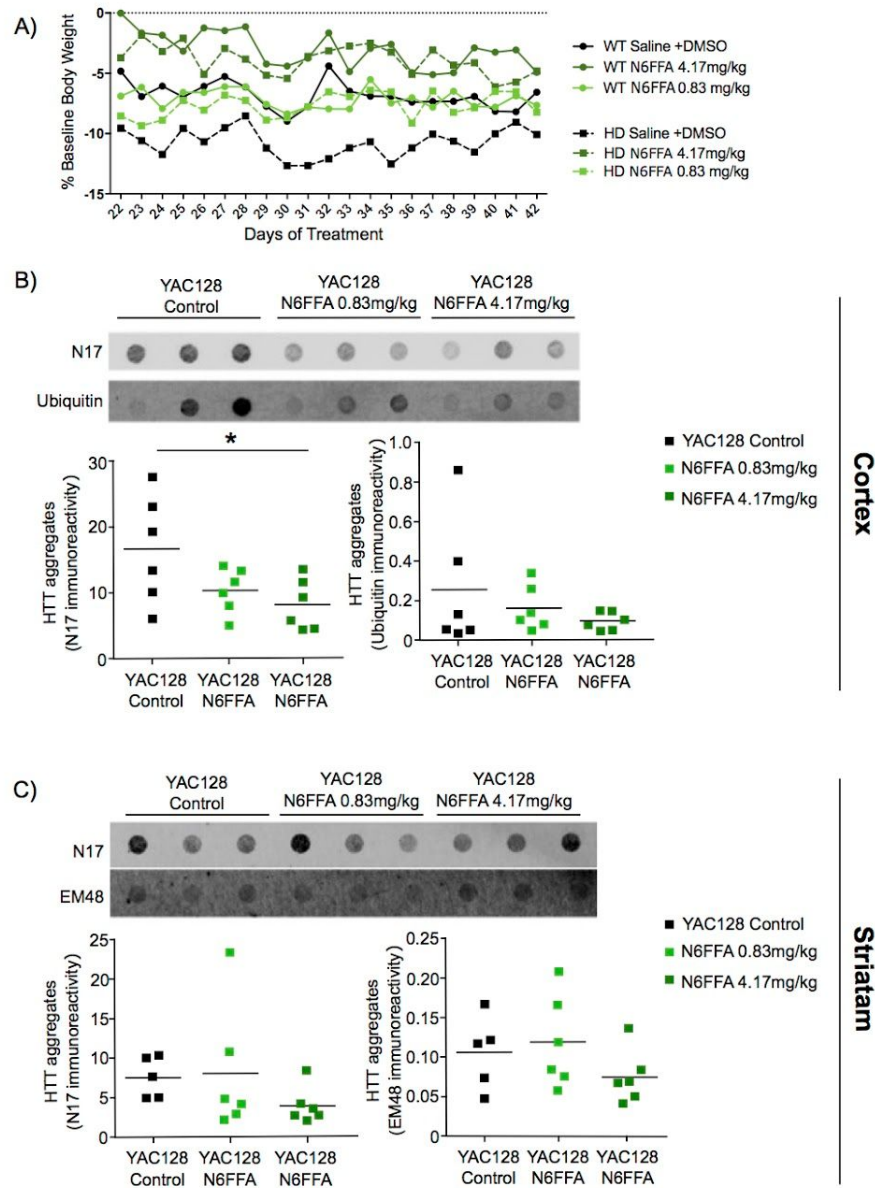
A

Ammonium Glycyrrhizinate	Parthenolide
Caffeic Acid	Phloretin
Dioscin	Phlorizin
DL-Carnitine Hydrochloride	Quercetin Dihydrate
Ecdysone	Rutacarpine
Glycyrrhizic Acid	Rutin
Kaempferol	Salicin
N6-furfuryladenine	Sclareol
Neo-hesperidin Dihydrochloride	Silibinin
Orotic Acid	Tanshinone IIA
Osthole	Yohimbine Hydrochloride
Oxymatrine	4-MU

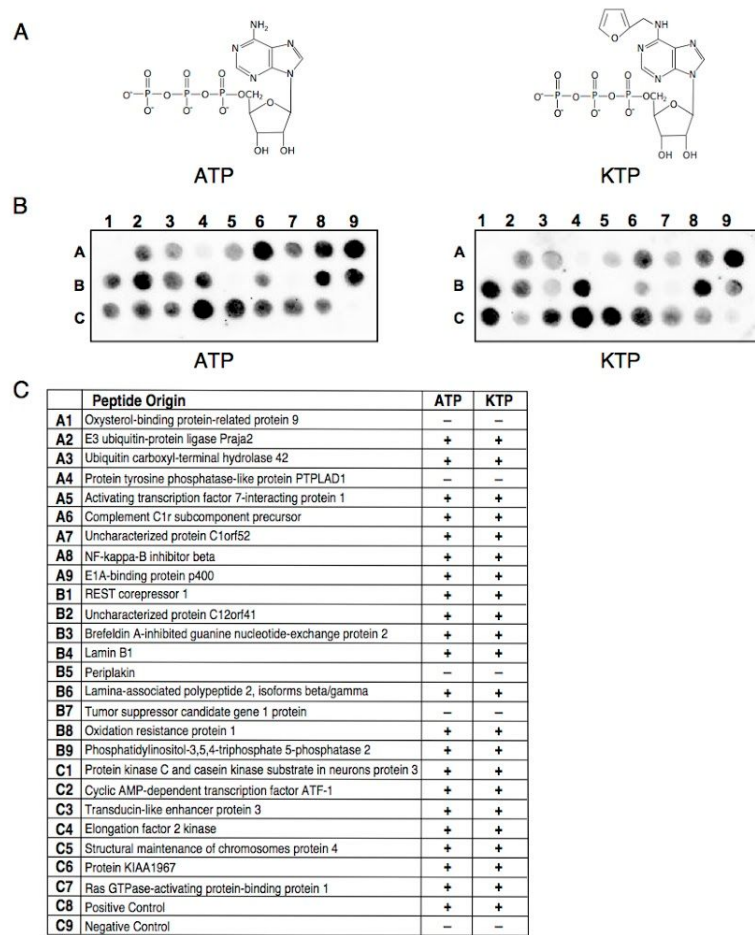
B



Supplemental Figure 2.1. Hit compound list and additional validation of N6FFA (A) List of compound hits from natural products screen. (B) STHdh cells were incubated in serum-free media for 9 h at 39°C and treated with the indicated concentrations of N6FFA. Flow cytometry was used after Annexin V staining to detect apoptotic cells. Results presented mean ± SD and significance was calculated by one-way ANOVA with Bonferroni post-test. **p<0.001 (N=8).



Supplemental Figure 2.2. Additional effects of N6FFA on YAC128 mice. (A) Percent change in body weight during treatment was calculated: $((\text{weight on day } x - \text{weight on day } 0) / \text{weight on day } 0) * 100$. All mice lost body weight during treatment, likely due to the stress of daily I.P. injections. Body weight loss was significantly decreased both in WT and YAC128 mice by N6FFA (* $p < 0.05$, ** $p < 0.01$, *** $p < 0.001$). (B) Effect of N6FFA on cortical aggregate levels. Representative blots (top) and quantification of of both N17 immunoreactivity (bottom left) and Ubiquitin reactivity (bottom right). (C) Effect of N6FFA on striatal aggregate levels. Representative blot (left) and quantification of N17 immunoreactivity (right). Blots were analyzed by one-Way Anova with Dunnet's post-test (* $p < 0.05$).



Supplemental Figure 2.3. CK2 can use KTP to phosphorylate substrates. (A) Chemical structures of ATP (left) and KTP (right). (B) CK2 phospho-specificity assay showing that CK2 can utilize KTP (right) to phosphorylate all of the same substrates as it does with ATP (left). (C) Summary of peptides used in peptide array in the CK2 phospho-specificity assay shown in (B).

CHAPTER 3

PKC ζ : A CANDIDATE N17 KINASE

The data described in this chapter is currently unpublished.
All experimental work was performed by the author, Laura Bowie.

3.1 Overview

In the previous chapter we fully validated CK2 as a kinase for the N17 domain of huntingtin, as well as identifying a compound that upregulates the action of this kinase in a protective manner (N6FFA). As action by CK2 requires “priming” of the N17 domain by phosphorylation, we next wanted to identify other potential N17 kinases. In the following chapter, I describe my efforts to identify these other kinases and my follow-up validation of one in particular.

3.2 Abstract

Huntingtin is modified by phosphorylation at a number of critical serine residues throughout the length of the protein. Modification of these residues impacts both protein function and mutant huntingtin toxicity. In the context of Huntington’s disease (HD), the huntingtin protein is hypo-phosphorylated, and increasing phosphorylation mitigates the toxicity of the mutant protein. CK2 is a ubiquitously expressed cellular kinase that has been shown to recognize and phosphorylate the huntingtin N17 domain at serine 16, but only when this domain is already primed by phosphorylation at serine 13. Using high content analysis and subsequent secondary validation, we here identify a potential kinase for N17 at serine 16, which may be acting as a priming kinase for CK2.

3.3 Introduction

The neurodegenerative disorder, Huntington's disease (HD), is characterized by degeneration of the striatal MSNs, and later, the cortical pyramidal neurons. Although the pathogenic mechanism of degeneration is multi-faceted, the root cause can be traced to an expansion of the CAG tract in the huntingtin gene (41, 99). This expansion translates to a toxic polyglutamine expansion in the huntingtin protein. HD usually manifests in the 4th to 5th decade of life in a characteristic triad of motor, cognitive, and behavioural deterioration. This disease is found in as many as 1/5500 people (43), and, as HD is transmitted in an autosomal dominant fashion, it places an enormous burden on the families affected. At present, there is no cure for this disease, and those afflicted must rely on symptomatic treatment.

In the past, most efforts in disease-modifying drug discovery have been targeted at modifying the downstream, supposedly toxic, consequences of the polyglutamine expansion, such as aggregation (275, 378–380). As these potential drugs have all failed to reach endpoints in clinical trials, more recently, drug discovery has begun to focus on the huntingtin protein itself. Much of this focus has been in the area of huntingtin lowering drugs, specifically ASOs targeting the huntingtin protein (381–383), and, currently, there are two major ASO clinical trials underway (279–281). While eliminating the problematic protein is a logical therapeutic goal, there are concerns that lowering the protein too much may have unintended consequences due to total loss of protein function (384). Another

approach, which still targets the huntingtin protein without the potential dangers of protein lowering, is to modulate protective, huntingtin PTMs with the goal of decreasing mutant huntingtin toxicity.

The huntingtin protein has known roles in vesicular trafficking, cell division, synaptic transmission, and the cell stress response (88, 141, 153, 161, 385–387). Recently, our lab has further described the involvement of huntingtin in the cellular response to oxidative stress and DNA damage (98, 171). In order to fulfill all of these roles, huntingtin must be able to move between a number of different cellular compartments and organelles. This movement is regulated by the N17 domain, which is an amphipathic alpha helix that allows huntingtin to dynamically associate with membranes (69). Localization of the huntingtin protein is mainly regulated by phosphorylation of this domain at serines 13 and 16 (69–71). While mutant huntingtin has been shown to be hypo-phosphorylated at these residues, increasing phosphorylation by addition of exogenous compounds or phospho-mimetic mutations is protective in cell and animal models of disease (72, 287). The Sipione lab has shown phosphorylation of this domain can be upregulated by administration of ganglioside GM1 with protective effects in the YAC128 HD mouse model (287). Additionally, in the previous chapter, we demonstrate that exogenous administration of an adenine analogue, N6-furfuryladenine (N6FFA), also increases phosphorylation of this domain, again with protective effects in the YAC128 mouse. This small molecule is converted to an ATP analogue that can be used by CK2, a kinase we had previously identified as N17-modifying (71). As

phosphorylation of this domain clearly plays a role in reducing toxicity induced by mutant huntingtin, we wanted to identify other potential N17 kinases that could ideally be targeted to increase huntingtin phosphorylation in a similar manner to CK2.

Therefore, using a validated antibody to N17 phosphorylated at S13 and S16 (71), we conducted a high content screen with a library of kinase inhibitors with the goal of finding modulators of N17 phosphorylation and identifying putative N17 kinases. The results of this screen were analyzed by unbiased computer software using PCA (388). Potential hits were compared to results from kinase prediction software (389). This combination of analyses led us to identify protein kinase C ζ (PKC ζ) as a potential N17 modifying kinase.

PKC ζ is an atypical PKC with known roles in cell growth and survival, cell polarization, embryogenesis, and filamentous actin reorganization downstream of Ras-related C3 botulinum toxin substrate 1 (Rac1) (390–392). It has also been implicated in several different cell responses to stress, including oxidative stress and DNA damage (391, 393–395). We here give evidence that PKC ζ can phosphorylate the huntingtin N17 domain, which could act as a prime to allow subsequent phosphorylation by CK2 in a hierarchical manner.

3.4 Results

High content screening and sequence analysis identifies PKC ζ as a potential N17 priming kinase

We have shown in the previous chapter that CK2 is responsible for phosphorylating huntingtin N17, and that this action, in the context of mutant huntingtin, can be augmented by addition of exogenous N6FFA. However, in order for this phosphorylation event to occur, CK2 requires N17 to be already primed with a phosphate at a nearby serine residue. With the goal of identifying the kinase responsible for this “priming” phosphorylation, we conducted a high content screen of a small kinase inhibitor library (Selleckchem), using an antibody against N17 phosphorylated on S13 and S16 (71) directly conjugated to Alexa Fluor 488 as a read-out of inhibitor effect.

Direct immunofluorescence was performed on *STHdh^{Q7/Q7}* cells treated with the kinase inhibitor library for 4 hours at 37 °C. Images were taken in an unbiased manner at 10 software-randomized locations using a 40x air objective. There was no investigator bias except to set initial exposure settings. Images were analyzed by unbiased computer software (388), assaying textures in a single channel. From these textures, the 3 most variant textures are used to plot a unitless vector in 3D space such that the points farthest from each other represent images that are the most dissimilar. Compound hits were selected based on which ones plotted furthest from the control, 0.01% DMSO (**Figure 3.1a**).

As kinases often have a multitude of cross-pathway effects, we next sought to narrow down our list of potential hit compounds using a kinase prediction software, GPS 2.0 (389). This software analyzes amino acid sequences and identifies likely kinases for serine, threonine, and tyrosine residues based on consensus sequence (389). For this

analysis, the N17 sequence was used: MATLEKLMKAFESLKSF. From the list of hits generated, only one was also identified by GPS as a likely N17 kinase, PKC ζ (**Figure 3.2b**).

PKC ζ is an atypical PKC that is not activated by either calcium (Ca²⁺) or diacylglycerol due to the lack of a C2 domain and the presence of an atypical C1 domain, respectively. Instead, this kinase can be activated by lipid species, such as ceramides (396), and is often regulated by protein-protein interactions via its Phox/Bem 1p (PB1) domain (397, 398). Similar to huntingtin, PKC ζ is found at high levels in the brain and testes, with the brain containing an additional brain-specific isoform, called protein kinase M ζ (PKM ζ), which lacks the PKC ζ regulatory domain (399, 400) (**Figure 3.1c**). PKM ζ has been found to play a critical role in long-term potentiation and memory maintenance (401–403).

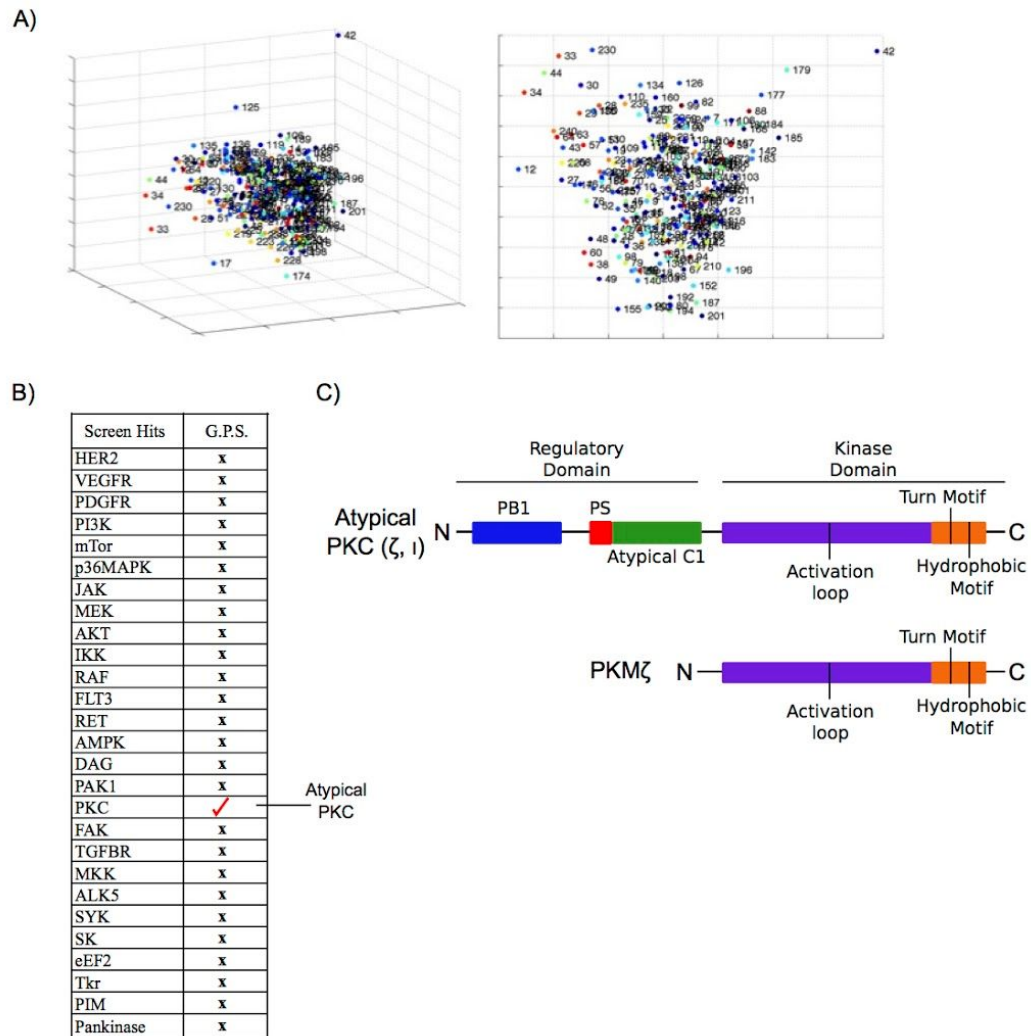


Figure 3.1. Identification of PKC ζ as a modulator of huntingtin N17 phosphorylation *STHdh*^{Q7/Q7} cells were treated for 4 hours with kinase inhibitors. Cells were fixed and incubated with an antibody to N17S13pS16p conjugated to Alexa Fluor 488. 10 images per well were taken and analyzed by Phenoripper, the results of this analysis are shown in (A). GPS 2.0 was used to analyze the N17 sequence to identify potential kinases, a list of phenoripper hits as well as their confirmation by GPS are shown in (B). The structure of atypical PKC, PKC ζ , is shown in (C).

PKC ζ can phosphorylates N17, but may not prime for CK2

To confirm that PKC ζ can act directly on huntingtin N17, we asked whether this kinase could phosphorylate N17 *in vitro*. Unfortunately, there is no commercially available antibody recognizing N17 phosphorylated at S13 alone, but our antibody to N17S13pS16p also recognizes S13p alone, though to a lesser degree than N17 phosphorylated on both residues (71). We see from this assay that PKC ζ can phosphorylate N17 *in vitro*, and that this likely occurs at the S13 site as our antibody is not sensitive to N17 phosphorylated at only the S16 site (**Figure 3.2**) (71).

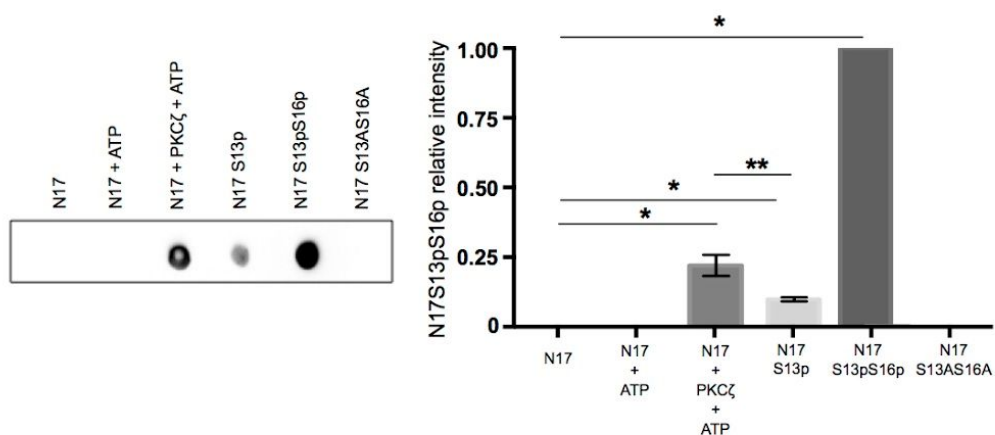


Figure 3.2. PKC ζ can phosphorylate N17 *in vitro*. Representative blot (left) and quantification (right) of an *in vitro* N17 phosphorylation assay using PKC ζ with either ATP as phospho-donor. Analysis by Mann-Whitney test (n=3 independent replicates, **p<0.001).

As we have previously shown that CK2 can phosphorylate N17 at S16 when S13 is already primed by phosphorylation, we wanted to look for kinases that could phosphorylate S13 when N17 is not primed. Therefore, we used GPS 2.0 software to look for kinases in our hit list that were likely to phosphorylate S13 based on consensus sequence. However, as CK2 is an acidophilic kinase, it is possible that CK2 can also

phosphorylate S13 if S16 is primed. To determine if CK2 could potentially also phosphorylate the putative PKC ζ site, a kinase assay was again used. Phosphorylation of phospho-primed peptides by CK2 was observed for both S13 and S16 primed, indicating that CK2 can phosphorylate N17 at either residue using both ATP and the N6FFA metabolite, KTP (**Figure 3.3**). This suggests that while PKC ζ may be phosphorylating N17 at S13, it is not necessarily priming the N17 domain for phosphorylation by CK2.

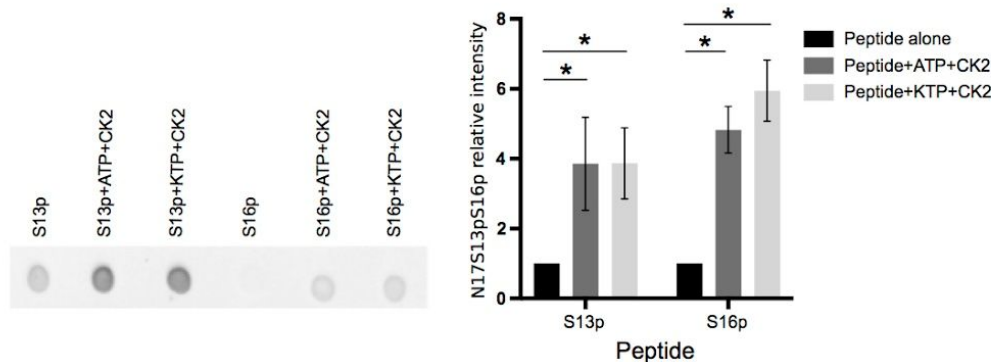


Figure 3.3. CK2 can phosphorylate N17 at either S13 or S16. Representative blot (left) and quantification of an *in vitro* N17 phosphorylation assay using CK2 with ATP or KTP as phospho-donor. Quantified intensity for each dot is relative to the respective peptide alone control. Analysis by Mann-Whitney test (n=4 independent replicates, *p<0.05).

Modulation of PKC ζ levels and activity modulates phosphorylation of the N17 domain

To validate PKC ζ as an N17 kinase, we first sought to inhibit its action by two methods. We first used both a general inhibitor of PKCs (Go 6850) and a specific inhibitor of PKC ζ at known effective concentrations. *STHdh*^{Q7/Q7} cells were treated for 4 hours with these compounds and the resulting levels of N17 phosphorylation were determined by western blot. Immunoblotting using a highly validated anti-N17S13pS16p

antibody shows that, in both cases, there is a significant decrease in N17 phosphorylation following inhibition of PKC ζ (**Figure 3.4a**).

To further validate these findings, we also wanted to determine if the converse was true, if increasing the activity of PKC ζ resulted in an increase in N17 phosphorylation. As specific targeting of PKC ζ is difficult, in part due to its strong homology with PKC ι/λ (approximately 72 % overall) (400), and also due to the nature of its activation, we chose to do this by overexpressing either PKC ζ or a control, kinase dead, mutant. Following 24 hours transfection, analysis by western blot shows a significant increase in N17 phosphorylation upon over-expression of PKC ζ that is not seen in cells transfected with the kinase dead mutant, suggesting that this effect is directly related to the kinase activity of PKC ζ rather than expression of the protein itself (**Figure 3.4b**).

Taken together, these findings show that modulation of PKC ζ levels and activity results in corresponding changes in N17 phosphorylation, suggesting that this kinase is a good candidate an N17 kinase.

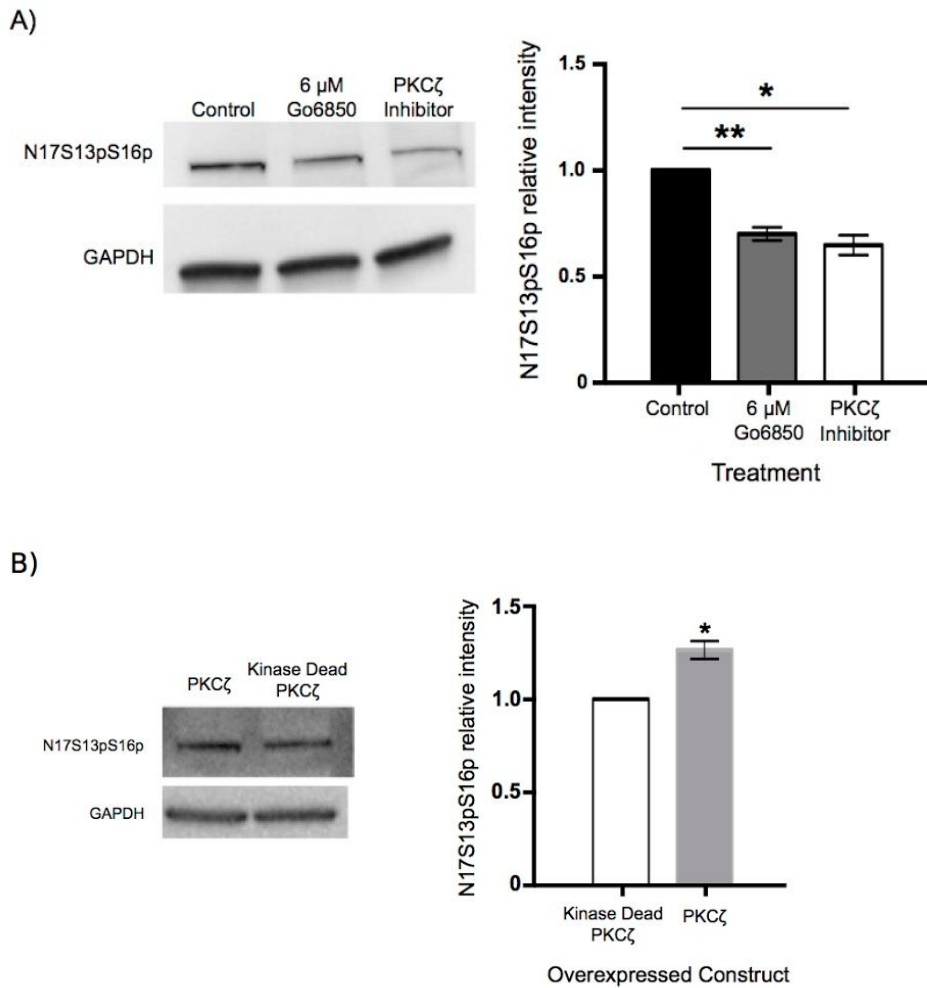


Figure 3.4. Modulation of PKC ζ results in corresponding changes in N17 phosphorylation *STHdh*^{Q7/Q7} cells were treated for 4 hours with Go6850, a general inhibitor of PKCs, as well as a specific inhibitor of PKC ζ . Proteins were separated by SDS-PAGE and immunoblotted. Representative blot (left) and quantification (right) are presented in A, * $p < 0.05$, ** $p < 0.001$, $n = 3$. B shows the results of an experiment where PKC ζ and a kinase dead PKC ζ mutant were overexpressed in *STHdh*^{Q7/Q7} cells for 24 hours. Representative blots (left) and quantification (right) are presented, * $p < 0.05$, $n = 3$.

PKC ζ colocalizes with N17 phosphorylated huntingtin in the nucleus

Our lab has previously shown that phosphorylated huntingtin colocalizes with known interactors, such as the DNA damage response protein ATM and protein kinase CK2, at nuclear speckles (171, 305). As CK2 is a known N17 kinase, we wanted to determine if PKC ζ might also co-localize with phosphorylated huntingtin in the nucleus. Thus, hTERT-immortalized wild-type human fibroblasts (TruHD-Q21Q18F) cells were fixed with methanol and incubated with an anti-PKC ζ directly conjugated to Alexa Fluor 594 followed by a rabbit anti-N17S13pS16p antibody directly conjugated to Alexa Fluor 488. We see considerable colocalization at punctate regions within the nucleus, which may suggest that huntingtin and PKC ζ have a proximity-dependent relationship (**Figure 3.4a and b**). This, in combination with our other findings, indicates that PKC ζ may have activity in the nucleus as an N17 kinase.

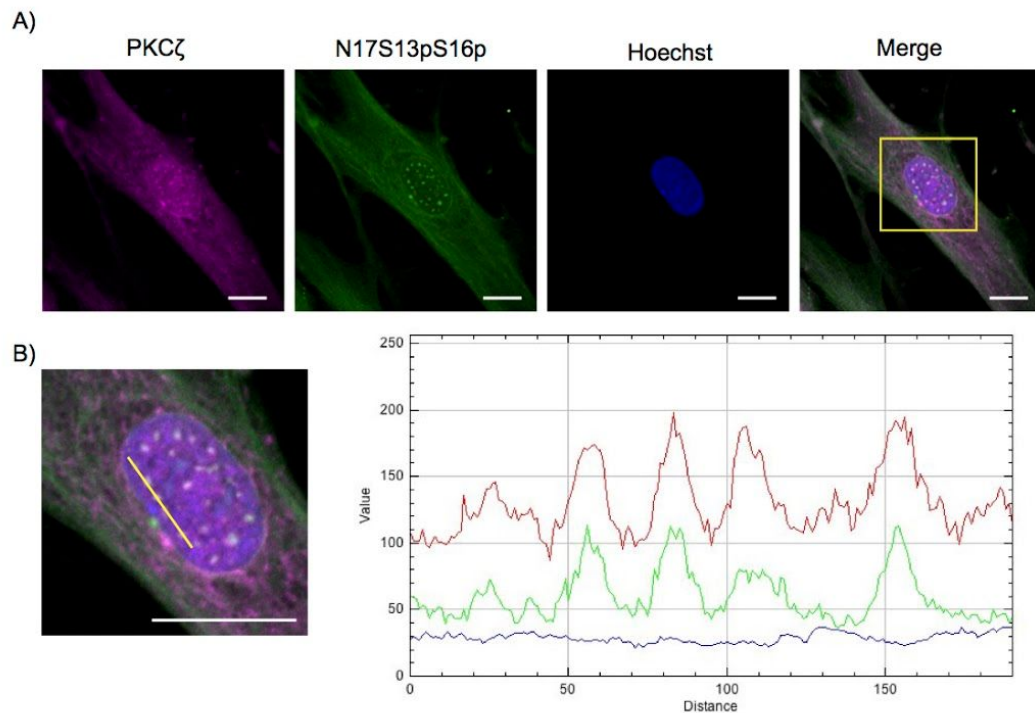


Figure 3.5. Colocalization of N17P and PKC ζ at nuclear puncta. (A) TruHD-Q21Q18F cells were fixed with methanol and incubated sequentially with a primary antibody against PKC ζ directly conjugated to Alexa Fluor 594, and a primary antibody against N17S13pS16p directly conjugated to Alexa Fluor 488. Images of protein localization in the nucleus, as stained by hoechst, are shown. The region indicated by the yellow square is shown enlarged in (B). An intensity profile across the nucleus of one of these cells is shown in (B), the yellow line indicates the region across which the intensity profile was taken. Red profile = PKC ζ intensity, green profile = N17S13pS16p intensity, and blue profile = hoechst intensity. Scale bar = 10 μ M.

3.5 Discussion

In this study, we used high content analysis with unbiased software analysis to identify kinase inhibitors that modulated phosphorylation of the N17 domain. From this screen we ended up with an extensive list of kinases, which made testing all of our hits prohibitively difficult. As many of the hits from this screen are found near the beginning of kinase signalling cascades, such as cell surface receptors human epidermal growth factor receptor 2 (HER2), vascular endothelial growth factor receptor (VEGFR), and

platelet-derived growth factor receptor (PDGFR), with pleiotropic effects in cells, it seemed unlikely that these enzymes would act directly on huntingtin. Indeed, one of the caveats of screening with kinase inhibitors is that they can affect multiple different pathways due to lack of inhibitor specificity and pathway cross-talk, convoluting results. To narrow down our list of hits to those that were most likely to act directly on huntingtin, we cross-referenced our findings with a list of potential N17 kinases generated by the GPS 2.0 software (389). Of all the potential kinases identified in our screen, the only group that was also pulled out by the GPS analysis were the atypical PKCs, specifically PKC ζ .

To follow up these initial findings, we next showed that this kinase could directly phosphorylate huntingtin N17 *in vitro* and that by modulating PKC ζ activity, via inhibition or over-expression, we induced a resulting decrease and increase in N17 phosphorylation levels, respectively. Taken together, these results indicate that PKC ζ may indeed be responsible for phosphorylating N17. This is consistent with the study by DiPardo et. al, that found treatment with ganglioside GM1 results in increased N17 phosphorylation. As GM1 is a ceramide derivative, and ceramides are known to activate atypical PKCs via activation of tropomyosin receptor kinase A (TrkA) receptor (404, 405), it follows that application of this compound could result in activation of atypical PKC ζ and increased N17 phosphorylation. This kinase has been mentioned in conjunction with huntingtin in the literature a few times in the past. In 2003, Zemskov *et al.* found PKC ζ associated with N-terminal fragments of mutant huntingtin in aggregates (406), and

later, in 2007, Fan *et al.* identified PKC ζ amongst several kinases that were elevated in HD cells (407). Interestingly, this group of kinases also included CK2, which we have also shown, in the previous chapter, to phosphorylate N17 (408). Like CK2, we see that PKC ζ colocalizes with phosphorylated huntingtin at punctate regions within the nucleus. In order for CK2 to phosphorylate S16, it is necessary that the N17 domain be already phosphorylated, or “primed”, at S13. Our findings suggest the PKC ζ may be the kinase responsible for priming N17 for subsequent CK2 phosphorylation. This is not the first time that PKC ζ has acted as a priming kinase, phosphorylating S680 of Drosophila Smoothed protein and targeting CK1 to phosphorylate S683 (409).

PKC ζ is a constitutively active kinase, but can be up-regulated by oxidative stress and DNA damage. Under conditions of oxidative stress, PKC ζ mediates Nrf2 activation through phosphorylation of S40 (393), and its interaction with NF-KB is required for the transcription factor to translocate to the nucleus and stimulate transcription of stress-associated genes (390). Additionally, PKC ζ translocates to the nucleus and mediates cell resistance to low and high doses of radiation (394), and enhances cell resistance to genotoxic stress by increasing nucleotide excision repair (395), implicating this kinase in the cellular response to DNA damage. This is consistent with the role of phosphorylated huntingtin as an oxidative stress response protein and as a member of the ATM DNA repair complex (98, 171).

Based on the above results, we believe that PKC ζ likely phosphorylates the N17 domain of huntingtin in response to stress, allowing for subsequent phosphorylation by

CK2. However, it is important to note that we have also determined that CK2 can phosphorylate either S13 or S16 depending on the location of the priming phosphate, which suggests that while PKC ζ may be priming for CK2, it may also be competing with CK2 to phosphorylate this domain. Determining the nature of the interaction between these two kinases will be an important future direction for this study. Future studies should investigate the combined effects of PKC ζ and CK2 activation and inhibition. Additionally, it would be prudent to identify compounds that increase PKC ζ kinase activity on the N17 domain, similar to the way N6FFA increases CK2 activity on this domain. The synergistic effect of this compound and N6FFA on N17 phosphorylation may have therapeutic benefit in HD.

3.6 Materials and Methods

Reagents and antibodies

Polyclonal antibody against huntingtin phosphorylated at S13 and S16 of the N17 domain (anti-N17-S13pS16p, New England Peptides) was previously characterized and validated (71). To directly conjugate the anti-N17-S13pS16p antibody to Alexa Fluor 488 succinimidyl ester dye (Molecular Probes/Life Technologies), 1 μ L dye per 10 μ L antibody and 5% NaHCO₃ was incubated overnight at 4°C with rotation. The conjugate antibody was then run through a Sephadex G-25 bead (Amersham Pharmacia Biotech AB) column and collected by elution with PBS until the visible dye front reached the base of the column. Other immunofluorescence antibodies were acquired commercially:

anti-PKC ζ -Alexa 594 (Santa Cruz). Western primary antibodies: anti-N17-S13pS16p (New England Peptides), anti-PKC ζ (Abcam), and anti-GAPDH (Abcam). Secondary antibodies against rabbit and mouse IgG, conjugated to HRP (Abcam).

All peptides were made by GenScript with the following amino acid sequences:

N17 peptide:	MATLEKLMKAFESLKSF
N17 S13p peptide:	MATLEKLMKAFepSLKSF
N17 S16p peptide:	MATLEKLMKAFESLKpSF
N17 S13pS16p peptide:	MATLEKLMKAFepSLKpSF
N17 S13AS16A peptide:	MATLEKLMKAFEALKAF

Plasmids

FLAG.PKC ζ and the kinase dead mutant FLAG.PKC ζ .K/W were gifts from Alex Toker (Addgene plasmid #10799) (410).

Cells

Cells, derived from mouse striatum, *STHdh*^{Q7/Q7} (a kind gift from M.E. MacDonald), were grown in Dulbecco's modified Eagle's medium with 10% fetal bovine serum (FBS) at 33°C in a 5% CO₂ incubator. Human hTERT immortalized retinal pigment epithelial-1 (RPE1) cells (ATCC) were grown in Dulbecco's modified Eagle's F12 medium with 10% FBS and hygromycin at 37°C with 5% CO₂. Immortalized human fibroblasts (TruHD-Q21Q18F) were grown in minimal Eagle's medium with 15% FBS and 1% Glutamax at 37°C with 5% CO₂. All media and supplements were from Gibco Life Technologies.

High content screen and analysis

STHdh^{Q7/Q7} cells were grown to approximately 80 % confluence in 96-well ibiTreat dishes (Ibidi) before treatment with a kinase inhibitor library (Selleckchem) for 4 h at 37°C. Fixation and permeabilization were by methanol at -20°C for 10 min followed by washing with wash buffer (PBS) and blocking for 1 h at room temperature with blocking buffer (wash buffer + 2% FBS). Cells were incubated overnight at 4°C with Alexa Fluor 488-conjugated anti-N17-S13pS16p antibody at 1:15 dilution in blocking buffer + 0.1% Tween before washing. After washing, nuclei were stained with Hoechst (0.2 µg/ml in PBS) for 8 min at room temperature, washed, and imaged in PBS. Images, taken with 40X objective, were analyzed using Phenoripper (388) where 5 images per well were thresholded by random sampling and analysis was carried out using a block size of 15. Hits were scored by selecting points on the resulting PCA plot lying furthest from controls where they fell outside of an arbitrarily defined radius.

Compound Application

All compounds were administered in cell-appropriate media with 10 % FBS for 4 hours unless otherwise indicated. Go6850 (Sigma) was used at 4 µM and the PKCζ pseudosubstrate inhibitor (Santa Cruz) was used at 10 µM.

Transfection

Plasmid transfection was performed using the Transit X2 system (Mirus). Briefly,

4 µg plasmid DNA was mixed with 400 µL opti-MEM and 20 µL Transit X2 and mixed by brief vortex. Mixture was incubated for 20 min at room temperature and then applied to cells. For PKC ζ overexpression assay, cells were left to express plasmid for 24 h before cells were collected, and for PKC ζ knock-down assay, cells were left to express shRNA for 72 h before cells were collected.

Microscopy

For screening, wide-field epifluorescence microscopy was done on a Nikon Eclipse Ti wide-field epifluorescent inverted microscope using the PLAN FLUOR 40 \times /0.6 air objective). Images were captured using a Hamamatsu Orca-Flash 4.0 CMOS camera (Hamamatsu, Japan). Image acquisition was done with NIS-Elements Advanced Research version 4.30 64-bit acquisition software (Nikon Instruments, Melville, NY, USA).

For colocalization experiments, cells were grown to approximately 80% confluence in 35 mm glass-bottom tissue culture dishes. Fixation and permeabilization by methanol at -20°C for 10 min followed by washing with wash buffer (50 mM Tris-HCl, pH 7.5, 150 mM NaCl, 0.1% Triton X-100) and blocking for 1 h at room temperature with blocking buffer (wash buffer + 2% FBS). Cells were incubated with primary conjugate antibodies diluted in blocking buffer overnight at 4°C before washing 3x with PBS. After washing, nuclei were stained with Hoechst (0.2 µg/ml in PBS) for 5 min at room temperature, washed, and imaged in PBS on A1 confocal microscope.

Protein extraction and immunoblotting

Cells were lysed in RIPA lysis buffer (50 mM Tris-HCl pH 8.0, 150 mM NaCl, 1% NP-40, 0.25% sodium deoxycholate, 1 mM EDTA) containing 10 % protease and phosphatase inhibitors (Roche). Lysates were centrifuged at 17000 x g for 12 min at 4°C and the supernatant was collected for immunoblot analysis. Equal amounts of protein were separated by SDS-PAGE on pre-cast 4-20% polyacrylamide gradient gels (Biorad) and electroblotted onto Immobilon poly-vinyl difluoride (PVDF) membrane (EMD Millipore). Membranes were blocked in TBS-T (50 mM Tris-HCl, pH 7.5, 150 mM NaCl, 0.1% Tween-20) containing 5% non-fat dry milk for 1.5 h at room temperature, followed by overnight incubation with primary antibodies diluted in blocking buffer at 4°C (anti-N17-S13pS16p 1:2500; anti-PKC ζ 1:1500; or anti-GAPDH 1:7500 as appropriate). After 3 x 15-min TBS-T washes, membranes were incubated with HRP-conjugated secondary antibodies diluted in blocking buffer (1:50000) for 45 min at room temperature, and visualized using Immobilon enhanced chemiluminescent HRP substrate (EMD Millipore) on a MicroChemi system (DNR Bio-imaging Systems). Bands were quantified using NIH Image J software and normalized to GAPDH controls.

In vitro kinase assays

Assays used 1000 ng peptides, as described above, incubated with 1 uL NEBuffer for Protein Kinases (New England Biolabs), 1000 ng ATP (Sigma-Aldrich) or KTP

(Biolog) and 100 ng PKC ζ (Cedarlane) (specific activity 103 nmol/min/mg) or 500 units CK2 (New England Biolabs) (specific activity 859,000 units/mg) for 1 hour in shaking incubator at 30°C. Following incubation, the reaction was stopped by placing on ice. 8 μ L kinase assay mixture was spotted (2 μ L x 4) onto nitrocellulose membrane and allowed to dry for 45 minutes. Membranes were blocked in 5% non-fat milk in TBS-T for 1.5 hours and incubated in anti-N17S13pS16p (1:2500) (New England Peptides) overnight at 4°C on a rocker. Membranes were washed in TBS-T and incubated in the appropriate HRP-conjugated secondary antibody diluted in blocking buffer (1:50000) and were visualized using Immobilon enhanced chemiluminescent HRP substrate (EMD Millipore) using a MicroChemi system (DNR Bio-imaging Systems). Quantification was done using NIH Image J software.

Statistical Analysis

All statistical calculations were performed using the Graphpad Prism 7 software. Results were considered significant if $p < 0.05$. Statistical tests were used as recommended by the software, with normal data using the student's T test and non-normal data using Mann-Whitney analysis.

CHAPTER 4

FURTHER EXPLORATION OF N6-FURFURYLADENINE IN DISEASE: INSIGHTS ON MECHANISM

The data described in this chapter is currently unpublished.

All experimental work was conducted by the author, Laura Bowie, with the exception of:

Figure 4.1D: experiments by Mina Falcone, and

Fig 4.5B and 4.6: microscopy was conducted by Dr. Tamara Maiuri.

All statistical calculations were done by Laura Bowie.

Note that not all experiments in this chapter were performed in triplicate, this will be indicated in the text or figure legend.

4.1 Overview

As our investigation of N6FFA developed, various experiments were conducted with the goal of validating the effect of this small molecule on phosphorylation of N17, as well as elucidating the mechanism by which this compound is acting. In this chapter, I describe and discuss some of the efforts undertaken to achieve this goal, as well as our ongoing efforts in this area. A full discussion of this data and how it expands on my earlier findings, described in Chapters 2 and 3, will take place in Chapter 5.

4.2 Abstract

N6-furfuryladenine (N6FFA) is a product of DNA damage that is protective against oxidative stress and onset of age-related phenotypes in human fibroblasts. We have recently shown that this compound protects against motor and anxiety-like phenotypes in a mouse model of Huntington's disease (HD) via phosphorylation of huntingtin downstream of DNA damage. Here we show additional effects of N6FFA following DNA damage, as well as effects on other hallmarks of HD, such as aggregation of mutant huntingtin protein. We also investigate a potential role of huntingtin in familial dysautonomia (FD) through the action of N6FFA.

4.3 Introduction

N6-furfuryladenine (N6FFA), colloquially known as kinetin, is a small molecule with a structure similar to the purine adenine that is typically annotated as a plant growth

hormone (411). Originally, N6FFA was identified in autoclaved herring sperm DNA and was considered to be an unnatural byproduct of DNA damage (411). In 1996, N6FFA was found endogenously in plant extracts, but was not believed to occur naturally in humans until 2000 when it was identified in human urine (310, 412). The structural similarity between N6FFA and adenine led one group to speculate that N6FFA may be a product of oxidative DNA damage (363, 413). This was later confirmed by our own group when we demonstrated that N6FFA was generated upon laser-induced DNA damage (408).

Previous studies have shown that this plant cytokine has biological effects in both plant and mammalian cells, including protection against oxidative stress, stimulation of cell differentiation, and delay of age-related phenotypes (307, 414–417). These effects, in conjunction with the structure of N6FFA suggest protective role of this molecule downstream of DNA damage. In our recent publication, we have shown that N6FFA signals oxidative DNA damage through phosphorylation of huntingtin N17, and is protective in cell and animal models of HD (408). This process is dependent on the metabolism of N6FFA to a triphosphate form, KTP, by nucleotide salvaging enzymes, as well as the subsequent use of this triphosphate by the kinase CK2 (408). In a Parkinson's disease (PD) model, N6FFA was again shown to act as a kinase neo-substrate, although this time through PINK1 rather than CK2 (311).

In addition to these new-found effects in HD and PD models, N6FFA has also been reported to correct mis-splicing of the inhibitor of kappa light polypeptide gene enhancer in B-cells, kinase complex-associated protein (IKBKAP) mRNA, which is the

main cause of familial dysautonomia (FD). The, apparently, diverse effects of this oxidative DNA damage product point to a complex mechanism-of-action.

In this chapter, we continue our investigation into the action of N6FFA in disease. We begin by testing derivatives to identify those that, like N6FFA, increase mutant huntingtin phosphorylation, and may represent therapeutic leads amenable to patient treatment. We additionally investigate a potential connection between the huntingtin protein and the effect of N6FFA on IKBKAP splicing. Finally, the effects of this compound in HD were further explored by looking at modulation of disease hallmarks, such as aggregate formation, and expanding on the role of N6FFA as a signaling molecule in DNA damage repair.

4.4 Further experimentation with N6FFA derivatives

In the process of validating the effects of N6FFA on N17 phosphorylation, several other assays were performed. In addition to determining levels of N17 phosphorylation following treatment with an N6FFA derivative, 9DK, which cannot be metabolized to KTP, the levels of N17 phosphorylation following treatment with another N6FFA derivative, 9-methyl-kinetin (9MK) were determined. 9MK was initially developed as a N6FFA derivative that could not be metabolized to KTP by the nucleotide salvager APRT (similar to 9DK) (418), but this derivative is amenable to metabolism by cellular demethylases, allowing subsequent conversion to KTP by nucleotide salvaging enzymes. Consistent with this, while N17 phosphorylation upon 9MK treatment was not

significantly different from the negative control, it was also not significantly different from N6FFA treatment, which was significantly increased compared to control (**Figure 4.1a**). This could suggest that 9MK does affect N17 phosphorylation, but in an inconsistent manner, possibly due to the necessity of demethylase action on this molecule prior to salvaging.

As protective effects of N6FFA were noted in both cell and animal models of HD, we wanted to follow-up on this finding by investigating the effects of derivatives of N6FFA in striatal cells expressing mutant huntingtin. Using the methodology presented in Chapter 2, we screened a derivatives library for those with the greatest effect on N17 phosphorylation in *STHdh*^{Q111/Q111} cells. Analysis with Phenoripper identified several compounds with, apparently, greater effects on N17 phosphorylation than N6FFA, encircled in green (**Figure 4.1b**). Of these more efficacious compounds, we proceeded to validate one of these hits (encircled in blue), called N6FFA-O. Subsequent immunoblot analysis reveals that N6FFA-O significantly increases phosphorylation of the N17 domain, even at low concentrations, validating the findings of our screen (**Figure 4.1c**). Taken together, these findings indicate that, as long as they are able to be metabolized to KTP, derivatives of N6FFA may be of therapeutic benefit in HD, and, as a result, the effects of a number of N6FFA derivatives are currently being investigated for beneficial effects in mouse models.

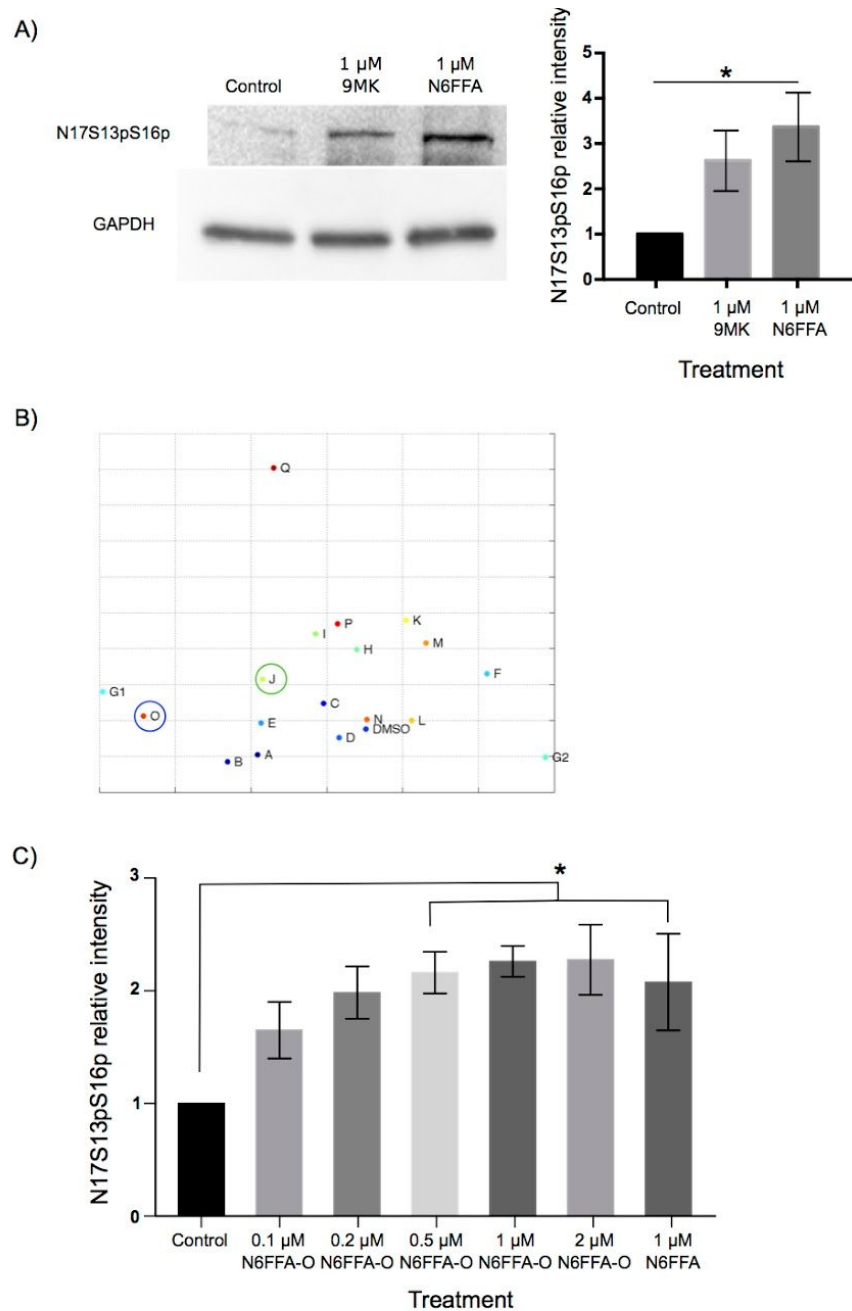


Figure 4.1. The effect of N6FFA derivatives on huntingtin N17 phosphorylation (A) STHdh^{Q111/Q111} cells were treated for 24 hours with with 1 μM N6FFA, 9DK, or vehicle control, 0.01% DMSO. A representative blot (left) and quantification (right) from n=3 immunoblotting experiments are shown, bars are mean±SEM *p<0.05. (B) Results of a screen of N6FFA derivatives, N6FFA is annotated as compound J (encircled in green), N6FFA-O (encircled in blue) was selected for further investigation. In a secondary assay, STHdh^{Q111/Q111} cells were treated with N6FFA-O at the

indicated concentrations or 1 μ M N6FFA for 24 h. Proteins were separated by SDS-PAGE and immunoblotted with an anti-N17S13pS16p antibody, the quantification of this analysis is presented in (C), bars are mean \pm SEM *p<0.05.

4.5 Increased inclusion of IKBKAP exon 20 by N6FFA treatment occurs through a mechanism unrelated to huntingtin phosphorylation by CK2

In addition to current investigations into the protective effects in HD and PD (418), N6FFA is also being explored as a potential treatment in a degenerative neuropathic condition known as familial dysautonomia (FD) (419). FD, or Riley-Day disease, is an autosomal recessive disorder that disproportionately affects the Ashkenazi Jewish population. This disease causes widespread sensory and autonomic dysfunction, leading to organ dysfunction and death, usually prior to age 30 (420).

In 1993 the FD causal mutation was mapped to chromosome 9 (421), and 8 years later, the same group narrowed this to two mutations in the IKBKAP gene (422). The majority of individuals possessed a T-to-C mutation in intron 20 of the IKBKAP gene that leads to tissue specific skipping of exon 20 in the IKK-complex-associated protein (IKAP) transcript (422). This mis-splicing results in a frameshift and leads to production of a truncated IKAP protein - a critical component of the Elongator complex involved in transcription of mRNA (423). Elongator is composed of 6 proteins, Elp1-6. IKAP, or Elp1, is responsible for scaffolding the Elongator complex and facilitating the activity of Elp3, which acts as a histone acetyltransferase (HAT), acetylating histone H3 and facilitating transcription of a subset of genes (424, 425). Although the identities of the

entirety of this subset are not fully known, a number of genes involved in cell motility seem to be regulated by the Elongator complex (426). In addition to its roles in the nucleus, Elongator also has a number of proposed roles in the cytoplasm, including actin skeleton organization via filamin A binding, regulation of exocytosis, and tRNA modification, and, most recently, as an α -tubulin acetyltransferase (427–430).

FD is not a fully penetrant disease in that, even in individuals homozygous for the FD mutation, the wild-type IKBKAP transcript is still produced, and the ratio of wild-type:mutant transcript (WT:MU) varies in a tissue-dependent manner (431). The WT:MU is highest in cultured patient lymphoblasts and lowest in central and nervous system tissues (431). This tissue-specific difference in splicing suggests that there are differences between tissues in the identity and levels of splice-associated RNA binding proteins (RBPs) (431). Recently, it has been found that N6FFA can correct exon 20 mis-splicing and is effective in increasing cellular IKAP levels, even in cells that do not possess the FD mutation (419, 432).

While there has been no implication of huntingtin in the development of FD in the past, the fact that N6FFA is having effects in both HD and FD is intriguing. A yeast two-hybrid screen has shown that huntingtin interacts with the IKAP protein (433); however, the effect of N6FFA in FD seems to be through correction of the splice defect (419). There has been some indirect evidence in the past that huntingtin may play a role in splicing. In 2002, Kegel *et al.* found that huntingtin colocalizes, amongst other things, with splice factor SC35 in the nucleus (93). Recently we were able to replicate this finding

with an independent antibody at nuclear puncta, indicating that these puncta are, in fact, nuclear splice speckles, suggesting huntingtin may be involved in the process of splicing, although the exact role of this protein in these regions is unknown (305). Consistent with this, huntingtin has been shown to regulate its own splicing and, in the context of mutant huntingtin, there are observable splice abnormalities in a number of different mRNA (434, 435). More recently, huntingtin has been shown to interact, and negatively regulate, its own mRNA (97) and mis-splicing of huntingtin has been suggested as a potential disease mechanism in HD (436). These data suggest that huntingtin could play a role in IKBKAP splicing that is modulated by N6FFA.

We first wanted to determine if there was an effect of N6FFA on IKBKAP splicing at the concentration at which we saw an effect on huntingtin phosphorylation. Increased proper splicing of the IKBKAP mRNA results in increased levels of the IKAP protein. Using this as a read-out, retinal pigment epithelial 1 (RPE1) cells were treated with 1 μ M N6FFA for 24 h and the levels of IKAP were determined. There was a consistent and significant increase in IKAP levels following N6FFA treatment, suggesting that, even at this low concentration, N6FFA can increase the incidence of proper IKBKAP mRNA splicing (**Figure 4.2a**). Therefore, it is possible that the effect of N6FFA on IKBKAP mRNA splicing may be through its effect on huntingtin. With this in mind, we knocked-down the huntingtin protein by siRNA to determine if there was an effect on IKAP levels. To our surprise, we did not see a corresponding decrease in IKAP levels, but instead noted a significant increase in IKAP levels (**Figure 4.2b**). This is

inconsistent with huntingtin phosphorylation increasing proper IKBKAP splicing, in fact, it suggests the opposite. Additionally, we noted that treatment with 9DK, which does not result in increased huntingtin phosphorylation, also increased IKAP levels, suggesting that the effect of N6FFA on IKBKAP splicing is not a result of this phenomenon (**Figure 4.2c**).

We also investigated splicing specifically using a splice reporter. This luciferase reporter contains exon 20 including the splice site mutated in FD. When exon 20 is correctly spliced, there is expression of the luciferase protein which can be measured using the Promega Dual-Luciferase Reporter System. This construct was a kind gift from the Slaugenhaupt lab, who initially described the effect of N6FFA on exon 20 inclusion in FD (422). To test whether this splice construct worked in our hands, immortalized human embryonic kidney (HEK293) cells were transfected for 24 h with 50 μ M N6FFA or DMSO control (**Figure 4.3a**). After confirmation of the response of the splice reporter to N6FFA, shown by the significant increase in luminescence, we then repeated this assay in *STHdh*^{Q7/Q7} and *STHdh*^{Q111/Q111} cells. N6FFA treatment significantly increased splicing in both cell types, but there was no difference in the effect of N6FFA on splicing between mutant and wild-type cells (**Figure 4.3b**).

Taken together, these results led us to conclude that, although the mechanism by which N6FFA increases inclusion of exon 20 is still undetermined, this mechanism is unlikely to be related to conversion of N6FFA to KTP and the subsequent phosphorylation of huntingtin N17. As a result, this avenue of investigation was

discontinued, but it would be interesting, in the future, to investigate further the connection between IKAP and huntingtin. Nguyen *et al.* proposed that the acetylation activity of Elongator on α -tubulin might promote anchoring of molecular motors and facilitate microtubule-based, intracellular trafficking, which is impaired in a number of neurodegenerative diseases, including HD (437). Therefore, it is possible that the protective effects of N6FFA in HD models could, in part, be due to increased activity of the Elongator complex in addition to the previously described increase in mutant huntingtin phosphorylation.

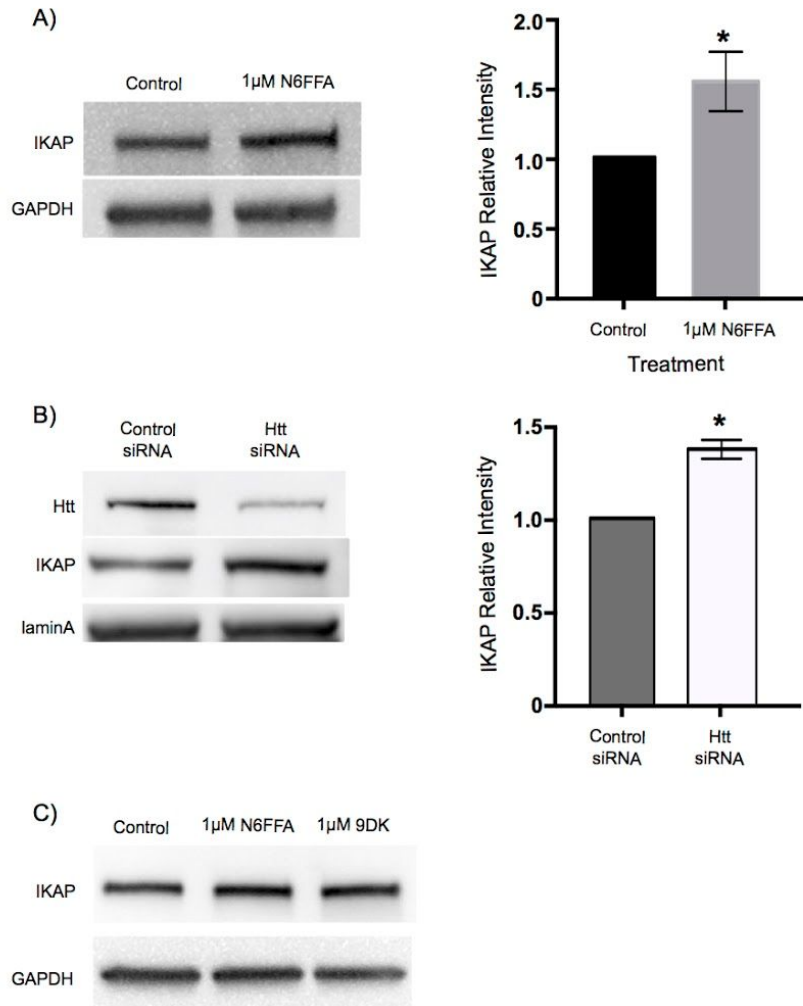


Figure 4.2. IKAP levels are modulated by huntingtin, but this effect does not seem to occur via N17 phosphorylation following N6FFA treatment A) RPE1(?) cells were treated for 24 hours with 1 μ M N6FFA or vehicle control, 0.01% DMSO. Cells were collected and lysed with RIPA buffer and proteins were separated by SDS-PAGE. IKAP levels were measured by immunoblotting, results were quantified for n=3 trials, *p<0.05. B) RPE1 cells were transfected with siRNA to huntingtin for 48 hours, after which time, cells were collected, lysed with RIPA and proteins were separated by SDS-PAGE. IKAP levels were measured by immunoblotting, results were quantified for n=3 trials, *p<0.05. C) Cells were treated with 1 μ M N6FFA, 9DK, or vehicle control, 0.01% DMSO, for 24 hours, protein levels were measured by immunoblotting.

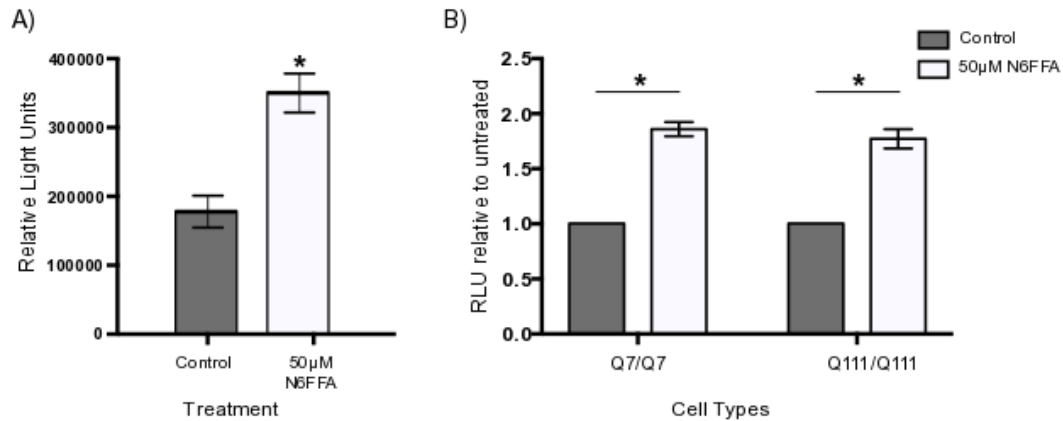


Fig 4.3. Treatment with N6FFA increases proper splicing of IKBKAP but there is no difference in this response between *STHdh*^{Q7/Q7} and *STHdh*^{Q111/Q111} A) HEK293 cells were transfected with an IKBKAP splice reporter construct and treated with N6FFA for 24 hours, * $p < 0.001$, $n = 3$. B) *STHdh*^{Q7/Q7} and *STHdh*^{Q111/Q111} were transfected with an IKBKAP splice reporter construct and treated with N6FFA for 24 hours. Results are shown relative to transfected, but untreated, control cells, * $p < 0.001$, $n = 3$.

4.6 N6FFA causes a consistent, but not significant, change in the ratio of globular to fibrillar type mutant huntingtin aggregates

We also wanted to show that N6FFA had an effect on a known cellular phenotype of mutant huntingtin. Our lab has previously found that the ratio of globular to fibrillar aggregates can be altered by the phosphorylation state of N17 (74). This study showed that cells expressing a fluorescently-tagged huntingtin exon1 construct with an expanded polyglutamine domain developed two types of huntingtin inclusions, loosely-packed globular inclusions, and tightly-packed fibrillar inclusions. Compounds known to increase N17 phosphorylation, as well as phospho-mimetic mutations of S13 and S16, shifted the ratio of globular:fibrillar inclusion formation towards fibrillar inclusions (74). Therefore,

to determine if N6FFA would have a similar effect on inclusion formation, *STHdh*^{Q111/Q111} cells were transfected with a fluorescently-tagged exon 1 fragment of huntingtin with 138 glutamine repeats (mCer-Exon1Q138-YFP) and the cells were subsequently treated with 1 μ M N6FFA or DMSO control. Following a 24 h incubation period, the number of globular and fibrillar inclusions were counted by a blinded investigator. Results in **Figure 4.4** show the percent change in the inclusion population upon N6FFA treatment. We saw a small but consistent trend towards decreased globular and increased fibrillar inclusions in cells treated with N6FFA, consistent with increased N17 phosphorylation, but this trend did not reach significance. This method of validation was discontinued as it was technically difficult and time consuming to acquire consistent results.

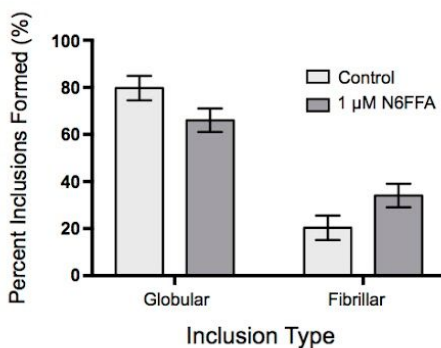


Figure 4.4. N6FFA influences inclusions formation (B) *STHdh*^{Q111/Q111} cells transfected with an Exon1Q138-YFP construct were treated with 1 μ M N6FFA and the number of globular and fibrillar inclusions were counted, quantification of n=3 trials is shown.

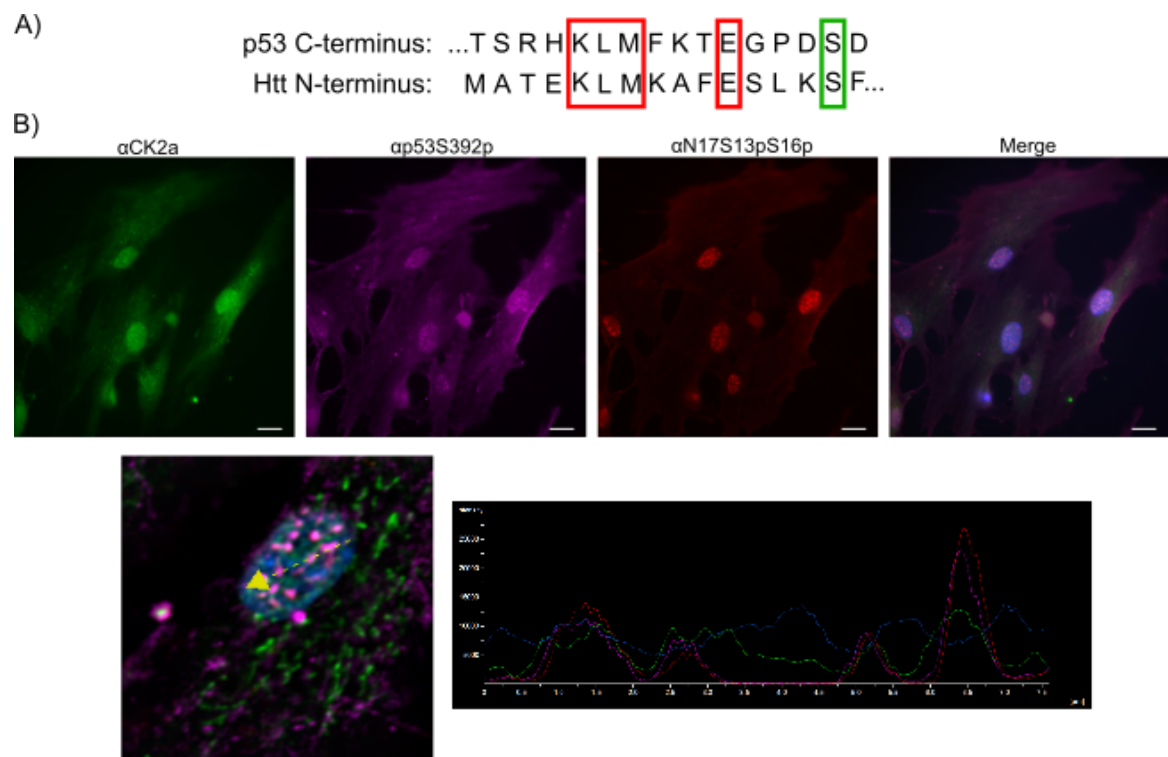
4.7 N6FFA increases phosphorylation of the p53 S392, which co-localizes with huntingtin at nuclear puncta and at sites of DNA damage.

While the N17 domain of huntingtin does not conform to the canonical phosphorylation consensus sequence for CK2, this pleiotropic kinase is known to phosphorylate a variety of substrate sequences (438). We therefore searched for known substrates of CK2 that possessed sequences similar to N17. The carboxyl terminus of tumor suppressor protein p53 has a serine residue at position 392 (S392) that is phosphorylated under diverse stress conditions, in part, by CK2 (439, 440). The sequence surrounding S392 is highly conserved in vertebrates (441) and has several key residues that align with N17, specifically residues K-L-M located at the -10, -9 and -8 positions, and E found at the -4 position relative to S392 (**Figure 4.4a**). We see that p53 phosphorylated at S392 site co-localizes with CK2 and N17 phosphorylated huntingtin at nuclear puncta, suggesting that p53 may be phosphorylated in a manner similar to huntingtin N17 at this site (**Figure 4.4b**). The priming of huntingtin by phosphorylation at S13 or S16, which we found necessary for CK2 kinase activity on N17, gives N17 additional charge similarity to the S392 substrate sequence. Consistent with the ability of CK2 to use KTP to phosphorylate its canonical substrates and N17, CK2 can use KTP to phosphorylate p53 S392 in the context of an *in vitro* kinase assay (**Figure 4.4c**). Furthermore, addition of N6FFA to *STHdh*^{Q111/Q111} cells increased phosphorylation of p53 at S389, the mouse homologue of human p53 S392 (**Figure 4.4d**). Together, these results

suggest a similar mechanism of action of CK2 on p53 and huntingtin, where the metabolic product of N6FFA, KTP, is used by CK2 on these similar substrate sequences. Both p53 S392 and N17 are phosphorylated in response to cellular stress (98, 439, 440); however, mutant huntingtin is hypophosphorylated at the N17 domain (287). It is therefore possible that the CK2-mediated stress response pathway is dysregulated in cells expressing polyglutamine-expanded huntingtin.

P53 is integral to the cellular response to stress, and the specific biological responses of this protein are controlled by protein expression levels and PTM patterns (442). Basal levels of p53 are, out of necessity, kept quite low, but this protein stands ready to form a stable complex upon DNA damage (443). Phosphorylation at S392 is associated with both increased formation of stable tetramers and regulation of the DNA binding domain of p53 (444). We know, from the work outlined in Chapter 2, that components of the N6FFA salvaging pathway co-localize at sites of microirradiation-induced DNA damage. To determine if phosphorylation of the p53 C-terminus by CK2 might also be a part of this pathway, we used a 405 nm laser to irradiate a line of DNA damage across the nuclei of cells. Following a 20-min incubation period, we saw enrichment of p53 S392p at these sites, along with N17S13pS16p, CK2 α , and N6FFA riboside (**Figure 4.5**). CK2 is a ubiquitous kinase known to modify proteins involved in DNA repair (445–447). We have found that CK2 can phosphorylate the N17 domain *in vitro*, and that it co-localizes with N17-phosphorylated huntingtin at sites of DNA damage. CK2 also phosphorylates p53 S392 in response to DNA damage (440),

which stabilizes the active form of p53 (448). The p53 S392p epitope, bearing sequence similarity to N17-S13pS16p, co-localized with huntingtin and CK2 at sites of DNA damage. Together, these findings point toward a functional interaction of these proteins. Co-regulation of huntingtin and p53 by CK2 would be complementary to previous reports describing transactivation of the huntingtin gene via p53 DNA-binding elements and the p53-dependent increase in huntingtin protein levels in response to DNA damage (173). Indeed, our work extends upon growing evidence that huntingtin has a role downstream of p53 in monitoring genomic integrity, implicated in HD pathology (51, 449, 450).



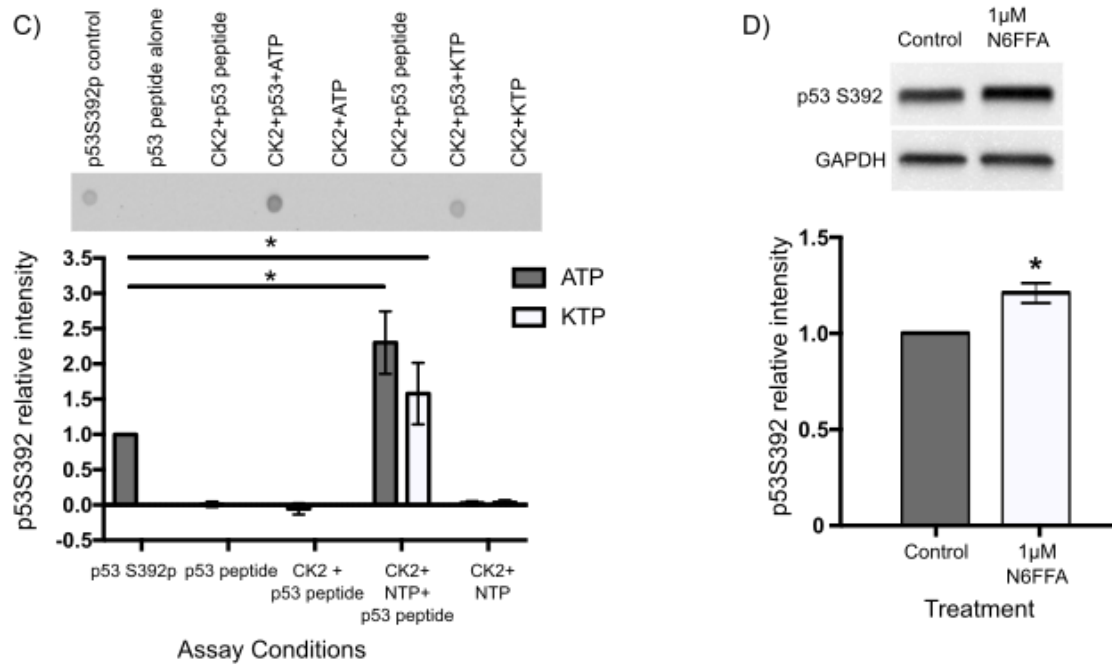


Figure 4.5. p53 S392 can be phosphorylated by CK2 using KTP and co-localizes with CK2 and phospho-huntingtin at nuclear puncta A) Sequence alignment of huntingtin N17 and the C-terminus of p53. B) Top panels show co-localization of CK2, p53 S392p, and N17S13pS16p at nuclear puncta in RPE1 cells; bottom panels show an enlarged, deconvolved RPE1 nucleus (left) and an intensity profile (right) across several nuclear puncta (line profile indicated by yellow arrow). Scale bars = 10 μ m. C) Representative blot (top) and quantification (bottom) of an *in vitro* p53 phosphorylation assay using CK2 with either ATP or KTP as phospho-donor, * $p < 0.05$, $n = 5$. D) Representative blot (top) and quantification (bottom) p53 S392p levels in *STHdh*^{Q111/Q111} cells after 24 hours treatment with N6FFA or control, * $p < 0.05$, $n = 3$.

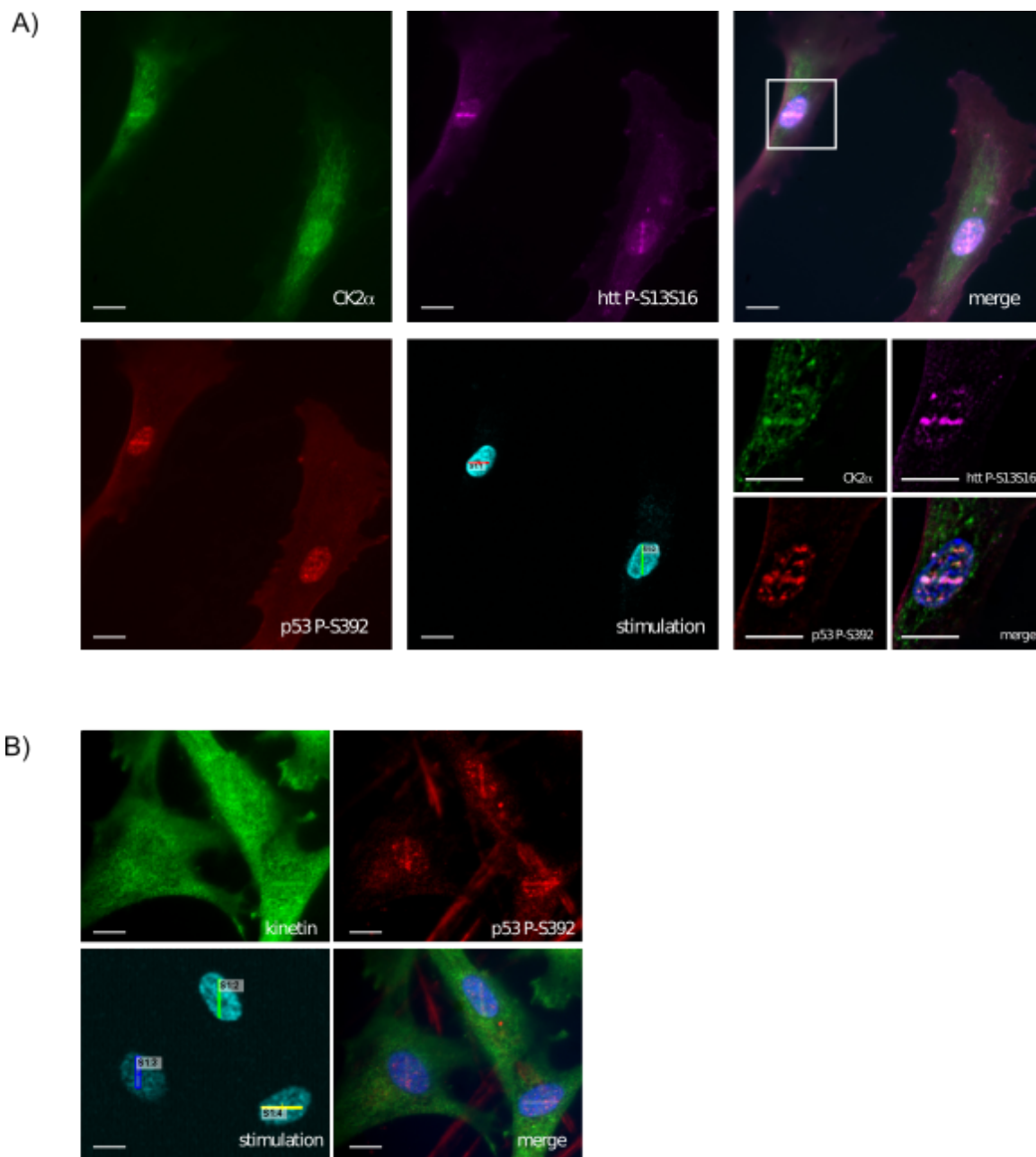


Figure 4.6. p53 S392p co-localizes with N6FFA/APRT/KTP/CK2/htt pathway at sites of DNA damage A) Upon microirradiation with a 405 nm laser, p53 S392p localizes to these sites of damage along with CK2 and N17S13pS16p. B) p53 S392p also co-localizes with N6FFA generated at these sites of laser-induced damage.

4.8 N6FFA riboside is elevated in cells expressing polyglutamine expanded huntingtin

There is mounting evidence that DNA repair is defective in HD. Previously, oxidative DNA damage in the form of the damaged nucleotide base 8-hydroxy-2-deoxyguanosine, has been noted in the urine, plasma, and striatum of HD mouse models (164), and it has been suggested that oxidative damage to DNA specifically may be a pathogenic mechanism in HD (228, 451, 452). Additionally, a recent GWAS has revealed that the most potent modifiers of HD age of onset to be those genes involved in mitochondrial function, redox control, and DNA damage repair (51).

Although it is well established that ROS levels, particularly in neurons, increase with age (144, 453), it is unclear in HD whether the apparently greater amount of ROS-related damage is due solely to increased ROS production or if this data also suggests that the cellular response to ROS stress is impaired. Our recent characterization of huntingtin as a part of the DNA damage repair response downstream of ATM (171) suggests that the improper functioning of mutant huntingtin may be the cause of defective repair of oxidative DNA damage. If this is true, we would expect to see increased N6FFA-riboside in the DNA of cells expressing polyglutamine-expanded huntingtin. Genomic DNA (gDNA) from hTERT immortalized human fibroblasts taken from a control individual and an HD patient with 43 glutamine repeats (TruHD-Q21Q18F and TruHD-Q43Q17M) was extracted and equal amounts were spotted onto a nitrocellulose

membrane. Immunoblotting with an N6FFA riboside antibody revealed that the HD cells had significantly more oxidative DNA damage, in the form of N6FFA riboside, than control cells (**Figure 4.7**) suggesting impaired repair of this oxidative lesion. This lack of excision would lead to lack of free N6FFA and, consequently, KTP, available for use by CK2. This may, in part, account for the hypo-phosphorylation of N17 in HD.

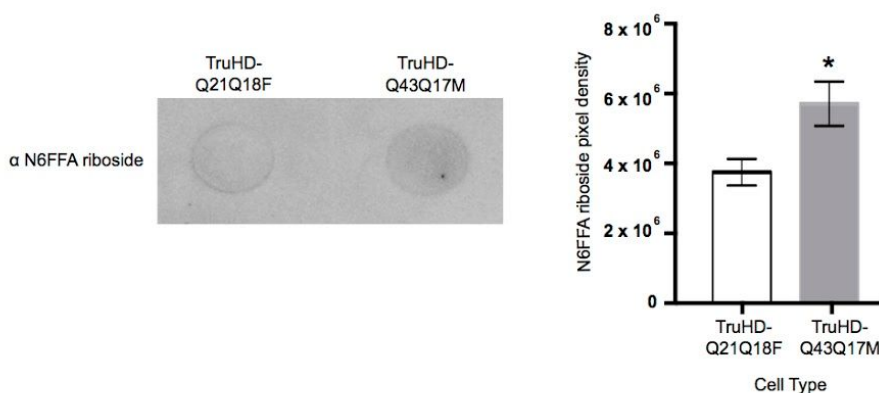


Figure 4.7. N6FFA riboside is increased in the genomic DNA of cells expressing mutant huntingtin. gDNA was extracted and spotted onto a nitrocellulose membrane and immunoblotted with an anti-N6FFA riboside antibody. A representative dot blot (left) and quantification of n=4 trials (right) are shown above.

4.9 N6-Furfuryladenine reduces DNA damage in *STHdh*^{Q111/Q111} cells upon MMS-induced stress

Finally, if N6FFA is upregulating the activity of CK2 on huntingtin as proposed in Chapter 2, and if it is also having a parallel action on p53, we should see increased DNA damage repair, and thus decreased DNA damage, in cells treated with N6FFA. To evaluate the extent of DNA damage, an alkaline comet assay was employed. In brief, *STHdh*^{Q7/Q7} and *STHdh*^{Q111/Q111} cells were treated with or without N6FFA for 24 h and then DNA damage was induced using methylmethanesulphonate (MMS). This assay

revealed that *STHdh*^{Q111/Q111} cells had significantly higher levels of DNA damage when treated with MMS than did *STHdh*^{Q7/Q7} cells. This damage was significantly decreased by treatment with N6FFA in *STHdh*^{Q111/Q111}, but not *STHdh*^{Q7/Q7}, cells (**Figure 4.8**). These results are consistent with our hypothesis that N6FFA may restore the DNA damage repair defect in HD through increasing phosphorylation of huntingtin and p53.

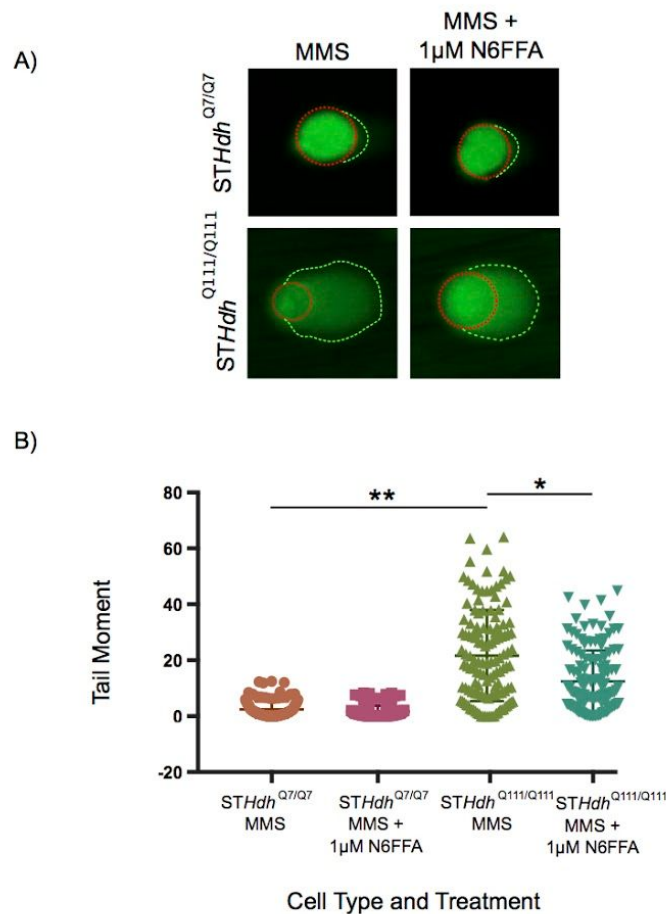


Figure 4.8. N6FFA decreases tail moment in *STHdh*^{Q111/Q111} cells with MMS-induced DNA damage. Cells were treated for 24 hours with kinetin and then stressed with MMS. Cells are lysed, suspended in low melt, and electrophoresis is performed. DNA is stained with Vista Green, and damaged DNA is measured by the amount of DNA in the “tail” of the comet, called the tail moment as measured by OpenComet. Increased tail moment is representative of the presence of increased DNA damage. (A) Representative images showing characteristic comets upon electrophoresis.

Red dashed areas show the comet head and green dashed areas show the comet tail. (B) Quantified results presented are from 1 trial with over 130 nuclei analysed per trial; * $p < 0.05$, ** $p < 0.001$.

4.10 Materials and Methods

Reagents and Antibodies

Polyclonal antibody against huntingtin phosphorylated at S13 and S16 of the N17 domain (anti-N17-S13pS16p, New England Peptides) was previously characterized and validated (71). Immunofluorescence antibodies: anti-N17S16pS16p (New England Peptides), anti-CK2 α (Abcam), anti-p53S392p (Santa Cruz), anti-N6FFA riboside (Agrisera). Secondary antibodies against rabbit, mouse, and goat IgG were conjugated to Alexa Fluor 488, 555, 594, or Cy5 (Invitrogen). Western primary antibodies: anti-N17S13pS16p (New England Peptides), anti-p53S392p (Abcam), and anti-GAPDH (Abcam). Secondary antibodies against rabbit and mouse IgG were conjugated to HRP (Abcam).

All peptides were made by GenScript with the following amino acid sequences:

p53 peptide (371-393):	SKKGQSTSRHKKLMFKTEGPDSD
P53 S392p peptide (371-393):	SKKGQSTSRHKKLMFKTEGPDpSD

Plasmids

Exon 1 fragments were cloned into an mCer-C1 plasmid with eYFP insert between BamHI and XbaI. Huntingtin exon 1 fragments were generated from cDNA using forward primer GATCTCCGGAATGGCGACCCTG with a BSPEI restriction site, and reverse primer GATCGGTACCGGGTTCGGTGCAGCGGCTC with a ACC65I

restriction site as described in (77). Renilla luciferase splice assay plasmid from the Slaughenhaupt lab contained IKBKAP exon 20 with intact splice sites.

Cells

Cells derived from mouse striatum, *STHdh*^{Q7/Q7} and *STHdh*^{Q111/Q111} (a kind gift from ME MacDonald), were grown in Dulbecco's modified Eagle's medium with 10% FBS at 33°C in a 5% CO₂ incubator. Human hTERT-immortalized foreskin fibroblast BJ-5ta cells (ATCC), primary human fibroblasts from Coriell Institute for Medical Research Biorepositories (ND30014 wild-type fibroblasts bearing 21/18 CAG repeats in *HTT* gene alleles), and immortalized human fibroblasts from control and HD patients (TruHD-Q21Q18F and TruHD-Q43Q17M, respectively) were grown in minimal Eagle's medium with 15% FBS and 1% Glutamax at 37°C with 5% CO₂. All media and supplements were from Gibco Life Technologies. HEK293 cells (ATCC) were grown in α -modified Eagle's medium with 10 % FBS at 37 °C in 5% CO₂. with 5% CO₂.

Treatment Protocol

All compounds were administered in cell-appropriate media with 0.2% FBS for 24 hours unless otherwise indicated.

Huntingtin Knockdown

RPE1 cells were transfected with siRNA to human huntingtin (Santa Cruz) using

lipofectamine RNAiMax (Invitrogen) diluted in Opti-MEM (Gibco) according to manufacturer's instructions.

Protein Extraction and Immunoblotting

Cells were lysed in either NP-40 lysis buffer (50 mM Tris-HCl pH 8.0, 150 mM NaCl, 1% NP-40) or RIPA lysis buffer (50 mM Tris-HCl pH 8.0, 150 mM NaCl, 1% NP-40, 0.25% sodium deoxycholate, 1 mM EDTA) containing protease and phosphatase inhibitors (Roche). Lysates were centrifuged at 17000 x *g* for 12 min and the supernatant was collected for immunoblot analysis. Equal amounts of protein were separated by SDS-PAGE on pre-cast 4-20% polyacrylamide gradient gels (Biorad) and electroblotted onto Immobilon poly-vinyl difluoride (PVDF) membrane (EMD Millipore). Membranes were blocked in TBS-T (50 mM Tris-HCl, pH 7.5, 150 mM NaCl, 0.1% Tween-20) containing 5% non-fat dry milk for 1.5 h at room temperature, followed by overnight incubation with primary antibodies diluted in blocking buffer at 4°C (anti-N17-S13pS16p 1:2500; anti-IKAP 1:1500; anti-GAPDH 1:7500, as appropriate). After 3x 15-min TBS-T washes, membranes were incubated with HRP-conjugated secondary antibodies diluted in blocking buffer (1:50000) for 45 min at room temperature, and visualized using Immobilon enhanced chemiluminescence HRP substrate (EMD Millipore) on a MicroChemi system (DNR Bio-imaging Systems). Bands were quantified using NIH Image J software and normalized to GAPDH controls.

Microscopy

Wide-field epifluorescence microscopy was done on a Nikon Eclipse Ti wide-field epifluorescent inverted microscope using the PLAN APO 60×/1.4 oil objective and Spectra X LED lamp (Lumencor, Beaverton, OR, USA). Images were captured using a Hamamatsu Orca-Flash 4.0 CMOS camera (Hamamatsu, Japan). Image acquisition and deconvolution of Z-stacks were done with NIS-Elements Advanced Research version 4.30 64-bit acquisition software (Nikon Instruments, Melville, NY, USA).

Super-resolution imaging was done on the Nikon N-SIM super-resolution microscope system attached to a Nikon Eclipse Ti inverted microscope using an APO TIRF 100×/1.49 oil objective, and 405 nm, 488 nm, and 561 nm lasers (Coherent Inc). Images were captured using a Hamamatsu Orca-Flash 4.0 CMOS camera and acquired with the NIS-Elements software version 4.50.

P53 Kinase Assay

Assays used 1000 ng peptides, as described above, incubated with 1 uL NEBuffer for Protein Kinases (New England Biolabs), 1000 ng ATP (Sigma-Aldrich) or KTP (Biolog) and 500 units CK2 (New England Biolabs) (specific activity 859,000 units/mg) for 1 hour in shaking incubator at 30°C. Following incubation, the reaction was stopped by placing on ice. 8 uL kinase assay mixture was spotted (2 uL x 4 replicates) onto nitrocellulose membrane and allowed to dry for 45 minutes. Membranes were blocked in 5 % non-fat milk in TBS-T for 1.5 hours and incubated in anti-p53S392p (1:1500)

overnight at 4°C on a rocker. Membranes were washed in TBS-T and incubated in the appropriate HRP-conjugated secondary antibody diluted in blocking buffer (1:50000) and were visualized using Immobilon enhanced chemiluminescence HRP substrate (EMD Millipore) using a MicroChemi system (DNR Bio-imaging Systems). Quantification was done using NIH Image J software.

Genomic DNA dot blot

TruHQ-Q21Q18F and TruHD-Q43Q17M cells were collected and gDNA was extracted using Purelink Genomic DNA Mini Kit (Invitrogen) according to manufacturer's instructions. From each sample 500 ng was diluted in autoclaved water to 9 uL volume and was then denatured for 20 min with 1 uL of 10 X denaturing solution (100 mM EDTA, 4M NaOH). Samples were then neutralized with 2M ice cold ammonium acetate and placed on ice. From each sample, 8 uL gDNA was spotted onto nitrocellulose membrane and was dried at 80 °C for 2 h. Blots were blocked in 5 % non-fat milk in TBS-T for 1 h and then immunoblotted as described above with anti-N6FFA riboside primary and anti-rabbit HRP secondary.

Comet Assay

STHdh^{Q7/Q7} and *STHdh*^{Q111/Q111} cells were grown to 60 % confluence and then treated for 24 hours with 1 µM N6FFA or DMSO control. Cells were then incubated in 0.01 % methylmethanesulphonate (MMS) (Sigma) for 15 minutes. Comet assay was

performed as in (171).

Statistical Analysis

All statistical calculations were performed using the Graphpad Prism 7 software. Results were considered significant if $p < 0.05$. Statistical tests were used as recommended by the software, with normal data using the student's t test or ANOVA, as appropriate, and non-normal data using Mann-Whitney or Kruskal-Wallis analysis, as appropriate.

CHAPTER 5

DISCUSSION AND FUTURE DIRECTIONS

5.1 Overview of major findings

Throughout my time as a Ph.D. student, I have worked to integrate high content analysis using a known disease phenotype with biochemical and cell biological techniques to identify lead compounds for HD therapeutics and also to learn more about the biological functions of the huntingtin protein. In short, this process of a primary screening assay, followed up by secondary validation and characterization has led to identification of a DNA damage product, N6FFA, as a modulator of huntingtin phosphorylation and mutant huntingtin toxicity. Follow-up assays led to validation of a previously suggested N17 kinase, CK2 (71), and, more importantly, the proposal of a novel DNA damage response pathway in which a product of said damage signals huntingtin phosphorylation, facilitating it to act as a scaffold in DNA damage. This is not the first time that a product of DNA damage has been shown to signal a cytoprotective downstream response. 8-oxo-dG, a common product of oxidative damage to guanine bases, complexes with its glycosylase, OGG1, to act a guanine nucleotide exchange factor (GEF) and activate mitogen activated protein kinase signalling (454, 455).

By the same methodology of screening and validation, another potential N17 kinase, PKC ζ , was identified. This atypical PKC has been previously noted in association with huntingtin, either with aggregated mutant huntingtin or as a part of the PAR3-aPKC complex, which mediates apical vesicular trafficking in polarized cells (406, 456). Atypical PKCs are unresponsive to calcium, phosphatidylinositol (3,4,5)-triphosphate

(PIP₃), and diacylglycerol (DG), but can be regulated by interactions with protein scaffolds, phosphatidylserine, ceramides, and neurotrophic factors (397, 457). Activation of PKC ζ by the ceramide derivative ganglioside GM1 could explain the effect of this compound on N17 phosphorylation (287). Additionally, similar to huntingtin, PKC ζ is responsive to oxidative stress and DNA damage (390, 393, 394). As we have shown that phosphorylation of the N17 domain by CK2 requires a “phospho-prime”, it is possible that PKC ζ is this priming kinase, phosphorylating S13 as predicted by GPS 2.0.

Finally, we also show that, through a mechanism identical to its action on N17, CK2 also uses KTP to phosphorylate p53 at S392. Modification at this residue is associated with p53 tetramerization and increased stability (444). It also releases carboxyl-terminal inhibition of the binding function of p53, allowing site-specific DNA binding of p53 (458). While there is no one kinase that is solely responsible for phosphorylation of this domain, CK2 specifically has been shown to phosphorylate p53 at S392 in response to UV-induced DNA damage in complex with a transcription elongator heterodimer, facilitates chromatin transcription (FACT) (459).

Based on these findings, we hypothesize a model where, under conditions of oxidative DNA damage, a product of this damage, N6FFA signals phosphorylation of huntingtin and p53, facilitating their participation in the DNA damage repair response. Phosphorylated huntingtin acts as a scaffold in the ATM complex during oxidative DNA damage repair and p53 fulfills its function as a transcription factor, increasing expression of DNA damage response proteins, including huntingtin. The presence of the N6FFA

derivative, KTP, is likely of importance during times of low cellular ATP, such as when cells are in the midst of responding to oxidative stress. In the presence of mutant huntingtin, excision of oxidative lesions is impaired, leading to decreased excision of N6FFA and thus minimal KTP production and phosphorylation of huntingtin N17 and p53 S392, further impairing cellular response to DNA damage. With the added stress of a high ADP:ATP ratio in HD (214, 318), and the high ROS load and energy needs of neurons, these factors culminate in neuronal death. Addition of exogenous N6FFA bypasses the need for BER and increases KTP levels artificially, allowing for increased phosphorylation of CK2 substrates huntingtin and p53 and restoration of DNA damage repair (**Figure 5.1**). As a result of this work, N6FFA derivatives are currently being tested in HD mouse models for efficacy in decreasing mutant huntingtin load in the cortex and striatum and for effects on HD-like phenotypes.

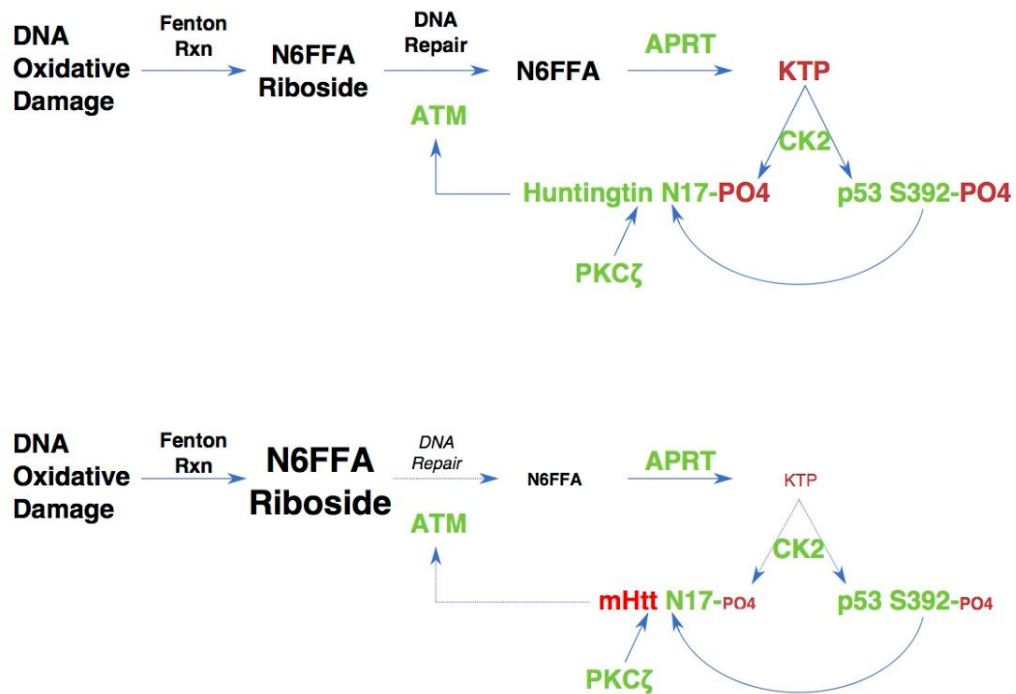


Figure 5.1: A metabolite of N6FFA increases N17 and p53 S392 phosphorylation in response to DNA damage. (Top) In a non-HD context, wild-type huntingtin acts as a part of the ATM complex to facilitate oxidative DNA damage repair. One of the products of this repair is N6FFA, which can be metabolized by APRT to produce KTP. KTP can be used by CK2 to phosphorylate huntingtin N17 and p53 S392. Phosphorylation of huntingtin N17 by CK2 requires a priming with another phospho-group, which may be added by the atypical PKC, PKC ζ . N17 phosphorylated huntingtin acts a scaffold in DNA damage repair, facilitating the release of more N6FFA until the damage is repaired. P53 facilitates DNA repair by acting as a transcription factor for DNA repair factors and, in dividing cells, arresting the cell cycle until damage is repaired. (Bottom) In the context of HD, this process is impaired as mutant huntingtin is hypo-phosphorylated and does not properly scaffold DNA repair. This leads to decreased excision of oxidative DNA damage products, including N6FFA. As a result there is less KTP, less phosphorylation of N17 and p53, which contributes to increasingly impaired DNA damage repair in a feedback loop.

5.2 DNA damage, p53, and the energy crisis in Huntington's Disease

During the process of aging, cells show signs of increased oxidative damage to DNA and other biomolecules. This damage has been linked to increased ROS production by the mitochondria as well as decreased activity of cellular antioxidant enzymes and DNA damage repair. In HD, DNA damage is further elevated, likely due to exacerbation

of these typical consequences of aging; a theory that is supported by the major pathways identified as modulators of age of onset in the recent GWAS: DNA repair, redox mechanisms, and mitochondrial function (51). Deficits in any of these processes can lead to impaired bioenergetics and cell death, particularly in high-energy cells such as neurons, and, indeed, neuronal dysfunction and neurodegeneration are common consequences of mutations in DNA repair genes in both mouse models and human patients (460, 461). It therefore follows that correction of these defects is likely to be protective.

This thesis presents analogous mechanisms of phosphorylation of DNA damage response proteins, huntingtin and p53, by protein kinase CK2, using the ATP analog, N6FFA. P53 has well known, and extensively documented, roles in the response to DNA damage, acting as an integrator of cellular responses to stress (462). Huntingtin also responds to DNA damage as a part of the ATM complex (171). This is consistent with the well-studied role of CK2 as a kinase for a number of DNA damage response proteins. CK2 is a heterotetrameric protein composed of 2 α and 2 β subunits, forming a holoenzyme, that is required for cell viability (463). The first indication that CK2 was involved in DNA damage repair came from the identification of p53 as a CK2 binding partner and substrate (464, 465). Subsequent studies showed that, upon UV-induced DNA damage, CK2 phosphorylated p53 at S392 (466–468). Depletion of CK2 by RNAi impairs the cellular response to DNA damage, highlighting the importance of this protein (469, 470). Specifically, depletion of CK2 was shown to attenuate phosphorylation of ATM at S1981, and Chk2 phosphorylation at T68, and decrease the formation of 53BP1

foci, which are critical for the repair of DNA DSBs (470). Conversely, increased activity of CK2 increases cleavage of the DNA damage product 8-oxo-dG, suggesting increased repair (471). Other DNA damage response proteins are directly phosphorylated by CK2, including xeroderma pigmentosa group B (XPB), apurinic/apyrimidinic endonuclease (APE), X-ray repair cross-complementing group 1 (XRCC1), and Msh1 and Msh6, in fact, most DNA damage repair mechanisms are, in some way, dependent on the activity of CK2 (472–476).

While it is likely that, under normal circumstances, CK2 utilizes the abundant cellular ATP as a source of energy for phosphorylation, the proposed KTP pathway becomes more important in situations where there is a shortage of this nucleotide triphosphate. During times when DNA damage is being repaired, there is a dramatic decrease in cellular levels of ATP due to the high energy cost of this process. This can be illustrated in the response of the DNA damage response protein, PARP-1. PARP-1 catalyzes assembly of poly(ADP-ribose) (PAR) chains, the result of which is depletion of cellular NAD^+ and ATP (477). In most cases, cells respond by increasing oxidative phosphorylation, but, especially in situations where mitochondrial respiration is impaired, this can lead to increased generation of oxygen free radicals and increased potential for additional damage to DNA (478). Additionally, excessive PARylation inhibits both glycolysis and oxidative phosphorylation, further depleting ATP stores, which can lead to apoptosis or necrosis (479). The process by which excessive PARylation induces cell death is called “parthanatos”.

In the context of HD, there is already low cellular ATP, which is exacerbated when DNA damage occurs (214). When cellular ATP levels are at these exceptionally low levels, KTP would provide a much needed source of phosphates for CK2 to phosphorylate its target proteins. Unfortunately, as DNA damage repair is impaired in HD cells (164, 171), less N6FFA would be excised to be converted to KTP; however, this lack of KTP could be overcome with addition of exogenous N6FFA, bypassing the need for intact oxidative DNA damage repair to produce this product. Consistent with this, there is a greater effect of N6FFA treatment on cells expressing mutant huntingtin than wild-type huntingtin with regards to huntingtin phosphorylation, protective effects in cell and animal models, and DNA repair under DNA-damaging conditions.

Future directions for this story will focus on the effect of N6FFA on other DNA damage response proteins that are substrates of CK2. It is likely that the effect of N6FFA on huntingtin and p53 phosphorylation is not restricted to these two proteins and that the protective effects of this compound in cell and animal models of HD are due to an overall increased activity of CK2 at a time when ATP is limited.

5.2.1 N6FFA riboside as a biomarker for Huntington's Disease

A long standing problem in HD is the lack of biomarkers that accurately correlate with disease progression. At present, most research has focused on CSF biomarkers, and, though there has been some success looking at mutant huntingtin levels (247), it would be beneficial if a biomarker could be found that was measurable in a more easily accessible

tissue, such as blood or skin fibroblasts. As previously mentioned, there is mounting evidence that DNA repair is defective in HD and that oxidative damage to DNA specifically may be a pathogenic mechanism (451, 452, 480). Given this, and our current hypothesis that there is impaired BER in HD due to the presence of mutant huntingtin, we would expect that oxidative lesions, such as N6FFA riboside, would correlate with disease progression.

In this thesis, we show that DNA-incorporated N6FFA riboside levels can be measured in skin fibroblasts and that this level is increased in HD. Though it remains to be seen if this level is correlated with disease progression, we propose that DNA-incorporated N6FFA may be a disease biomarker that can readily be measured in easily accessible tissue. To determine the validity of N6FFA as a biomarker of disease, levels of this DNA damaged product will be measured in human lymphocytes from HD patients that have been annotated from pre-manifest through the four Shoulson-Fahn stages of disease. In this way we will be able to determine if the level of DNA-incorporated N6FFA riboside is in any way correlated to disease progression.

5.3 The role of N6FFA and PINK1 in mitochondrial health and bioenergetics: implications for Huntington's Disease

As outlined in Chapter 1, there is strong evidence that mitochondrial dysfunction, disturbances in cellular energy homeostasis, and oxidative damage play a key role in HD pathogenesis. In addition to the action of N6FFA in DNA damage repair through CK2,

the salvaged form of this damaged nucleotide can also be used by PINK1 (311). PINK1 is a kinase that is mutated in a subset of early onset PD patients and has been characterized as a mitochondrial quality control protein. When mitochondria are healthy, PINK1 is quickly degraded, but when the mitochondrial membrane becomes depolarized, PINK1 is stabilized on the outer mitochondrial membrane and recruits the E3 ubiquitin ligase parkin (481). The kinase then phosphorylates both parkin and ubiquitin at S65, promoting arrest of mitochondrial movement and fusion, and removal of damaged mitochondria by selective autophagy, also called mitophagy (481–483). There are mutations in proteins in this PINK/parkin pathway in 3 variants of familial PD (206). In HD, deficient removal of damaged mitochondria has been reported in fly and cell models (484), and has been attributed to disruption of either autophagosome loading or fusion with the lysosome (158, 485). Interestingly, defective mitophagy in these fly and cell models of HD was corrected by over-expression of PINK1, resulting in increased ATP levels and survival in both models, suggesting that modulation of PINK1 activity may be a therapeutic target in HD (484). Based on these data, the effects of N6FFA on PINK1 activity and mitophagy will be an important avenue of future investigation, both further elucidating the mechanism by which N6FFA exerts its effects, both endogenously, in a biological context, and exogenously, as a potential HD therapeutic.

It should be noted that wild-type huntingtin itself is believed to have a physiological role in mitophagy that is disturbed by mutant huntingtin, although this role has not yet been characterized, nor has the manner in which mutant huntingtin interferes

with this role been determined. Never-the-less, evidence that the carboxyl-terminus of huntingtin bears remarkable similarity to yeast autophagy-related protein 11 (Atg11) and has been reported to interact with autophagy receptor, p62, as well as autophagy regulators BNIP3 and NIX, implies involvement of this protein in mitochondrial clearance (156). Therefore, it is also possible that increased phosphorylation of the mutant huntingtin protein by CK2 could restore its action in mitophagy and increase mitochondrial turnover, either in addition to, or instead of, upregulation of the PINK1/parkin pathway.

In addition to the role of PINK1/parkin in mitophagy, this pathway has also been implicated in mitochondrial biogenesis. Recently, it has been shown that PINK1 phosphorylates the pathological substrate of parkin, parkin interacting substrate (PARIS), priming it for ubiquitination by parkin and subsequent degradation by the proteasome (486). PARIS is elevated in sporadic and familial PD brains and is responsible for loss of dopaminergic neurons in parkin inactivation models of disease through repression of peroxisome proliferator-activated receptor gamma coactivator-1-alpha (PGC-1 α) (487–491). PGC-1 α is known to be the master regulator of mitochondrial biogenesis, in concert with nuclear respiratory factors 1 and 2 (Nrf1 and Nrf2) (492), tying PINK1 activity to both mitochondrial quality control and mitochondrial biogenesis. PGC-1 α has also been linked to HD pathogenesis, with impaired PGC-1 α activity and defective mitochondrial biogenesis being tied to striatal degeneration in PGC-1 α knockout mouse models (493). Additionally, in early-HD patient brains, and in several HD mouse models,

PGC-1 α mRNA levels are decreased, and upregulation of the PGC-1 α pathway by peroxisome proliferator-activated receptors (PPAR) agonists has shown promising, protective, results (494–496). This data suggests that not only is mitophagy impaired in HD, but mitochondrial biogenesis is also, which is consistent with the observation of morphologically abnormal mitochondria in HD patient brains, as well as the ATP deficiency in HD models (198, 214). Therefore, it would also be prudent to investigate the effects of N6FFA on PGC-1 α levels and mitochondrial biogenesis in HD models, as this too may contribute to the protective effects of this compound.

In HD, resting levels of cellular ATP are quite low compared to wild-type conditions (36, 214). This can likely be attributed to dysfunctional mitochondria and mitochondrial turnover and increased DNA damage with inefficient repair. Under stress conditions, both acute and as a result of aging, these deficiencies become more pronounced, resulting in an “energy crisis” and cell death, particularly in neurons. Although a number of mitochondria-targeting antioxidant molecules, as well as those upregulating mitochondrial biogenesis, have been tested and found to be protective in cell and animal models of disease (200, 275, 494, 497), we believe that N6FFA is unique in this category as it also addresses the DNA repair defects that also play a role in the progressive neuronal cell death in HD via a two-pronged effect on both CK2 and PINK1 (**Figure 5.2**), resulting in correction of the energy crisis and neuroprotection.

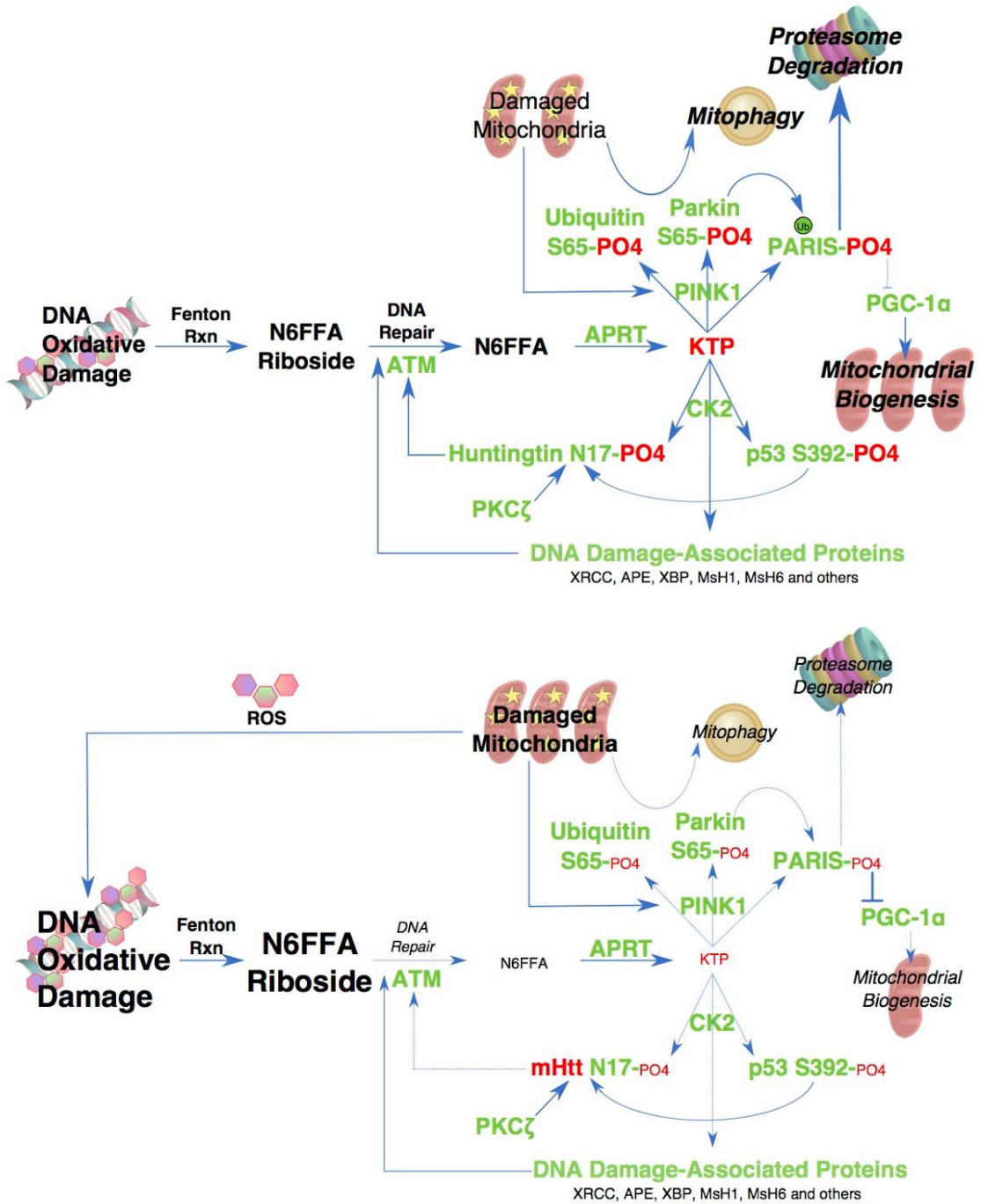


Figure 5.2. An expanded mechanism of action for DNA damage product N6FFA in DNA damage and mitochondrial turnover. (Top) In addition to the protective action of N6FFA in DNA damage repair through CK2, during times of ATP stress, it is also possible that there exists another protective mechanism through the kinase PINK1. PINK1 recruits and phosphorylates parkin and ubiquitin at S65, leading to turnover of damaged mitochondria by mitophagy. Additionally, PINK1 and parkin facilitate degradation of PARIS by the proteasome, resulting in increased

mitochondrial biogenesis through PGC-1 α . PINK1, like CK2, can utilize KTP to phosphorylate its substrates, which likely becomes a critical option during times of ATP stress. (Bottom) In the context of mutant huntingtin, less KTP is generated upon DNA damage, resulting in impairment of these processes and exacerbation of already low energy levels, or “energy crisis”.

5.4 Implication for other neurodegenerative diseases

The mechanism presented above, as well as the potential therapeutic applications of exogenously administered N6FFA, have implications not only for HD, but for other neurodegenerative diseases as well. Although these diseases, such as AD, PD, ALS, and the SCAs, differ in symptomatology as well as the primary neuronal type affected, they have a significant overlap in underlying pathology. Specifically, all of these diseases shown signs of prevalent DNA damage and dysfunctional bioenergetics (498–500). In some cases, as in HD and PD, mutations in proteins involved in either the DNA damage response pathway or the mitochondrial turnover pathway, respectively, have been directly implicated in disease development (171, 206), but even in those where no direct link has been found, defects in these two pathways still exist. Thus, identification of N6FFA as a modulator of mutant huntingtin function and toxicity through CK2, and the potential of this compound to correct DNA repair phenotypes has broad implications for neurodegenerative diseases in general, especially when taken with its known effect through PINK1 (418). We propose that there is a central mechanism in which both the processes of DNA damage repair and mitochondrial turnover are connected through a single DNA damage product. Therefore, it may be possible to target both of these dysfunctional pathways in neurodegenerative diseases simultaneously through exogenous

addition of N6FFA or a derivative thereof, and, indeed, protective effects of this compound in HD and PD have already been shown, both in this thesis, and in the literature (418).

5.5 Conclusions

The cellular processes of DNA damage repair and mitochondrial (dys)function and turnover are intricately connected, each with effects on the other (163, 501). When these processes are acting optimally, they promote DNA repair, energy production, and cell viability. When one of these pathways becomes dysfunctional, there are consequences in the others. In HD, this impairment may begin at the level of DNA damage repair due to improper function of the huntingtin scaffold (171). In PD, particularly in those variants arising from mutations in PINK1, parkin, and DJ-1, this impairment begins at the level of mitophagy (206). In fact, most neurodegenerative diseases have some evidence of impaired bioenergetics and/or response to DNA damage.

In this thesis, a mechanism is proposed where cells, when faced with ATP stress such as oxidative DNA damage, can use a product of the DNA damage as a source of energy. Specifically, two kinases, CK2 and PINK1, can utilize the N6FFA metabolite, KTP, to phosphorylate key substrates in DNA damage repair pathways and mitochondrial turnover pathways, respectively. Additionally, in HD there is decreased excision of N6FFA from damaged DNA and, consequently, decreased production of KTP, resulting in decreased activity of CK2 and PINK1 on their substrates in this time of ATP stress.

Dysfunctional DNA repair and mitochondria work in concert to create a cellular energy crisis and subsequent cell death. In HD models, this can be overcome by exogenous administration of N6FFA, which likely has a bifurcated cytoprotective mechanism through CK2 and PINK1. It makes sense that cells would evolve a mechanism to deal with both DNA damage and mitochondrial dysfunction through a pathway that utilizes an alternate source of energy, considering the incredibly low ATP in these conditions. The implications of this mechanism can be extended beyond just HD, to all neurodegenerative disorders where there are defects in DNA repair mechanisms and mitochondrial bioenergetics.

References

1. Roos RAC (2010) Huntington's disease: a clinical review. *Orphanet J Rare Dis* 5:40.
2. Tupper DE, Sondell SK (2004) Motor disorders and neuropsychological development: A historical appreciation. *Developmental motor disorders: A neuropsychological perspective*:3–25.
3. Tolosa E, Solé J (2004) Companion to Clinical Neurology 2nd Edition. William Pryse-Phillips. Oxford University Press, 2003. ISBN: 0-19-515938-1. *Clin Neurophysiol* 115(2):490–491.
4. Bhattacharyya KB (2016) The story of George Huntington and his disease. *Ann Indian Acad Neurol* 19(1):25–28.
5. Huntington G (1872) On chorea. Available at: <http://hdsa.org/wp-content/uploads/2017/08/On-Chorea.pdf>.
6. Donaldson IM, Marsden CD, Schneider SA, Bhatia KP (2012) Huntington's disease.
7. Paulsen JS, et al. (2001) Clinical markers of early disease in persons near onset of Huntington's disease. *Neurology* 57(4):658–662.
8. Lanska DJ, Lanska MJ, Lavine L, Schoenberg BS (1988) Conditions associated with Huntington's disease at death. A case-control study. *Arch Neurol* 45(8):878–880.
9. Sørensen SA, Fenger K (1992) Causes of death in patients with Huntington's disease and in unaffected first degree relatives. *J Med Genet* 29(12):911–914.
10. Yanagisawa N (1992) The spectrum of motor disorders in Huntington's disease. *Clin Neurol Neurosurg* 94 Suppl:S182–4.
11. Sturrock A, Leavitt BR (2010) The clinical and genetic features of Huntington disease. *J Geriatr Psychiatry Neurol* 23(4):243–259.
12. Butters N, Wolfe J, Martone M, Granholm E, Cermak LS (1985) Memory disorders associated with Huntington's disease: verbal recall, verbal recognition and procedural memory. *Neuropsychologia* 23(6):729–743.
13. Josiassen RC, Curry LM, Mancall EL (1983) Development of neuropsychological deficits in Huntington's disease. *Arch Neurol* 40(13):791–796.
14. Craufurd D, Thompson JC, Snowden JS (2001) Behavioral changes in Huntington

- Disease. *Neuropsychiatry Neuropsychol Behav Neurol* 14(4):219–226.
15. Eddy CM, Parkinson EG, Rickards HE (2016) Changes in mental state and behaviour in Huntington's disease. *Lancet Psychiatry* 3(11):1079–1086.
 16. Schoenfeld M, et al. (1984) Increased rate of suicide among patients with Huntington's disease. *J Neurol Neurosurg Psychiatry* 47(12):1283–1287.
 17. Sari Y (2011) Potential drugs and methods for preventing or delaying the progression of Huntington's disease. *Recent Pat CNS Drug Discov* 6(2):80–90.
 18. Vonsattel J-P, et al. (1985) Neuropathological Classification of Huntington's Disease. *J Neuropathol Exp Neurol* 44(6):559–577.
 19. Vonsattel JPG (2008) Huntington disease models and human neuropathology: similarities and differences. *Acta Neuropathol* 115(1):55–69.
 20. Ferrante RJ, et al. (1985) Selective sparing of a class of striatal neurons in Huntington's disease. *Science* 230(4725):561–563.
 21. Ferrante RJ, et al. (1987) Morphologic and histochemical characteristics of a spared subset of striatal neurons in Huntington's disease. *J Neuropathol Exp Neurol* 46(1):12–27.
 22. Reiner A, et al. (1988) Differential loss of striatal projection neurons in Huntington disease. *Proc Natl Acad Sci U S A* 85(15):5733–5737.
 23. Pillai JA, et al. (2012) Clinical severity of Huntington's disease does not always correlate with neuropathologic stage. *Mov Disord* 27(9):1099–1103.
 24. Vonsattel JPG, Keller C, Pilar Amaya M del (2008) Neuropathology of Huntington's Disease. *Handbook of Clinical Neurology* (Elsevier), pp 599–618.
 25. Vonsattel JP, DiFiglia M (1998) Huntington disease. *J Neuropathol Exp Neurol* 57(5):369–384.
 26. Kassubek J, et al. (2004) Topography of cerebral atrophy in early Huntington's disease: a voxel based morphometric MRI study. *J Neurol Neurosurg Psychiatry* 75(2):213–220.
 27. Politis M, et al. (2008) Hypothalamic involvement in Huntington's disease: an in vivo PET study. *Brain* 131(Pt 11):2860–2869.
 28. Rosas HD, et al. (2003) Evidence for more widespread cerebral pathology in early

- HD: an MRI-based morphometric analysis. *Neurology* 60(10):1615–1620.
29. Tabrizi SJ, et al. (2012) Potential endpoints for clinical trials in premanifest and early Huntington's disease in the TRACK-HD study: analysis of 24 month observational data. *Lancet Neurol* 11(1):42–53.
 30. Tabrizi SJ, et al. (2009) Biological and clinical manifestations of Huntington's disease in the longitudinal TRACK-HD study: cross-sectional analysis of baseline data. *Lancet Neurol* 8(9):791–801.
 31. Paulsen JS, et al. (2008) Detection of Huntington's disease decades before diagnosis: the Predict-HD study. *J Neurol Neurosurg Psychiatry* 79(8):874–880.
 32. Duff K, et al. (2010) Mild cognitive impairment in prediagnosed Huntington disease. *Neurology* 75(6):500–507.
 33. Stout JC, et al. (2011) Neurocognitive signs in prodromal Huntington disease. *Neuropsychology* 25(1):1–14.
 34. Menalled LB (2005) Knock-in mouse models of Huntington's disease. *NeuroRx* 2(3):465–470.
 35. Fossale E, et al. (2002) Identification of a presymptomatic molecular phenotype in Hdh CAG knock-in mice. *Hum Mol Genet* 11(19):2233–2241.
 36. Gines S, et al. (2003) Specific progressive cAMP reduction implicates energy deficit in presymptomatic Huntington's disease knock-in mice. *Hum Mol Genet* 12(5):497–508.
 37. Wheeler VC, et al. (2000) Long glutamine tracts cause nuclear localization of a novel form of huntingtin in medium spiny striatal neurons in HdhQ92 and HdhQ111 knock-in mice. *Hum Mol Genet* 9(4):503–513.
 38. Usdin MT, Shelbourne PF, Myers RM, Madison DV (1999) Impaired synaptic plasticity in mice carrying the Huntington's disease mutation. *Hum Mol Genet* 8(5):839–846.
 39. Gusella JF, et al. (1983) A polymorphic DNA marker genetically linked to Huntington's disease. *Nature* 306(5940):234–238.
 40. Wexler NS, et al. (2004) Venezuelan kindreds reveal that genetic and environmental factors modulate Huntington's disease age of onset. *Proc Natl Acad Sci U S A* 101(10):3498–3503.
 41. MacDonald ME, et al. (1993) A novel gene containing a trinucleotide repeat that is

- expanded and unstable on Huntington's disease chromosomes. *Cell* 72(6):971–983.
42. Squitieri F, et al. (2003) Homozygosity for CAG mutation in Huntington disease is associated with a more severe clinical course. *Brain* 126(Pt 4):946–955.
 43. Evans SJW, et al. (2013) Prevalence of adult Huntington's disease in the UK based on diagnoses recorded in general practice records. *J Neurol Neurosurg Psychiatry* 84(10):1156–1160.
 44. Stine OC, et al. (1993) Correlation between the onset age of Huntington's disease and length of the trinucleotide repeat in IT-15. *Hum Mol Genet* 2(10):1547–1549.
 45. McNeil SM, et al. (1997) Reduced penetrance of the Huntington's disease mutation. *Hum Mol Genet* 6(5):775–779.
 46. Duyao M, et al. (1993) Trinucleotide repeat length instability and age of onset in Huntington's disease. *Nat Genet* 4(4):387–392.
 47. Trottier Y, Biancalana V, Mandel JL (1994) Instability of CAG repeats in Huntington's disease: relation to parental transmission and age of onset. *J Med Genet* 31(5):377–382.
 48. McMurray CT (2010) Mechanisms of trinucleotide repeat instability during human development. *Nat Rev Genet* 11(11):786–799.
 49. Andrew SE, et al. (1993) The relationship between trinucleotide (CAG) repeat length and clinical features of Huntington's disease. *Nat Genet* 4(4):398–403.
 50. Nance MA, Myers RH (2001) Juvenile onset Huntington's disease—clinical and research perspectives. *Dev Disabil Res Rev* 7(3):153–157.
 51. Genetic Modifiers of Huntington's Disease (GeM-HD) Consortium (2015) Identification of Genetic Factors that Modify Clinical Onset of Huntington's Disease. *Cell* 162(3):516–526.
 52. Zoghbi HY, Orr HT (2000) Glutamine repeats and neurodegeneration. *Annu Rev Neurosci* 23:217–247.
 53. Behn-Krappa A, Doerfler W (1994) Enzymatic amplification of synthetic oligodeoxyribonucleotides: implications for triplet repeat expansions in the human genome. *Hum Mutat* 3(1):19–24.
 54. Crespan E, Hübscher U, Maga G (2015) Expansion of CAG triplet repeats by human DNA polymerases λ and β in vitro, is regulated by flap endonuclease 1 and DNA

- ligase 1. *DNA Repair* 29:101–111.
55. Truant R, et al. (2006) Canadian Association of Neurosciences Review: polyglutamine expansion neurodegenerative diseases. *Can J Neurol Sci* 33(3):278–291.
 56. Perutz MF (1996) Glutamine repeats and inherited neurodegenerative diseases: molecular aspects. *Curr Opin Struct Biol* 6(6):848–858.
 57. Orr HT (2000) The ins and outs of a polyglutamine neurodegenerative disease: spinocerebellar ataxia type 1 (SCA1). *Neurobiol Dis* 7(3):129–134.
 58. Takano H, Gusella JF (2002) The predominantly HEAT-like motif structure of huntingtin and its association and coincident nuclear entry with dorsal, an NF-kB/Rel/dorsal family transcription factor. *BMC Neurosci* 3:15.
 59. Andrade MA, Bork P (1995) HEAT repeats in the Huntington's disease protein. *Nat Genet* 11(2):115–116.
 60. Guo Q, et al. (2018) The cryo-electron microscopy structure of huntingtin. *Nature* 555(7694):117–120.
 61. Groves MR, Hanlon N, Turowski P, Hemmings BA, Barford D (1999) The structure of the protein phosphatase 2A PR65/A subunit reveals the conformation of its 15 tandemly repeated HEAT motifs. *Cell* 96(1):99–110.
 62. Groves MR, Barford D (1999) Topological characteristics of helical repeat proteins. *Curr Opin Struct Biol* 9(3):383–389.
 63. Kobe B, Kajava AV (2000) When protein folding is simplified to protein coiling: the continuum of solenoid protein structures. *Trends Biochem Sci* 25(10):509–515.
 64. Grinthal A, Adamovic I, Weiner B, Karplus M, Kleckner N (2010) PR65, the HEAT-repeat scaffold of phosphatase PP2A, is an elastic connector that links force and catalysis. *Proc Natl Acad Sci U S A* 107(6):2467–2472.
 65. Harjes P, Wanker EE (2003) The hunt for huntingtin function: interaction partners tell many different stories. *Trends Biochem Sci* 28(8):425–433.
 66. Shirasaki DI, et al. (2012) Network organization of the huntingtin proteomic interactome in mammalian brain. *Neuron* 75(1):41–57.
 67. Faber PW, et al. (1998) Huntingtin interacts with a family of WW domain proteins. *Hum Mol Genet* 7(9):1463–1474.

68. Kim MW, Chelliah Y, Kim SW, Otwinowski Z, Bezprozvanny I (2009) Secondary structure of Huntingtin amino-terminal region. *Structure* 17(9):1205–1212.
69. Atwal RS, et al. (2007) Huntingtin has a membrane association signal that can modulate huntingtin aggregation, nuclear entry and toxicity. *Hum Mol Genet* 16(21):2600–2615.
70. Maiuri T, Woloshansky T, Xia J, Truant R (2013) The huntingtin N17 domain is a multifunctional CRM1 and Ran-dependent nuclear and cilial export signal. *Hum Mol Genet* 22(7):1383–1394.
71. Atwal RS, et al. (2011) Kinase inhibitors modulate huntingtin cell localization and toxicity. *Nat Chem Biol* 7(7):453–460.
72. Gu X, et al. (2009) Serines 13 and 16 are critical determinants of full-length human mutant huntingtin induced disease pathogenesis in HD mice. *Neuron* 64(6):828–840.
73. Gu X, et al. (2015) N17 Modifies mutant Huntingtin nuclear pathogenesis and severity of disease in HD BAC transgenic mice. *Neuron* 85(4):726–741.
74. Caron NS, Hung CL, Atwal RS, Truant R (2014) Live cell imaging and biophotonic methods reveal two types of mutant huntingtin inclusions. *Hum Mol Genet* 23(9):2324–2338.
75. Tanaka M, Morishima I, Akagi T, Hashikawa T, Nukina N (2001) Intra- and intermolecular beta-pleated sheet formation in glutamine-repeat inserted myoglobin as a model for polyglutamine diseases. *J Biol Chem* 276(48):45470–45475.
76. Chen S, Bertheliev V, Yang W, Wetzel R (2001) Polyglutamine aggregation behavior in vitro supports a recruitment mechanism of cytotoxicity1. *J Mol Biol* 311(1):173–182.
77. Caron NS, Desmond CR, Xia J, Truant R (2013) Polyglutamine domain flexibility mediates the proximity between flanking sequences in huntingtin. *Proc Natl Acad Sci U S A* 110(36):14610–14615.
78. Crick SL, Ruff KM, Garai K, Frieden C, Pappu RV (2013) Unmasking the roles of N- and C-terminal flanking sequences from exon 1 of huntingtin as modulators of polyglutamine aggregation. *Proc Natl Acad Sci U S A* 110(50):20075–20080.
79. Chen M, Wolynes PG (2017) Aggregation landscapes of Huntingtin exon 1 protein fragments and the critical repeat length for the onset of Huntington’s disease. *Proc Natl Acad Sci U S A* 114(17):4406–4411.

80. Desmond CR, Atwal RS, Xia J, Truant R (2012) Identification of a karyopherin $\beta 1/\beta 2$ proline-tyrosine nuclear localization signal in huntingtin protein. *J Biol Chem* 287(47):39626–39633.
81. Xia J, Lee DH, Taylor J, Vandelft M, Truant R (2003) Huntingtin contains a highly conserved nuclear export signal. *Hum Mol Genet* 12(12):1393–1403.
82. Strong TV, et al. (1993) Widespread expression of the human and rat Huntington's disease gene in brain and nonneural tissues. *Nat Genet* 5(3):259–265.
83. DiFiglia M, et al. (1995) Huntingtin is a cytoplasmic protein associated with vesicles in human and rat brain neurons. *Neuron* 14(5):1075–1081.
84. Hoogeveen AT, et al. (1993) Characterization and localization of the Huntington disease gene product. *Hum Mol Genet* 2(12):2069–2073.
85. De Rooij KE, Dorsman JC, Smoor MA, Den Dunnen JT, Van Ommen GJ (1996) Subcellular localization of the Huntington's disease gene product in cell lines by immunofluorescence and biochemical subcellular fractionation. *Hum Mol Genet* 5(8):1093–1099.
86. Hoffner G, Kahlem P, Djian P (2002) Perinuclear localization of huntingtin as a consequence of its binding to microtubules through an interaction with beta-tubulin: relevance to Huntington's disease. *J Cell Sci* 115(Pt 5):941–948.
87. Angeli S, Shao J, Diamond MI (2010) F-actin binding regions on the androgen receptor and huntingtin increase aggregation and alter aggregate characteristics. *PLoS One* 5(2):e9053.
88. Munsie L, et al. (2011) Mutant huntingtin causes defective actin remodeling during stress: defining a new role for transglutaminase 2 in neurodegenerative disease. *Hum Mol Genet* 20(10):1937–1951.
89. Godin JD, et al. (2010) Huntingtin is required for mitotic spindle orientation and mammalian neurogenesis. *Neuron* 67(3):392–406.
90. Burke KA, Hensal KM, Umbaugh CS, Chaibva M, Legleiter J (2013) Huntingtin disrupts lipid bilayers in a polyQ-length dependent manner. *Biochim Biophys Acta* 1828(8):1953–1961.
91. Michalek M, Salnikov ES, Werten S, Bechinger B (2013) Membrane interactions of the amphipathic amino terminus of huntingtin. *Biochemistry* 52(5):847–858.
92. Tao T, Tartakoff AM (2001) Nuclear relocation of normal huntingtin. *Traffic*

2(6):385–394.

93. Kegel KB, et al. (2002) Huntingtin is present in the nucleus, interacts with the transcriptional corepressor C-terminal binding protein, and represses transcription. *J Biol Chem* 277(9):7466–7476.
94. Hilditch-Maguire P, et al. (2000) Huntingtin: an iron-regulated protein essential for normal nuclear and perinuclear organelles. *Hum Mol Genet* 9(19):2789–2797.
95. Benn CL, et al. (2008) Huntingtin Modulates Transcription, Occupies Gene Promoters In Vivo, and Binds Directly to DNA in a Polyglutamine-Dependent Manner. *J Neurosci* 28(42):10720–10733.
96. Savas JN, et al. (2010) A role for huntington disease protein in dendritic RNA granules. *J Biol Chem* 285(17):13142–13153.
97. Culver BP, et al. (2016) Huntington's Disease Protein Huntingtin Associates with its own mRNA. *J Huntingtons Dis* 5(1):39–51.
98. DiGiovanni LF, Mocle AJ, Xia J, Truant R (2016) Huntingtin N17 domain is a reactive oxygen species sensor regulating huntingtin phosphorylation and localization. *Hum Mol Genet* 25(18):3937–3945.
99. Zuccato C, Valenza M, Cattaneo E (2010) Molecular mechanisms and potential therapeutical targets in Huntington's disease. *Physiol Rev* 90(3):905–981.
100. Menalled LB, Sison JD, Dragatsis I, Zeitlin S, Chesselet M-F (2003) Time course of early motor and neuropathological anomalies in a knock-in mouse model of Huntington's disease with 140 CAG repeats. *J Comp Neurol* 465(1):11–26.
101. Hickey MA, Chesselet M-F (2003) The use of transgenic and knock-in mice to study Huntington's disease. *Cytogenet Genome Res* 100(1-4):276–286.
102. Lin CH, et al. (2001) Neurological abnormalities in a knock-in mouse model of Huntington's disease. *Hum Mol Genet* 10(2):137–144.
103. Huang CC, et al. (1998) Amyloid formation by mutant huntingtin: threshold, progressivity and recruitment of normal polyglutamine proteins. *Somat Cell Mol Genet* 24(4):217–233.
104. Saudou F, Finkbeiner S, Devys D, Greenberg ME (1998) Huntingtin acts in the nucleus to induce apoptosis but death does not correlate with the formation of intranuclear inclusions. *Cell* 95(1):55–66.
105. Kuemmerle S, et al. (1999) Huntingtin aggregates may not predict neuronal death

- in Huntington's disease. *Ann Neurol* 46(6):842–849.
106. MacDonald ME (2003) Huntingtin: alive and well and working in middle management. *Sci STKE* 2003(207):e48.
 107. Duyao MP, et al. (1995) Inactivation of the mouse Huntington's disease gene homolog Hdh. *Science* 269(5222):407–410.
 108. Nasir J, et al. (1995) Targeted disruption of the Huntington's disease gene results in embryonic lethality and behavioral and morphological changes in heterozygotes. *Cell* 81(5):811–823.
 109. Nguyen GD, Molero AE, Gokhan S, Mehler MF (2013) Functions of huntingtin in germ layer specification and organogenesis. *PLoS One* 8(8):e72698.
 110. Dragatsis I, Efstratiadis A, Zeitlin S (1998) Mouse mutant embryos lacking huntingtin are rescued from lethality by wild-type extraembryonic tissues. *Development* 125(8):1529–1539.
 111. Liu J-P, Zeitlin SO (2017) Is Huntingtin Dispensable in the Adult Brain? *J Huntingtons Dis* 6(1):1–17.
 112. Dragatsis I, Levine MS, Zeitlin S (2000) Inactivation of Hdh in the brain and testis results in progressive neurodegeneration and sterility in mice. *Nat Genet* 26(3):300–306.
 113. Arteaga-Bracho EE, et al. (2016) Postnatal and adult consequences of loss of huntingtin during development: Implications for Huntington's disease. *Neurobiol Dis* 96:144–155.
 114. Yao J, Ong S-E, Bajjalieh S (2014) Huntingtin is associated with cytomatrix proteins at the presynaptic terminal. *Mol Cell Neurosci* 63:96–100.
 115. Sun Y, Savanenin A, Reddy PH, Liu YF (2001) Polyglutamine-expanded huntingtin promotes sensitization of N-methyl-D-aspartate receptors via post-synaptic density 95. *J Biol Chem* 276(27):24713–24718.
 116. Garcia EP, et al. (1998) SAP90 binds and clusters kainate receptors causing incomplete desensitization. *Neuron* 21(4):727–739.
 117. Migaud M, et al. (1998) Enhanced long-term potentiation and impaired learning in mice with mutant postsynaptic density-95 protein. *Nature* 396(6710):433–439.
 118. Sattler R, et al. (1999) Specific coupling of NMDA receptor activation to nitric

- oxide neurotoxicity by PSD-95 protein. *Science* 284(5421):1845–1848.
119. Modregger J, DiProspero NA, Charles V, Tagle DA, Plomann M (2002) PACSIN 1 interacts with huntingtin and is absent from synaptic varicosities in presymptomatic Huntington's disease brains. *Hum Mol Genet* 11(21):2547–2558.
 120. Pérez-Otaño I, et al. (2006) Endocytosis and synaptic removal of NR3A-containing NMDA receptors by PACSIN1/syndapin1. *Nat Neurosci* 9(5):611–621.
 121. Tabrizi SJ, et al. (1999) Biochemical abnormalities and excitotoxicity in Huntington's disease brain. *Ann Neurol* 45(1):25–32.
 122. Borrell-Pages M, Zala D, Humbert S, Saudou F (2006) Huntington's disease: from huntingtin function and dysfunction to therapeutic strategies. *Cell Mol Life Sci* 63(22):2642–2660.
 123. Block-Galarza J, et al. (1997) Fast transport and retrograde movement of huntingtin and HAP 1 in axons. *Neuroreport* 8(9-10):2247–2251.
 124. Caviston JP, Ross JL, Antony SM, Tokito M, Holzbaur ELF (2007) Huntingtin facilitates dynein/dynactin-mediated vesicle transport. *Proc Natl Acad Sci U S A* 104(24):10045–10050.
 125. Engelender S, et al. (1997) Huntingtin-associated protein 1 (HAP1) interacts with the p150Glued subunit of dynactin. *Hum Mol Genet* 6(13):2205–2212.
 126. McGuire JR, Rong J, Li S-H, Li X-J (2006) Interaction of Huntingtin-associated protein-1 with kinesin light chain: implications in intracellular trafficking in neurons. *J Biol Chem* 281(6):3552–3559.
 127. Gunawardena S, et al. (2003) Disruption of axonal transport by loss of huntingtin or expression of pathogenic polyQ proteins in Drosophila. *Neuron* 40(1):25–40.
 128. Gauthier LR, et al. (2004) Huntingtin controls neurotrophic support and survival of neurons by enhancing BDNF vesicular transport along microtubules. *Cell* 118(1):127–138.
 129. Zala D, et al. (2008) Phosphorylation of mutant huntingtin at S421 restores anterograde and retrograde transport in neurons. *Hum Mol Genet* 17(24):3837–3846.
 130. Colin E, et al. (2008) Huntingtin phosphorylation acts as a molecular switch for anterograde/retrograde transport in neurons. *EMBO J* 27(15):2124–2134.
 131. Altar CA, et al. (1997) Anterograde transport of brain-derived neurotrophic factor

- and its role in the brain. *Nature* 389(6653):856–860.
132. Baquet ZC, Gorski JA, Jones KR (2004) Early striatal dendrite deficits followed by neuron loss with advanced age in the absence of anterograde cortical brain-derived neurotrophic factor. *J Neurosci* 24(17):4250–4258.
 133. Ferrer I, Goutan E, Marín C, Rey MJ, Ribalta T (2000) Brain-derived neurotrophic factor in Huntington disease. *Brain Res* 866(1-2):257–261.
 134. Humbert S, et al. (2002) The IGF-1/Akt pathway is neuroprotective in Huntington's disease and involves Huntingtin phosphorylation by Akt. *Dev Cell* 2(6):831–837.
 135. Merdes A, Heald R, Samejima K, Earnshaw WC, Cleveland DW (2000) Formation of spindle poles by dynein/dynactin-dependent transport of NuMA. *J Cell Biol* 149(4):851–862.
 136. Pfarr CM, et al. (1990) Cytoplasmic dynein is localized to kinetochores during mitosis. *Nature* 345(6272):263–265.
 137. Steuer ER, Wordeman L, Schroer TA, Sheetz MP (1990) Localization of cytoplasmic dynein to mitotic spindles and kinetochores. *Nature* 345(6272):266–268.
 138. Quinyne NJ, et al. (1999) Dynactin is required for microtubule anchoring at centrosomes. *J Cell Biol* 147(2):321–334.
 139. Sawin KE, LeGuellec K, Philippe M, Mitchison TJ (1992) Mitotic spindle organization by a plus-end-directed microtubule motor. *Nature* 359(6395):540–543.
 140. Martin EJ, et al. (1999) Analysis of Huntingtin-associated protein 1 in mouse brain and immortalized striatal neurons. *J Comp Neurol* 403(4):421–430.
 141. Molina-Calavita M, et al. (2014) Mutant huntingtin affects cortical progenitor cell division and development of the mouse neocortex. *J Neurosci* 34(30):10034–10040.
 142. Godin JD, Humbert S (2011) Mitotic spindle: focus on the function of huntingtin. *Int J Biochem Cell Biol* 43(6):852–856.
 143. Chan DC (2006) Mitochondria: dynamic organelles in disease, aging, and development. *Cell* 125(7):1241–1252.
 144. Chen X, Guo C, Kong J (2012) Oxidative stress in neurodegenerative diseases. *Neural Regeneration Res* 7(5):376–385.

145. Jenkins BG, et al. (2005) Effects of CAG repeat length, HTT protein length and protein context on cerebral metabolism measured using magnetic resonance spectroscopy in transgenic mouse models of Huntington's disease. *J Neurochem* 95(2):553–562.
146. Milakovic T, Johnson GVW (2005) Mitochondrial respiration and ATP production are significantly impaired in striatal cells expressing mutant huntingtin. *J Biol Chem* 280(35):30773–30782.
147. Ludolph AC, He F, Spencer PS, Hammerstad J, Sabri M (1991) 3-Nitropropionic acid-exogenous animal neurotoxin and possible human striatal toxin. *Can J Neurol Sci* 18(4):492–498.
148. Palfi S, et al. (1996) Chronic 3-nitropropionic acid treatment in baboons replicates the cognitive and motor deficits of Huntington's disease. *J Neurosci* 16(9):3019–3025.
149. Guedes-Dias P, et al. (2015) HDAC6 inhibition induces mitochondrial fusion, autophagic flux and reduces diffuse mutant huntingtin in striatal neurons. *Biochim Biophys Acta* 1852(11):2484–2493.
150. Pellman JJ, Hamilton J, Brustovetsky T, Brustovetsky N (2015) Ca²⁺ handling in isolated brain mitochondria and cultured neurons derived from the YAC128 mouse model of Huntington's disease. *J Neurochem* 134(4):652–667.
151. Trushina E, et al. (2004) Mutant huntingtin impairs axonal trafficking in mammalian neurons in vivo and in vitro. *Mol Cell Biol* 24(18):8195–8209.
152. Gutekunst CA, et al. (1998) The cellular and subcellular localization of huntingtin-associated protein 1 (HAP1): comparison with huntingtin in rat and human. *J Neurosci* 18(19):7674–7686.
153. Caviston JP, Holzbaur ELF (2009) Huntingtin as an essential integrator of intracellular vesicular trafficking. *Trends Cell Biol* 19(4):147–155.
154. Ismailoglu I, et al. (2014) Huntingtin protein is essential for mitochondrial metabolism, bioenergetics and structure in murine embryonic stem cells. *Dev Biol* 391(2):230–240.
155. Choo YS, Johnson GVW, MacDonald M, Detloff PJ, Lesort M (2004) Mutant huntingtin directly increases susceptibility of mitochondria to the calcium-induced permeability transition and cytochrome c release. *Hum Mol Genet* 13(14):1407–1420.

156. Ochaba J, et al. (2014) Potential function for the Huntingtin protein as a scaffold for selective autophagy. *Proc Natl Acad Sci U S A* 111(47):16889–16894.
157. Komatsu M, et al. (2006) Loss of autophagy in the central nervous system causes neurodegeneration in mice. *Nature* 441(7095):880–884.
158. Wong YC, Holzbaur ELF (2014) The regulation of autophagosome dynamics by huntingtin and HAP1 is disrupted by expression of mutant huntingtin, leading to defective cargo degradation. *J Neurosci* 34(4):1293–1305.
159. Morimoto RI (2008) Proteotoxic stress and inducible chaperone networks in neurodegenerative disease and aging. *Genes Dev* 22(11):1427–1438.
160. Drummond IA, McClure SA, Poenie M, Tsien RY, Steinhardt RA (1986) Large changes in intracellular pH and calcium observed during heat shock are not responsible for the induction of heat shock proteins in *Drosophila melanogaster*. *Mol Cell Biol* 6(5):1767–1775.
161. Nath S, Munsie LN, Truant R (2015) A huntingtin-mediated fast stress response halting endosomal trafficking is defective in Huntington's disease. *Hum Mol Genet* 24(2):450–462.
162. Illuzzi J, Yerkes S, Parekh-Olmedo H, Kmiec EB (2009) DNA breakage and induction of DNA damage response proteins precede the appearance of visible mutant huntingtin aggregates. *J Neurosci Res* 87(3):733–747.
163. Acevedo-Torres K, et al. (2009) Mitochondrial DNA damage is a hallmark of chemically induced and the R6/2 transgenic model of Huntington's disease. *DNA Repair* 8(1):126–136.
164. Bogdanov MB, Andreassen OA, Dedeoglu A, Ferrante RJ, Beal MF (2001) Increased oxidative damage to DNA in a transgenic mouse model of Huntington's disease. *J Neurochem* 79(6):1246–1249.
165. Browne SE, et al. (1997) Oxidative damage and metabolic dysfunction in Huntington's disease: selective vulnerability of the basal ganglia. *Ann Neurol* 41(5):646–653.
166. Enokido Y, et al. (2010) Mutant huntingtin impairs Ku70-mediated DNA repair. *J Cell Biol* 189(3):425–443.
167. Khoronenkova SV, Dianov GL (2015) ATM prevents DSB formation by coordinating SSB repair and cell cycle progression. *Proc Natl Acad Sci U S A*

- 112(13):3997–4002.
168. Guo Z, Kozlov S, Lavin MF, Person MD, Paull TT (2010) ATM activation by oxidative stress. *Science* 330(6003):517–521.
169. Bakkenist CJ, Kastan MB (2003) DNA damage activates ATM through intermolecular autophosphorylation and dimer dissociation. *Nature* 421(6922):499–506.
170. Lu X-H, et al. (2014) Targeting ATM ameliorates mutant Huntingtin toxicity in cell and animal models of Huntington’s disease. *Sci Transl Med* 6(268):268ra178.
171. Maiuri T, et al. (2017) Huntingtin is a scaffolding protein in the ATM oxidative DNA damage response complex. *Hum Mol Genet* 26(2):395–406.
172. Anne SL, Saudou F, Humbert S (2007) Phosphorylation of huntingtin by cyclin-dependent kinase 5 is induced by DNA damage and regulates wild-type and mutant huntingtin toxicity in neurons. *J Neurosci* 27(27):7318–7328.
173. Feng Z, et al. (2006) p53 tumor suppressor protein regulates the levels of huntingtin gene expression. *Oncogene* 25(1):1–7.
174. Ryan AB, Zeitlin SO, Scrabble H (2006) Genetic interaction between expanded murine Hdh alleles and p53 reveal deleterious effects of p53 on Huntington’s disease pathogenesis. *Neurobiol Dis* 24(2):419–427.
175. Kim M (2013) Beta conformation of polyglutamine track revealed by a crystal structure of Huntingtin N-terminal region with insertion of three histidine residues. *Prion* 7(3):221–228.
176. Zuccato C, et al. (2008) Systematic assessment of BDNF and its receptor levels in human cortices affected by Huntington’s disease. *Brain Pathol* 18(2):225–238.
177. Fan MMY, Raymond LA (2007) N-methyl-D-aspartate (NMDA) receptor function and excitotoxicity in Huntington’s disease. *Prog Neurobiol* 81(5-6):272–293.
178. Cepeda C, Wu N, André VM, Cummings DM, Levine MS (2007) The corticostriatal pathway in Huntington’s disease. *Prog Neurobiol* 81(5-6):253–271.
179. Goldberg YP, et al. (1996) Cleavage of huntingtin by apopain, a proapoptotic cysteine protease, is modulated by the polyglutamine tract. *Nat Genet* 13(4):442–449.
180. DiFiglia M, et al. (1997) Aggregation of huntingtin in neuronal intranuclear

- inclusions and dystrophic neurites in brain. *Science* 277(5334):1990–1993.
181. Davies SW, et al. (1997) Formation of neuronal intranuclear inclusions underlies the neurological dysfunction in mice transgenic for the HD mutation. *Cell* 90(3):537–548.
182. Yang W, Dunlap JR, Andrews RB, Wetzel R (2002) Aggregated polyglutamine peptides delivered to nuclei are toxic to mammalian cells. *Hum Mol Genet* 11(23):2905–2917.
183. Cuervo AM, Dice JF (2000) Regulation of lamp2a levels in the lysosomal membrane. *Traffic* 1(7):570–583.
184. Horton TM, et al. (1995) Marked increase in mitochondrial DNA deletion levels in the cerebral cortex of Huntington's disease patients. *Neurology* 45(10):1879–1883.
185. Correia K, et al. (2015) The Genetic Modifiers of Motor OnsetAge (GeM MOA) Website: Genome-wide Association Analysis for Genetic Modifiers of Huntington's Disease. *J Huntingtons Dis* 4(3):279–284.
186. Ross CA, Poirier MA (2004) Protein aggregation and neurodegenerative disease. *Nat Med* 10 Suppl:S10–7.
187. Roizin L, Stellar S, Willson N, Whittier J, Liu JC (1974) Electron microscope and enzyme studies in cerebral biopsies of Huntington's chorea. *Trans Am Neurol Assoc* 99:240–243.
188. Hackam AS, et al. (1998) The influence of huntingtin protein size on nuclear localization and cellular toxicity. *J Cell Biol* 141(5):1097–1105.
189. Ho LW, Brown R, Maxwell M, Wyttenbach A, Rubinsztein DC (2001) Wild type Huntingtin reduces the cellular toxicity of mutant Huntingtin in mammalian cell models of Huntington's disease. *J Med Genet* 38(7):450–452.
190. Bence NF, Sampat RM, Kopito RR (2001) Impairment of the ubiquitin-proteasome system by protein aggregation. *Science* 292(5521):1552–1555.
191. Cha J-HJ (2007) Transcriptional signatures in Huntington's disease. *Prog Neurobiol* 83(4):228–248.
192. Arrasate M, Mitra S, Schweitzer ES, Segal MR, Finkbeiner S (2004) Inclusion body formation reduces levels of mutant huntingtin and the risk of neuronal death. *Nature* 431(7010):805–810.

193. Bodner RA, et al. (2006) Pharmacological promotion of inclusion formation: a therapeutic approach for Huntington's and Parkinson's diseases. *Proc Natl Acad Sci U S A* 103(11):4246–4251.
194. Morris GP, Clark IA, Vissel B (2014) Inconsistencies and controversies surrounding the amyloid hypothesis of Alzheimer's disease. *Acta Neuropathol Commun* 2:135.
195. Castello MA, Jeppson JD, Soriano S (2014) Moving beyond anti-amyloid therapy for the prevention and treatment of Alzheimer's disease. *BMC Neurol* 14:169.
196. Mink JW, Blumenschine RJ, Adams DB (1981) Ratio of central nervous system to body metabolism in vertebrates: its constancy and functional basis. *Am J Physiol* 241(3):R203–12.
197. Bélanger M, Allaman I, Magistretti PJ (2011) Brain energy metabolism: focus on astrocyte-neuron metabolic cooperation. *Cell Metab* 14(6):724–738.
198. Goebel HH, Heipertz R, Scholz W, Iqbal K, Tellez-Nagel I (1978) Juvenile Huntington chorea: clinical, ultrastructural, and biochemical studies. *Neurology* 28(1):23–31.
199. Feigin A, et al. (2001) Metabolic network abnormalities in early Huntington's disease: an [18F] FDG PET study. *J Nucl Med* 42(11):1591–1595.
200. Ferrante RJ, et al. (2002) Therapeutic effects of coenzyme Q10 and remacemide in transgenic mouse models of Huntington's disease. *J Neurosci* 22(5):1592–1599.
201. Jenkins BG, Koroshetz WJ, Flint Beal M, Rosen BR (1993) Evidence for impairment of energy metabolism in vivo in Huntington's disease using localized 1H NMR spectroscopy. *Neurology* 43(12):2689–2689.
202. Panov AV, et al. (2002) Early mitochondrial calcium defects in Huntington's disease are a direct effect of polyglutamines. *Nat Neurosci* 5(8):731–736.
203. Brouillet E, et al. (1995) Chronic mitochondrial energy impairment produces selective striatal degeneration and abnormal choreiform movements in primates. *Proc Natl Acad Sci U S A* 92(15):7105–7109.
204. Przedborski S, Tieu K, Perier C, Vila M (2004) MPTP as a mitochondrial neurotoxic model of Parkinson's disease. *J Bioenerg Biomembr* 36(4):375–379.
205. Porras G, Li Q, Bezard E (2012) Modeling Parkinson's disease in primates: The MPTP model. *Cold Spring Harb Perspect Med* 2(3):a009308.

206. Klein C, Westenberger A (2012) Genetics of Parkinson's disease. *Cold Spring Harb Perspect Med* 2(1):a008888.
207. Valente EM, et al. (2004) PINK1 mutations are associated with sporadic early-onset parkinsonism. *Ann Neurol* 56(3):336–341.
208. Rogaeva E, et al. (2004) Analysis of the PINK1 gene in a large cohort of cases with Parkinson disease. *Arch Neurol* 61(12):1898–1904.
209. Lücking CB, et al. (2000) Association between early-onset Parkinson's disease and mutations in the parkin gene. *N Engl J Med* 342(21):1560–1567.
210. Canet-Avilés RM, et al. (2004) The Parkinson's disease protein DJ-1 is neuroprotective due to cysteine-sulfinic acid-driven mitochondrial localization. *Proc Natl Acad Sci U S A* 101(24):9103–9108.
211. Junn E, et al. (2005) Interaction of DJ-1 with Daxx inhibits apoptosis signal-regulating kinase 1 activity and cell death. *Proc Natl Acad Sci U S A* 102(27):9691–9696.
212. Junn E, Jang WH, Zhao X, Jeong BS, Mouradian MM (2009) Mitochondrial localization of DJ-1 leads to enhanced neuroprotection. *J Neurosci Res* 87(1):123–129.
213. Eckert A, Schulz KL, Rhein V, Götz J (2010) Convergence of amyloid-beta and tau pathologies on mitochondria in vivo. *Mol Neurobiol* 41(2-3):107–114.
214. Seong IS, et al. (2005) HD CAG repeat implicates a dominant property of huntingtin in mitochondrial energy metabolism. *Hum Mol Genet* 14(19):2871–2880.
215. Thies E, Mandelkow E-M (2007) Missorting of tau in neurons causes degeneration of synapses that can be rescued by the kinase MARK2/Par-1. *J Neurosci* 27(11):2896–2907.
216. Mortiboys H, Johansen KK, Aasly JO, Bandmann O (2010) Mitochondrial impairment in patients with Parkinson disease with the G2019S mutation in LRRK2. *Neurology* 75(22):2017–2020.
217. Lovell MA, Gabbita SP, Markesbery WR (1999) Increased DNA oxidation and decreased levels of repair products in Alzheimer's disease ventricular CSF. *J Neurochem* 72(2):771–776.
218. Zhang J, et al. (1999) Parkinson's disease is associated with oxidative damage to cytoplasmic DNA and RNA in substantia nigra neurons. *Am J Pathol*

- 154(5):1423–1429.
219. Bjelland S, Seeberg E (2003) Mutagenicity, toxicity and repair of DNA base damage induced by oxidation. *Mutat Res* 531(1-2):37–80.
220. Sancar A, Lindsey-Boltz LA, Unsal-Kaçmaz K, Linn S (2004) Molecular mechanisms of mammalian DNA repair and the DNA damage checkpoints. *Annu Rev Biochem* 73:39–85.
221. Hoeijmakers JHJ (2009) DNA damage, aging, and cancer. *N Engl J Med* 361(15):1475–1485.
222. McKinnon PJ, Caldecott KW (2007) DNA strand break repair and human genetic disease. *Annu Rev Genomics Hum Genet* 8:37–55.
223. Wei W, Englander EW (2008) DNA polymerase beta-catalyzed-PCNA independent long patch base excision repair synthesis: a mechanism for repair of oxidatively damaged DNA ends in post-mitotic brain. *J Neurochem* 107(3):734–744.
224. Rao KS, Annapurna VV, Raji NS, Harikrishna T (2000) Loss of base excision repair in aging rat neurons and its restoration by DNA polymerase beta. *Brain Res Mol Brain Res* 85(1-2):251–259.
225. Gabbita SP, Lovell MA, Markesbery WR (1998) Increased nuclear DNA oxidation in the brain in Alzheimer's disease. *J Neurochem* 71(5):2034–2040.
226. Leandro GS, Sykora P, Bohr VA (2015) The impact of base excision DNA repair in age-related neurodegenerative diseases. *Mutat Res* 776:31–39.
227. Arai T, et al. (2006) Up-regulation of hMUTYH, a DNA repair enzyme, in the mitochondria of substantia nigra in Parkinson's disease. *Acta Neuropathol* 112(2):139–145.
228. Ayala-Peña S (2013) Role of oxidative DNA damage in mitochondrial dysfunction and Huntington's disease pathogenesis. *Free Radical Biology and Medicine* 62:102–110.
229. Sanchez-Ramos JR (1994) A marker of oxyradical-mediated DNA damage (8-hydroxy-2'-deoxyguanosine) is increased in nigro-striatum of Parkinson's disease brain. *Neurodegeneration* 3:197–204.
230. Bettencourt C, et al. (2016) DNA repair pathways underlie a common genetic mechanism modulating onset in polyglutamine diseases. *Ann Neurol* 79(6):983–990.
231. Frappart P-O, McKinnon PJ (2006) Ataxia-telangiectasia and related diseases.

Neuromolecular Med 8(4):495–511.

232. Vinters HV, Gatti RA, Rakic P (1985) Sequence of cellular events in cerebellar ontogeny relevant to expression of neuronal abnormalities in ataxia-telangiectasia. *Kroc Found Ser* 19:233–255.
233. Stadelmann C, Brück W, Bancher C, Jellinger K, Lassmann H (1998) Alzheimer disease: DNA fragmentation indicates increased neuronal vulnerability, but not apoptosis. *J Neuropathol Exp Neurol* 57(5):456–464.
234. Suberbielle E, et al. (2013) Physiologic brain activity causes DNA double-strand breaks in neurons, with exacerbation by amyloid- β . *Nat Neurosci* 16(5):613–621.
235. Jacobsen E, Beach T, Shen Y, Li R, Chang Y (2004) Deficiency of the Mre11 DNA repair complex in Alzheimer's disease brains. *Brain Res Mol Brain Res* 128(1):1–7.
236. Shackelford DA (2006) DNA end joining activity is reduced in Alzheimer's disease. *Neurobiol Aging* 27(4):596–605.
237. Lovell MA, Xie C, Markesbery WR (2000) Decreased base excision repair and increased helicase activity in Alzheimer's disease brain. *Brain Res* 855(1):116–123.
238. Sepe S, et al. (2016) Inefficient DNA Repair Is an Aging-Related Modifier of Parkinson's Disease. *Cell Rep* 15(9):1866–1875.
239. Nospikel T (2008) Nucleotide excision repair and neurological diseases. *DNA Repair* 7(7):1155–1167.
240. Martire S, Mosca L, d'Erme M (2015) PARP-1 involvement in neurodegeneration: A focus on Alzheimer's and Parkinson's diseases. *Mech Ageing Dev* 146-148:53–64.
241. McColgan P, Tabrizi SJ (2018) Huntington's disease: a clinical review. *Eur J Neurol* 25(1):24–34.
242. Stout JC, et al. (2012) Evaluation of longitudinal 12 and 24 month cognitive outcomes in premanifest and early Huntington's disease. *J Neurol Neurosurg Psychiatry* 83(7):687–694.
243. Tabrizi SJ, et al. (2013) Predictors of phenotypic progression and disease onset in premanifest and early-stage Huntington's disease in the TRACK-HD study: analysis of 36-month observational data. *Lancet Neurol* 12(7):637–649.
244. Byrne LM, et al. (2017) Neurofilament light protein in blood as a potential

- biomarker of neurodegeneration in Huntington's disease: a retrospective cohort analysis. *Lancet Neurol* 16(8):601–609.
245. Dalrymple A, et al. (2007) Proteomic profiling of plasma in Huntington's disease reveals neuroinflammatory activation and biomarker candidates. *J Proteome Res* 6(7):2833–2840.
246. Weiss A, et al. (2012) Mutant huntingtin fragmentation in immune cells tracks Huntington's disease progression. *J Clin Invest* 122(10):3731–3736.
247. Wild EJ, et al. (2015) Quantification of mutant huntingtin protein in cerebrospinal fluid from Huntington's disease patients. *J Clin Invest* 125(5):1979–1986.
248. ClinicalTrials.gov (2018) Safety, Tolerability, Pharmacokinetics, and Pharmacodynamics of IONIS-HTTRx in Patients With Early Manifest Huntington's Disease. *Identifier: NCT02519036*. Available at: <https://clinicaltrials.gov/ct2/show/NCT02519036?recrs=eh&type=Intr&cond=Huntington+Disease&draw=2&rank=4> [Accessed June 1, 2018].
249. Dumas EM, et al. (2012) Early changes in white matter pathways of the sensorimotor cortex in premanifest Huntington's disease. *Hum Brain Mapp* 33(1):203–212.
250. Gregory S, et al. (2015) Longitudinal Diffusion Tensor Imaging Shows Progressive Changes in White Matter in Huntington's Disease. *J Huntingtons Dis* 4(4):333–346.
251. Niccolini F, et al. (2015) Altered PDE10A expression detectable early before symptomatic onset in Huntington's disease. *Brain* 138(Pt 10):3016–3029.
252. Huntington Study Group (2006) Tetrabenazine as antichorea therapy in Huntington disease: a randomized controlled trial. *Neurology* 66(3):366–372.
253. Yero T, Rey JA (2008) Tetrabenazine (Xenazine), An FDA-Approved Treatment Option For Huntington's Disease-Related Chorea. *P T* 33(12):690–694.
254. Huntington Study Group, et al. (2016) Effect of Deutetrabenazine on Chorea Among Patients With Huntington Disease: A Randomized Clinical Trial. *JAMA* 316(1):40–50.
255. Li Y, Hai S, Zhou Y, Dong BR (2015) Cholinesterase inhibitors for rarer dementias associated with neurological conditions. *Cochrane Database Syst Rev* (3):CD009444.

256. Beglinger LJ, et al. (2014) Results of the citalopram to enhance cognition in Huntington disease trial. *Mov Disord* 29(3):401–405.
257. Travessa AM, Rodrigues FB, Mestre TA, Ferreira JJ (2017) Fifteen Years of Clinical Trials in Huntington's Disease: A Very Low Clinical Drug Development Success Rate. *J Huntingtons Dis* 6(2):157–163.
258. Seeman P, et al. (2009) The dopaminergic stabilizer ASP2314/ACR16 selectively interacts with D2(High) receptors. *Synapse* 63(10):930–934.
259. Ponten H, et al. (2010) In vivo pharmacology of the dopaminergic stabilizer pridopidine. *Eur J Pharmacol* 644(1-3):88–95.
260. Lundin A, et al. (2010) Efficacy and safety of the dopaminergic stabilizer Pridopidine (ACR16) in patients with Huntington's disease. *Clin Neuropharmacol* 33(5):260–264.
261. de Yebenes JG, et al. (2011) Pridopidine for the treatment of motor function in patients with Huntington's disease (MermaiHD): a phase 3, randomised, double-blind, placebo-controlled trial. *Lancet Neurol* 10(12):1049–1057.
262. Investigators HSGH (2013) A randomized, double-blind, placebo-controlled trial of pridopidine in Huntington's disease. *Mov Disord* 28(10):1407–1415.
263. ClinicalTrials.gov Randomized, Placebo Controlled Study Of The Efficacy And Safety Of PF-02545920 In Subjects With Huntington's Disease. *Identifier: NCT02197130*. Available at: <https://clinicaltrials.gov/ct2/show/results/NCT02197130?term=Pfizer&type=Intr&cond=Huntington+Disease&rank=2&view=results>.
264. Coskran TM, et al. (2006) Immunohistochemical localization of phosphodiesterase 10A in multiple mammalian species. *J Histochem Cytochem* 54(11):1205–1213.
265. Nishi A, et al. (2008) Distinct roles of PDE4 and PDE10A in the regulation of cAMP/PKA signaling in the striatum. *J Neurosci* 28(42):10460–10471.
266. Girault J-A (2012) Integrating Neurotransmission in Striatal Medium Spiny Neurons. *Synaptic Plasticity: Dynamics, Development and Disease*, eds Kreutz MR, Sala C (Springer Vienna, Vienna), pp 407–429.
267. Giampà C, et al. (2010) Inhibition of the striatal specific phosphodiesterase PDE10A ameliorates striatal and cortical pathology in R6/2 mouse model of

- Huntington's disease. *PLoS One* 5(10):e13417.
268. Giampà C, et al. (2009) Phosphodiesterase 10 inhibition reduces striatal excitotoxicity in the quinolinic acid model of Huntington's disease. *Neurobiol Dis* 34(3):450–456.
269. Hemmer W, Wallimann T (1993) Functional aspects of creatine kinase in brain. *Dev Neurosci* 15(3-5):249–260.
270. Lenaz G (1988) Role of mobility of redox components in the inner mitochondrial membrane. *J Membr Biol* 104(3):193–209.
271. Schneider H, Lemasters JJ, Hackenbrock CR (1982) Lateral diffusion of ubiquinone during electron transfer in phospholipid- and ubiquinone-enriched mitochondrial membranes. *J Biol Chem* 257(18):10789–10793.
272. Spindler M, Beal MF, Henchcliffe C (2009) Coenzyme Q10 effects in neurodegenerative disease. *Neuropsychiatr Dis Treat* 5:597–610.
273. Beal MF, et al. (1993) Age-dependent striatal excitotoxic lesions produced by the endogenous mitochondrial inhibitor malonate. *J Neurochem* 61(3):1147–1150.
274. Ferrante RJ, et al. (2000) Neuroprotective effects of creatine in a transgenic mouse model of Huntington's disease. *J Neurosci* 20(12):4389–4397.
275. Matthews RT, et al. (1998) Neuroprotective effects of creatine and cyclocreatine in animal models of Huntington's disease. *J Neurosci* 18(1):156–163.
276. Coenzyme Q10 in Huntington's Disease (HD) - Full Text View - ClinicalTrials.gov Available at:
<https://clinicaltrials.gov/ct2/show/NCT00608881?term=Coenzyme+Q10&type=Intr&cond=Huntington+Disease&rank=2> [Accessed June 2, 2018].
277. Creatine Safety, Tolerability, & Efficacy in Huntington's Disease (CREST-E) - Full Text View - ClinicalTrials.gov Available at:
<https://clinicaltrials.gov/ct2/show/NCT00712426?term=Creatine&type=Intr&cond=Huntington+Disease&rank=4> [Accessed June 2, 2018].
278. Larrouy B, et al. (1992) RNase H-mediated inhibition of translation by antisense oligodeoxyribonucleotides: use of backbone modification to improve specificity. *Gene* 121(2):189–194.
279. Safety, Tolerability, Pharmacokinetics, and Pharmacodynamics of IONIS-HTTRx in Patients With Early Manifest Huntington's Disease - Full Text View -

ClinicalTrials.gov Available at:

<https://clinicaltrials.gov/ct2/show/NCT02519036?term=Ionis&type=Intr&cond=Huntington+Disease&rank=1> [Accessed June 2, 2018].

280. Safety and Tolerability of WVE-120102 in Patients With Huntington's Disease - Full Text View - ClinicalTrials.gov Available at: <https://clinicaltrials.gov/ct2/show/NCT03225846?term=Wave&type=Intr&cond=Huntington+Disease&rank=1> [Accessed June 2, 2018].
281. Safety and Tolerability of WVE-120101 in Patients With Huntington's Disease - Full Text View - ClinicalTrials.gov Available at: <https://clinicaltrials.gov/ct2/show/NCT03225833?term=Wave&type=Intr&cond=Huntington+Disease&rank=2> [Accessed June 2, 2018].
282. Wild EJ, Tabrizi SJ (2017) Therapies targeting DNA and RNA in Huntington's disease. *Lancet Neurol* 16(10):837–847.
283. Agustín-Pavón C, Mielcarek M, Garriga-Canut M, Isalan M (2016) Deimmunization for gene therapy: host matching of synthetic zinc finger constructs enables long-term mutant Huntingtin repression in mice. *Mol Neurodegener* 11(1):64.
284. Shin JW, et al. (2016) Permanent inactivation of Huntington's disease mutation by personalized allele-specific CRISPR/Cas9. *Hum Mol Genet* 25(20):4566–4576.
285. Yang S, et al. (2017) CRISPR/Cas9-mediated gene editing ameliorates neurotoxicity in mouse model of Huntington's disease. *J Clin Invest* 127(7):2719–2724.
286. Ehrnhoefer DE, Sutton L, Hayden MR (2011) Small changes, big impact: posttranslational modifications and function of huntingtin in Huntington disease. *Neuroscientist* 17(5):475–492.
287. Di Pardo A, et al. (2012) Ganglioside GM1 induces phosphorylation of mutant huntingtin and restores normal motor behavior in Huntington disease mice. *Proc Natl Acad Sci U S A* 109(9):3528–3533.
288. Thompson LM, et al. (2009) IKK phosphorylates Huntingtin and targets it for degradation by the proteasome and lysosome. *J Cell Biol* 187(7):1083–1099.
289. Keum JW, et al. (2016) The HTT CAG-Expansion Mutation Determines Age at Death but Not Disease Duration in Huntington Disease. *Am J Hum Genet* 98(2):287–298.

290. Genetic Modifiers of Huntington's Disease (GeM-HD) Consortium (2015) Identification of Genetic Factors that Modify Clinical Onset of Huntington's Disease. *Cell* 162(3):516–526.
291. Moss DJH, et al. (2017) Identification of genetic variants associated with Huntington's disease progression: a genome-wide association study. *Lancet Neurol* 16(9):701–711.
292. Maiuri T, et al. (2017) Huntingtin is a scaffolding protein in the ATM oxidative DNA damage response complex. *Hum Mol Genet* 26(2):395–406.
293. Atwal RS, et al. (2007) Huntingtin has a membrane association signal that can modulate huntingtin aggregation, nuclear entry and toxicity. *Hum Mol Genet* 16(21):2600–2615.
294. Vidal RL, Hetz C (2012) Crosstalk between the UPR and autophagy pathway contributes to handling cellular stress in neurodegenerative disease. *Autophagy* 8(6):970–972.
295. DiGiovanni LF, Mocle AJ, Xia J, Truant R (2016) Huntingtin N17 domain is a reactive oxygen species sensor regulating huntingtin phosphorylation and localization. *Hum Mol Genet* 25(18):3937–3945.
296. Gu X, et al. (2009) Serines 13 and 16 Are Critical Determinants of Full-Length Human Mutant Huntingtin Induced Disease Pathogenesis in HD Mice. *Neuron* 64(6):828–840.
297. Atwal RS, et al. (2011) Kinase inhibitors modulate huntingtin cell localization and toxicity. *Nat Chem Biol* 7(7):453–460.
298. Atwal RS, et al. (2007) Huntingtin has a membrane association signal that can modulate huntingtin aggregation, nuclear entry and toxicity. *Hum Mol Genet* 16(21):2600–2615.
299. Michalek M, Salnikov ES, Bechinger B (2013) Structure and topology of the huntingtin 1-17 membrane anchor by a combined solution and solid-state NMR approach. *Biophys J* 105(3):699–710.
300. Maiuri T, Woloshansky T, Xia J, Truant R (2013) The huntingtin N17 domain is a multifunctional CRM1 and Ran-dependent nuclear and cilial export signal. *Hum Mol Genet* 22(7):1383–1394.
301. Atwal RS, et al. (2007) Huntingtin has a membrane association signal that can modulate huntingtin aggregation, nuclear entry and toxicity. *Hum Mol Genet*

- 16(21):2600–2615.
302. Gu X, et al. (2015) N17 Modifies mutant Huntingtin nuclear pathogenesis and severity of disease in HD BAC transgenic mice. *Neuron* 85(4):726–741.
303. Veldman MB, et al. (2015) The N17 domain mitigates nuclear toxicity in a novel zebrafish Huntington's disease model. *Mol Neurodegener* 10:67.
304. Di Pardo A, et al. (2012) Ganglioside GM1 induces phosphorylation of mutant huntingtin and restores normal motor behavior in Huntington disease mice. *Proceedings of the National Academy of Sciences* 109(9):3528–3533.
305. Hung CLK, et al. (2018) A Patient-Derived Cellular Model for Huntington Disease Reveals Phenotypes at Clinically Relevant CAG Lengths. *bioRxiv*:291575.
306. Barciszewski J, Massino F, Clark BFC (2007) Kinetin--a multiactive molecule. *Int J Biol Macromol* 40(3):182–192.
307. Olsen A, Siboska GE, Clark BF, Rattan SI (1999) N(6)-Furfuryladenine, kinetin, protects against Fenton reaction-mediated oxidative damage to DNA. *Biochem Biophys Res Commun* 265(2):499–502.
308. Rattan SIS, Clark BFC (1994) Kinetin Delays the Onset of Aging Characteristics in Human Fibroblasts. *Biochem Biophys Res Commun* 201(2):665–672.
309. Barciszewski J, Barciszewska MZ, Siboska G, Rattan SI, Clark BF (1999) Some unusual nucleic acid bases are products of hydroxyl radical oxidation of DNA and RNA. *Mol Biol Rep* 26(4):231–238.
310. Barciszewski J, Mielcarek M, Stobiecki M, Siboska G, Clark BF (2000) Identification of 6-furfuryladenine (kinetin) in human urine. *Biochem Biophys Res Commun* 279(1):69–73.
311. Hertz NT, et al. (2013) A Neo-Substrate that Amplifies Catalytic Activity of Parkinson's-Disease-Related Kinase PINK1. *Cell* 154(4):737–747.
312. Arnér ES, Eriksson S (1995) Mammalian deoxyribonucleoside kinases. *Pharmacol Ther* 67(2):155–186.
313. Micheli V, et al. (2011) Neurological disorders of purine and pyrimidine metabolism. *Curr Top Med Chem* 11(8):923–947.
314. Formentini L, et al. (2009) Poly(ADP-ribose) catabolism triggers AMP-dependent mitochondrial energy failure. *J Biol Chem* 284(26):17668–17676.

315. Thompson LM, et al. (2009) IKK phosphorylates Huntingtin and targets it for degradation by the proteasome and lysosome. *J Cell Biol* 187(7):1083–1099.
316. Shetty RS, et al. (2011) Specific correction of a splice defect in brain by nutritional supplementation. *Hum Mol Genet* 20(21):4093–4101.
317. Caron NS, Desmond CR, Xia J, Truant R (2013) Polyglutamine domain flexibility mediates the proximity between flanking sequences in huntingtin. *Proc Natl Acad Sci U S A* 110(36):14610–14615.
318. Trettel F, et al. (2000) Dominant phenotypes produced by the HD mutation in STHdh(Q111) striatal cells. *Hum Mol Genet* 9(19):2799–2809.
319. Rajaram S, Pavie B, Wu LF, Altschuler SJ (2012) PhenoRipper: software for rapidly profiling microscopy images. *Nat Methods* 9(7):635–637.
320. Thompson LM, et al. (2009) IKK phosphorylates Huntingtin and targets it for degradation by the proteasome and lysosome. *J Cell Biol* 187(7):1083–1099.
321. Axelrod FB, et al. (2011) Kinetin improves IKBKAP mRNA splicing in patients with familial dysautonomia. *Pediatr Res* 70(5):480–483.
322. Shetty RS, et al. (2011) Specific correction of a splice defect in brain by nutritional supplementation. *Hum Mol Genet* 20(21):4093–4101.
323. Gu X, et al. (2015) N17 Modifies mutant Huntingtin nuclear pathogenesis and severity of disease in HD BAC transgenic mice. *Neuron* 85(4):726–741.
324. Othman EM, Naseem M, Awad E, Dandekar T, Stopper H (2016) The Plant Hormone Cytokinin Confers Protection against Oxidative Stress in Mammalian Cells. *PLoS One* 11(12):e0168386.
325. Jabłońska-Trypuć A, Matejczyk M, Czerpak R (2016) N6-benzyladenine and kinetin influence antioxidative stress parameters in human skin fibroblasts. *Mol Cell Biochem* 413(1-2):97–107.
326. Watkin EE, et al. (2014) Phosphorylation of mutant huntingtin at serine 116 modulates neuronal toxicity. *PLoS One* 9(2):e88284.
327. Slow EJ (2003) Selective striatal neuronal loss in a YAC128 mouse model of Huntington disease. *Hum Mol Genet* 12(13):1555–1567.
328. Niefind K, Pütter M, Guerra B, Issinger OG, Schomburg D (1999) GTP plus water mimic ATP in the active site of protein kinase CK2. *Nat Struct Biol*

6(12):1100–1103.

329. Pagano MA, et al. (2004)
2-Dimethylamino-4,5,6,7-tetrabromo-1H-benzimidazole: a novel powerful and selective inhibitor of protein kinase CK2. *Biochem Biophys Res Commun* 321(4):1040–1044.
330. Nuñez de Villavicencio-Diaz T, Rabalski AJ, Litchfield DW (2017) Protein Kinase CK2: Intricate Relationships within Regulatory Cellular Networks. *Pharmaceuticals* 10(1). doi:10.3390/ph10010027.
331. Pagano MA, et al. (2004)
2-Dimethylamino-4,5,6,7-tetrabromo-1H-benzimidazole: a novel powerful and selective inhibitor of protein kinase CK2. *Biochem Biophys Res Commun* 321(4):1040–1044.
332. Olsten MEK, Litchfield DW (2004) Order or chaos? An evaluation of the regulation of protein kinase CK2. *Biochem Cell Biol* 82(6):681–693.
333. Montenarh M (2016) Protein kinase CK2 in DNA damage and repair. *Transl Cancer Res* 5(1):49–63.
334. Tsutakawa SE, Lafrance-Vanasse J, Tainer JA (2014) The cutting edges in DNA repair, licensing, and fidelity: DNA and RNA repair nucleases sculpt DNA to measure twice, cut once. *DNA Repair* 19:95–107.
335. Morales JC (2004) Breaking in a New Function for Casein Kinase 2. *Sci Aging Knowledge Environ* 2004(22):e24–pe24.
336. Guerra B, Iwabuchi K, Issinger O-G (2014) Protein kinase CK2 is required for the recruitment of 53BP1 to sites of DNA double-strand break induced by radiomimetic drugs. *Cancer Lett* 345(1):115–123.
337. Barciszewski J, Barciszewska MZ, Siboska G, Rattan SI, Clark BF (1999) Some unusual nucleic acid bases are products of hydroxyl radical oxidation of DNA and RNA. *Mol Biol Rep* 26(4):231–238.
338. Wyszko E, et al. (2003) “Action-at-a distance” of a new DNA oxidative damage product 6-furfuryl-adenine (kinetin) on template properties of modified DNA. *Biochimica et Biophysica Acta (BBA) - Gene Structure and Expression* 1625(3):239–245.
339. Radhakrishna V, et al. (2017) Evaluation of the Potency of Kinetin on Radiation Induced Behavioural Changes in Swiss Albino Mice. *J Clin Diagn Res*

11(7):TF01–TF04.

340. Hickson I, et al. (2004) Identification and characterization of a novel and specific inhibitor of the ataxia-telangiectasia mutated kinase ATM. *Cancer Res* 64(24):9152–9159.
341. Guerra B, Iwabuchi K, Issinger O-G (2014) Protein kinase CK2 is required for the recruitment of 53BP1 to sites of DNA double-strand break induced by radiomimetic drugs. *Cancer Lett* 345(1):115–123.
342. Formentini L, et al. (2009) Poly(ADP-ribose) catabolism triggers AMP-dependent mitochondrial energy failure. *J Biol Chem* 284(26):17668–17676.
343. Fecke W, Gianfriddo M, Gaviraghi G, Terstappen GC, Heitz F (2009) Small molecule drug discovery for Huntington's Disease. *Drug Discov Today* 14(9-10):453–464.
344. Thompson LM, et al. (2009) IKK phosphorylates Huntingtin and targets it for degradation by the proteasome and lysosome. *J Cell Biol* 187(7):1083–1099.
345. Kumar A, Ratan RR (2016) Oxidative Stress and Huntington's Disease: The Good, The Bad, and The Ugly. *J Huntingtons Dis* 5(3):217–237.
346. Polyzos A, et al. (2016) Mitochondrial targeting of XJB-5-131 attenuates or improves pathophysiology in HdhQ150 animals with well-developed disease phenotypes. *Hum Mol Genet* 25(9):1792–1802.
347. Tilstra JS, et al. (2014) Pharmacologic IKK/NF- κ B inhibition causes antigen presenting cells to undergo TNF α dependent ROS-mediated programmed cell death. *Sci Rep* 4:3631.
348. Shetty RS, et al. (2011) Specific correction of a splice defect in brain by nutritional supplementation. *Hum Mol Genet* 20(21):4093–4101.
349. Wei Y, et al. (2017) Neuroprotective Effects of Kinetin Against Glutamate-Induced Oxidative Cytotoxicity in HT22 Cells: Involvement of Nrf2 and Heme Oxygenase-1. *Neurotox Res*. doi:10.1007/s12640-017-9811-0.
350. Wei Y, et al. (2017) Protective effects of kinetin against aluminum chloride and D-galactose induced cognitive impairment and oxidative damage in mouse. *Brain Res Bull* 134:262–272.
351. Rattan SIS, Clark BFC (1994) Kinetin Delays the Onset of Aging Characteristics in Human Fibroblasts. *Biochem Biophys Res Commun* 201(2):665–672.

352. Olsen A, Siboska GE, Clark BF, Rattan SI (1999) N(6)-Furfuryladenine, kinetin, protects against Fenton reaction-mediated oxidative damage to DNA. *Biochem Biophys Res Commun* 265(2):499–502.
353. Kratter IH, et al. (2016) Serine 421 regulates mutant huntingtin toxicity and clearance in mice. *J Clin Invest* 126(9):3585–3597.
354. Warby SC, et al. (2009) Phosphorylation of huntingtin reduces the accumulation of its nuclear fragments. *Mol Cell Neurosci* 40(2):121–127.
355. Thompson LM, et al. (2009) IKK phosphorylates Huntingtin and targets it for degradation by the proteasome and lysosome. *J Cell Biol* 187(7):1083–1099.
356. Arbez N, et al. (2017) Posttranslational modifications clustering within proteolytic domains decrease mutant huntingtin toxicity. *J Biol Chem*. doi:10.1074/jbc.M117.782300.
357. Thompson LM, et al. (2009) IKK phosphorylates Huntingtin and targets it for degradation by the proteasome and lysosome. *J Cell Biol* 187(7):1083–1099.
358. Nuñez de Villavicencio-Diaz T, Rabalski AJ, Litchfield DW (2017) Protein Kinase CK2: Intricate Relationships within Regulatory Cellular Networks. *Pharmaceuticals* 10(1). doi:10.3390/ph10010027.
359. Sorrentino V, et al. (2017) Enhancing mitochondrial proteostasis reduces amyloid- β proteotoxicity. *Nature*. doi:10.1038/nature25143.
360. Morales JC (2004) Breaking in a New Function for Casein Kinase 2. *Sci Aging Knowledge Environ* 2004(22):e24–pe24.
361. Sakaguchi K, et al. (1997) Phosphorylation of serine 392 stabilizes the tetramer formation of tumor suppressor protein p53. *Biochemistry* 36(33):10117–10124.
362. Herhaus L, et al. (2015) Casein kinase 2 (CK2) phosphorylates the deubiquitylase OTUB1 at Ser16 to trigger its nuclear localization. *Sci Signal* 8(372):ra35.
363. Barciszewski J, Siboska GE, Pedersen BO, Clark BF, Rattan SI (1997) A mechanism for the in vivo formation of N6-furfuryladenine, kinetin, as a secondary oxidative damage product of DNA. *FEBS Lett* 414(2):457–460.
364. Schütt F, Aretz S, Auffarth GU (2012) ... Reduced ATP Levels Promote Oxidative Stress and Debilitate Autophagic and Phagocytic Capacities in Human RPE Cells Moderately Reduced ATP Levels *Invest Ophthalmol Vis Sci*. Available at: <http://iovs.arvojournals.org/article.aspx?articleid=2165977>.

365. Mochel F, Haller RG (2011) Energy deficit in Huntington disease: why it matters. *J Clin Invest* 121(2):493–499.
366. Vishnu N, et al. (2014) ATP increases within the lumen of the endoplasmic reticulum upon intracellular Ca²⁺ release. *Mol Biol Cell* 25(3):368–379.
367. Vidal R, Caballero B, Couve A, Hetz C (2011) Converging pathways in the occurrence of endoplasmic reticulum (ER) stress in Huntington's disease. *Curr Mol Med* 11(1):1–12.
368. Formentini L, et al. (2009) Poly(ADP-ribose) catabolism triggers AMP-dependent mitochondrial energy failure. *J Biol Chem* 284(26):17668–17676.
369. Micheli V, et al. (2011) Neurological disorders of purine and pyrimidine metabolism. *Curr Top Med Chem* 11(8):923–947.
370. Jiang B, Glover JNM, Weinfeld M (2017) Neurological disorders associated with DNA strand-break processing enzymes. *Mech Ageing Dev* 161(Pt A):130–140.
371. Turowec JP, et al. (2010) Protein Kinase CK2 is a Constitutively Active Enzyme that Promotes Cell Survival: Strategies to Identify CK2 Substrates and Manipulate its Activity in Mammalian Cells. *Methods in Enzymology*, pp 471–493.
372. Frank R (2002) The SPOT-synthesis technique. Synthetic peptide arrays on membrane supports--principles and applications. *J Immunol Methods* 267(1):13–26.
373. Duncan JS, et al. (2011) A peptide-based target screen implicates the protein kinase CK2 in the global regulation of caspase signaling. *Sci Signal* 4(172):ra30.
374. Slow EJ (2003) Selective striatal neuronal loss in a YAC128 mouse model of Huntington disease. *Hum Mol Genet* 12(13):1555–1567.
375. Porsolt RD, Le Pichon M, Jalfre M (1977) Depression: a new animal model sensitive to antidepressant treatments. *Nature* 266(5604):730–732.
376. Wanker EE, et al. (1999) Membrane filter assay for detection of amyloid-like polyglutamine-containing protein aggregates. *Methods Enzymol* 309:375–386.
377. Slow EJ (2003) Selective striatal neuronal loss in a YAC128 mouse model of Huntington disease. *Hum Mol Genet* 12(13):1555–1567.
378. Kornhuber, J., Weller, M., Schoppmeyer, K. & Riederer, P (1994) Amantadine and memantine are NMDA receptor antagonists with neuroprotective properties. *J Neural Transm* 43:91–104.

379. Chen M, et al. (2000) Minocycline inhibits caspase-1 and caspase-3 expression and delays mortality in a transgenic mouse model of Huntington disease. *Nat Med* 6(7):797–801.
380. Heiser V, et al. (2002) Identification of benzothiazoles as potential polyglutamine aggregation inhibitors of Huntington's disease by using an automated filter retardation assay. *Proc Natl Acad Sci U S A* 99 Suppl 4:16400–16406.
381. Carroll JB, et al. (2011) Potent and selective antisense oligonucleotides targeting single-nucleotide polymorphisms in the Huntington disease gene / allele-specific silencing of mutant huntingtin. *Mol Ther* 19(12):2178–2185.
382. Kordasiewicz HB, et al. (2012) Sustained therapeutic reversal of Huntington's disease by transient repression of huntingtin synthesis. *Neuron* 74(6):1031–1044.
383. Gagnon KT, et al. (2010) Allele-selective inhibition of mutant huntingtin expression with antisense oligonucleotides targeting the expanded CAG repeat. *Biochemistry* 49(47):10166–10178.
384. Dietrich P, Johnson IM, Alli S, Dragatsis I (2017) Elimination of huntingtin in the adult mouse leads to progressive behavioral deficits, bilateral thalamic calcification, and altered brain iron homeostasis. *PLoS Genet* 13(7):e1006846.
385. Munsie LN, Desmond CR, Truant R (2012) Cofilin nuclear--cytoplasmic shuttling affects cofilin--actin rod formation during stress. *J Cell Sci* 125(17):3977–3988.
386. Truant R, Atwal R, Burtnik A (2006) Hypothesis: Huntingtin may function in membrane association and vesicular trafficking. *Biochem Cell Biol* 84(6):912–917.
387. Tyebji S, Hannan AJ (2017) Synaptopathic mechanisms of neurodegeneration and dementia: Insights from Huntington's disease. *Prog Neurobiol* 153:18–45.
388. Rajaram S, Pavie B, Wu LF, Altschuler SJ (2012) PhenoRipper: software for rapidly profiling microscopy images. *Nat Methods* 9(7):635–637.
389. Xue Y, et al. (2008) GPS 2.0, a tool to predict kinase-specific phosphorylation sites in hierarchy. *Mol Cell Proteomics* 7(9):1598–1608.
390. Moscat J, Rennert P, Diaz-Meco MT (2005) PKC ζ at the crossroad of NF- κ B and Jak1/Stat6 signaling pathways. *Cell Death Differ* 13:702.
391. Kovac J, Oster H, Leitges M (2007) Expression of the atypical protein kinase C (aPKC) isoforms iota/lambda and zeta during mouse embryogenesis. *Gene Expr Patterns* 7(1-2):187–196.

392. Uberall F, et al. (1999) Evidence that atypical protein kinase C-lambda and atypical protein kinase C-zeta participate in Ras-mediated reorganization of the F-actin cytoskeleton. *J Cell Biol* 144(3):413–425.
393. Numazawa S, Ishikawa M, Yoshida A, Tanaka S, Yoshida T (2003) Atypical protein kinase C mediates activation of NF-E2-related factor 2 in response to oxidative stress. *Am J Physiol Cell Physiol* 285(2):C334–42.
394. Cataldi A, et al. (2003) Protein kinase C zeta nuclear translocation mediates the occurrence of radioresistance in friend erythroleukemia cells. *J Cell Biochem* 88(1):144–151.
395. Louat T, et al. (2004) Atypical protein kinase C stimulates nucleotide excision repair activity. *FEBS Lett* 574(1-3):121–125.
396. Ruvolo PP (2003) Intracellular signal transduction pathways activated by ceramide and its metabolites. *Pharmacol Res* 47(5):383–392.
397. Newton AC (2010) Protein kinase C: poised to signal. *Am J Physiol Endocrinol Metab* 298(3):E395–402.
398. Lamark T, et al. (2003) Interaction codes within the family of mammalian Phox and Bem1p domain-containing proteins. *J Biol Chem* 278(36):34568–34581.
399. Callender JA, Newton AC (2017) Conventional protein kinase C in the brain: 40 years later. *Neuronal Signaling* 1(2):NS20160005.
400. Akimoto K, et al. (1994) A new member of the third class in the protein kinase C family, PKC lambda, expressed dominantly in an undifferentiated mouse embryonal carcinoma cell line and also in many tissues and cells. *J Biol Chem* 269(17):12677–12683.
401. Tsokas P, et al. (2016) Compensation for PKM ζ in long-term potentiation and spatial long-term memory in mutant mice. *Elife* 5. doi:10.7554/eLife.14846.
402. Yao Y, et al. (2008) PKM zeta maintains late long-term potentiation by N-ethylmaleimide-sensitive factor/GluR2-dependent trafficking of postsynaptic AMPA receptors. *J Neurosci* 28(31):7820–7827.
403. Hsieh C, et al. (2017) Persistent increased PKM ζ in long-term and remote spatial memory. *Neurobiol Learn Mem* 138:135–144.
404. Kronfeld I, Kazimirsky G, Gelfand EW, Brodie C (2002) NGF rescues human B lymphocytes from anti-IgM induced apoptosis by activation of PKC ζ . *Eur J*

- Immunol* 32(1):136–143.
405. Duchemin A-M, Ren Q, Mo L, Neff NH, Hadjiconstantinou M (2002) GM1 ganglioside induces phosphorylation and activation of Trk and Erk in brain. *J Neurochem* 81(4):696–707.
406. Zemskov EA, et al. (2003) Pro-apoptotic protein kinase C δ is associated with intranuclear inclusions in a transgenic model of Huntington's disease. *J Neurochem* 87(2):395–406.
407. Fan MMY, Zhang H, Hayden MR, Pelech SL, Raymond LA (2008) Protective up-regulation of CK2 by mutant huntingtin in cells co-expressing NMDA receptors. *J Neurochem* 104(3):790–805.
408. Bowie LE, et al. (2018) N6-Furfuryladenine is protective in Huntington's disease models by signaling huntingtin phosphorylation. *Proc Natl Acad Sci U S A* 115(30):E7081–E7090.
409. Jiang K, et al. (2014) Hedgehog-regulated atypical PKC promotes phosphorylation and activation of Smoothed and Cubitus interruptus in Drosophila. *Proc Natl Acad Sci U S A* 111(45):E4842–50.
410. Chou MM, et al. (1998) Regulation of protein kinase C zeta by PI 3-kinase and PDK-1. *Curr Biol* 8(19):1069–1077.
411. Miller CO, Skoog F, Von Saltza MH, Strong FM (1955) KINETIN, A CELL DIVISION FACTOR FROM DEOXYRIBONUCLEIC ACID1. *J Am Chem Soc* 77(5):1392–1392.
412. Barciszewski J, Siboska GE, Pedersen BO, Clark BF, Rattan SI (1996) Evidence for the presence of kinetin in DNA and cell extracts. *FEBS Lett* 393(2-3):197–200.
413. Barciszewski J, Siboska GE, Pedersen BO, Clark BF, Rattan SI (1997) Furfural, a precursor of the cytokinin hormone kinetin, and base propenals are formed by hydroxyl radical damage of DNA. *Biochem Biophys Res Commun* 238(2):317–319.
414. Kowalska E (1992) Influence of kinetin (6-furfurylo-amino-purine) on human fibroblasts in the cell culture. *Folia Morphol* 51(2):109–118.
415. Rattan SI, Clark BF (1994) Kinetin delays the onset of ageing characteristics in human fibroblasts. *Biochem Biophys Res Commun* 201(2):665–672.
416. Verbeke P, Siboska GE, Clark BF, Rattan SI (2000) Kinetin inhibits protein oxidation and glycooxidation in vitro. *Biochem Biophys Res Commun*

276(3):1265–1270.

417. Sharma SP, Kaur P, Rattan SI (1995) Plant growth hormone kinetin delays ageing, prolongs the lifespan and slows down development of the fruitfly *Zaprionus parvittiger*. *Biochem Biophys Res Commun* 216(3):1067–1071.
418. Hertz NT, et al. (2013) A neo-substrate that amplifies catalytic activity of parkinson's-disease-related kinase PINK1. *Cell* 154(4):737–747.
419. Slaugenhaupt SA, et al. (2004) Rescue of a human mRNA splicing defect by the plant cytokinin kinetin. *Hum Mol Genet* 13(4):429–436.
420. Norcliffe-Kaufmann L, Slaugenhaupt SA, Kaufmann H (2017) Familial dysautonomia: History, genotype, phenotype and translational research. *Prog Neurobiol* 152:131–148.
421. Blumenfeld A, et al. (1993) Localization of the gene for familial dysautonomia on chromosome 9 and definition of DNA markers for genetic diagnosis. *Nat Genet* 4(2):160–164.
422. Slaugenhaupt SA, et al. (2001) Tissue-specific expression of a splicing mutation in the IKBKAP gene causes familial dysautonomia. *Am J Hum Genet* 68(3):598–605.
423. Svejstrup JQ (2007) Elongator complex: how many roles does it play? *Curr Opin Cell Biol* 19(3):331–336.
424. Wittschieben BO, et al. (1999) A novel histone acetyltransferase is an integral subunit of elongating RNA polymerase II holoenzyme. *Mol Cell* 4(1):123–128.
425. Winkler GS, Kristjuhan A, Erdjument-Bromage H, Tempst P, Svejstrup JQ (2002) Elongator is a histone H3 and H4 acetyltransferase important for normal histone acetylation levels in vivo. *Proc Natl Acad Sci U S A* 99(6):3517–3522.
426. Close P, et al. (2006) Transcription impairment and cell migration defects in elongator-depleted cells: implication for familial dysautonomia. *Mol Cell* 22(4):521–531.
427. Huang B, Johansson MJO, Byström AS (2005) An early step in wobble uridine tRNA modification requires the Elongator complex. *RNA* 11(4):424–436.
428. Rahl PB, Chen CZ, Collins RN (2005) Elp1p, the yeast homolog of the FD disease syndrome protein, negatively regulates exocytosis independently of transcriptional elongation. *Mol Cell* 17(6):841–853.

429. Johansen LD, et al. (2008) IKAP localizes to membrane ruffles with filamin A and regulates actin cytoskeleton organization and cell migration. *J Cell Sci* 121(Pt 6):854–864.
430. Creppe C, et al. (2009) Elongator controls the migration and differentiation of cortical neurons through acetylation of alpha-tubulin. *Cell* 136(3):551–564.
431. Cuajungco MP, et al. (2003) Tissue-specific reduction in splicing efficiency of IKBKAP due to the major mutation associated with familial dysautonomia. *Am J Hum Genet* 72(3):749–758.
432. Axelrod FB, et al. (2011) Kinetin improves IKBKAP mRNA splicing in patients with familial dysautonomia. *Pediatr Res* 70(5):480–483.
433. Goehler H, et al. (2004) A protein interaction network links GIT1, an enhancer of huntingtin aggregation, to Huntington's disease. *Mol Cell* 15(6):853–865.
434. Fernández-Nogales M, Santos-Galindo M, Hernández IH, Cabrera JR, Lucas JJ (2016) Faulty splicing and cytoskeleton abnormalities in Huntington's disease. *Brain Pathol* 26(6):772–778.
435. Jiang Y-J, et al. (2011) Interaction with polyglutamine-expanded huntingtin alters cellular distribution and RNA processing of huntingtin yeast two-hybrid protein A (HYPA). *J Biol Chem* 286(28):25236–25245.
436. Sathasivam K, et al. (2013) Aberrant splicing of HTT generates the pathogenic exon 1 protein in Huntington disease. *Proc Natl Acad Sci U S A* 110(6):2366–2370.
437. Nguyen L, Humbert S, Saudou F, Chariot A (2010) Elongator - an emerging role in neurological disorders. *Trends Mol Med* 16(1):1–6.
438. Meggio F, Pinna LA (2003) One-thousand-and-one substrates of protein kinase CK2? *FASEB J* 17(3):349–368.
439. Blaydes JP, Hupp TR (1998) DNA damage triggers DRB-resistant phosphorylation of human p53 at the CK2 site. *Oncogene* 17(8):1045–1052.
440. Cox ML, Meek DW (2010) Phosphorylation of serine 392 in p53 is a common and integral event during p53 induction by diverse stimuli. *Cell Signal* 22(3):564–571.
441. MacLaine NJ, Hupp TR (2011) How phosphorylation controls p53. *Cell Cycle* 10(6):916–921.
442. Meek DW, Anderson CW (2009) Posttranslational modification of p53:

- cooperative integrators of function. *Cold Spring Harb Perspect Biol* 1(6):a000950.
443. López-Sánchez I, et al. (2014) Vrk1 interacts with p53 forming a basal complex that is activated by UV-induced DNA damage. *FEBS Lett* 588(5):692–700.
444. Hupp TR, Sparks A, Lane DP (1995) Small peptides activate the latent sequence-specific DNA binding function of p53. *Cell* 83(2):237–245.
445. Litchfield DW, Lüscher B (1993) Casein kinase II in signal transduction and cell cycle regulation. *Mol Cell Biochem* 127-128:187–199.
446. Litchfield DW (2003) Protein kinase CK2: structure, regulation and role in cellular decisions of life and death. *Biochem J* 369(Pt 1):1.
447. Morales JC, Carpenter PB (2004) Breaking in a new function for casein kinase 2. *Sci Aging Knowledge Environ* 2004(22):e24.
448. Sakaguchi K, et al. (1997) Phosphorylation of serine 392 stabilizes the tetramer formation of tumor suppressor protein p53. *Biochemistry* 36(33):10117–10124.
449. Bae B-I, et al. (2005) p53 mediates cellular dysfunction and behavioral abnormalities in Huntington's disease. *Neuron* 47(1):29–41.
450. Szlachcic WJ, Switonski PM, Krzyzosiak WJ, Figlerowicz M, Figiel M (2015) Huntington disease iPSCs show early molecular changes in intracellular signaling, the expression of oxidative stress proteins and the p53 pathway. *Dis Model Mech* 8(9):1047–1057.
451. Kovtun IV, et al. (2007) OGG1 initiates age-dependent CAG trinucleotide expansion in somatic cells. *Nature* 447(7143):447–452.
452. Goula AV, Berquist BR, Wilson DM III, Wheeler VC (2009) Stoichiometry of base excision repair proteins correlates with increased somatic CAG instability in striatum over cerebellum in Huntington's disease transgenic *PLoS*. Available at: <http://journals.plos.org/plosgenetics/article?id=10.1371/journal.pgen.1000749>.
453. Hegde ML, et al. (2012) Oxidative genome damage and its repair: implications in aging and neurodegenerative diseases. *Mech Ageing Dev* 133(4):157–168.
454. German P, et al. (2013) Activation of cellular signaling by 8-oxoguanine DNA glycosylase-1-initiated DNA base excision repair. *DNA Repair* 12(10):856–863.
455. Boldogh I, et al. (2012) Activation of ras signaling pathway by 8-oxoguanine DNA glycosylase bound to its excision product, 8-oxoguanine. *J Biol Chem*

287(25):20769–20773.

456. Elias S, McGuire JR, Yu H, Humbert S (2015) Huntingtin Is Required for Epithelial Polarity through RAB11A-Mediated Apical Trafficking of PAR3-aPKC. *PLoS Biol* 13(5):e1002142.
457. Toker A (1998) Signaling through protein kinase C. *Front Biosci* 3:D1134–47.
458. Hupp TR, Lane DP (1994) Allosteric activation of latent p53 tetramers. *Curr Biol* 4(10):865–875.
459. Keller DM, et al. (2001) A DNA Damage-Induced p53 Serine 392 Kinase Complex Contains CK2, hSpt16, and SSRP1. *Mol Cell* 7(2):283–292.
460. McKinnon PJ (2009) DNA repair deficiency and neurological disease. *Nat Rev Neurosci* 10(2):100–112.
461. Jeppesen DK, Bohr VA, Stevnsner T (2011) DNA repair deficiency in neurodegeneration. *Prog Neurobiol* 94(2):166–200.
462. Oren M (2003) Decision making by p53: life, death and cancer. *Cell Death Differ* 10(4):431–442.
463. St-Denis NA, Litchfield DW (2009) Protein kinase CK2 in health and disease: From birth to death: the role of protein kinase CK2 in the regulation of cell proliferation and survival. *Cell Mol Life Sci* 66(11-12):1817–1829.
464. Kraiss S, Barnekow A, Montenarh M (1990) Protein kinase activity associated with immunopurified p53 protein. *Oncogene* 5(6):845–855.
465. Meek DW, Simon S, Kikkawa U, Eckhart W (1990) The p53 tumour suppressor protein is phosphorylated at serine 389 by casein kinase II. *EMBO J* 9(10):3253–3260.
466. Rossi R, et al. (1999) The replication factory targeting sequence/PCNA-binding site is required in G1 to control the phosphorylation status of DNA ligase I. *EMBO J* 18(20):5745–5754.
467. Lorenz A, Herrmann C, Issinger O, Montenarh M (1992) Phosphorylation of wild-type and mutant phenotypes of p53 by an associated protein-kinase. *Int J Oncol* 1(5):571–579.
468. Shieh SY, Ikeda M, Taya Y, Prives C (1997) DNA damage-induced phosphorylation of p53 alleviates inhibition by MDM2. *Cell* 91(3):325–334.

469. Olsen BB, Issinger O-G, Guerra B (2010) Regulation of DNA-dependent protein kinase by protein kinase CK2 in human glioblastoma cells. *Oncogene* 29(45):6016–6026.
470. Guerra B, Iwabuchi K, Issinger O-G (2014) Protein kinase CK2 is required for the recruitment of 53BP1 to sites of DNA double-strand break induced by radiomimetic drugs. *Cancer Lett* 345(1):115–123.
471. Parker AR, et al. (2003) Defective human MutY phosphorylation exists in colorectal cancer cell lines with wild-type MutY alleles. *J Biol Chem* 278(48):47937–47945.
472. Montenarh M (2016) Protein kinase CK2 in DNA damage and repair. *Transl Cancer Res* 5(1):49–63.
473. Parsons JL, et al. (2010) XRCC1 phosphorylation by CK2 is required for its stability and efficient DNA repair. *DNA Repair* 9(7):835–841.
474. Fritz G, Kaina B (1999) Phosphorylation of the DNA repair protein APE/REF-1 by CKII affects redox regulation of AP-1. *Oncogene* 18(4):1033–1040.
475. Christmann M, Tomicic MT, Kaina B (2002) Phosphorylation of mismatch repair proteins MSH2 and MSH6 affecting MutSalpha mismatch-binding activity. *Nucleic Acids Res* 30(9):1959–1966.
476. Coin F, et al. (2004) Phosphorylation of XPB helicase regulates TFIIH nucleotide excision repair activity. *EMBO J* 23(24):4835–4846.
477. Alano CC, et al. (2010) NAD⁺ depletion is necessary and sufficient for poly(ADP-ribose) polymerase-1-mediated neuronal death. *J Neurosci* 30(8):2967–2978.
478. Marczuk-Krynicka D, Hryniewiecki T, Piatek J, Paluszak J (2003) The effect of brief food withdrawal on the level of free radicals and other parameters of oxidative status in the liver. *Med Sci Monit* 9(3):BR131–5.
479. Andrabi SA, et al. (2014) Poly(ADP-ribose) polymerase-dependent energy depletion occurs through inhibition of glycolysis. *Proc Natl Acad Sci U S A* 111(28):10209–10214.
480. Ayala-Peña S (2013) Role of oxidative DNA damage in mitochondrial dysfunction and Huntington's disease pathogenesis. *Free Radical Biology and Medicine* 62:102–110.

481. Matsuda N, et al. (2010) PINK1 stabilized by mitochondrial depolarization recruits Parkin to damaged mitochondria and activates latent Parkin for mitophagy. *J Cell Biol* 189(2):211–221.
482. Koyano F, et al. (2014) Ubiquitin is phosphorylated by PINK1 to activate parkin. *Nature* 510(7503):162–166.
483. Kane LA, et al. (2014) PINK1 phosphorylates ubiquitin to activate Parkin E3 ubiquitin ligase activity. *J Cell Biol* 205(2):143–153.
484. Khalil B, et al. (2015) PINK1-induced mitophagy promotes neuroprotection in Huntington's disease. *Cell Death Dis* 6:e1617.
485. Martinez-Vicente M, et al. (2010) Cargo recognition failure is responsible for inefficient autophagy in Huntington's disease. *Nat Neurosci* 13(5):567–576.
486. Lee Y, et al. (2017) PINK1 Primes Parkin-Mediated Ubiquitination of PARIS in Dopaminergic Neuronal Survival. *Cell Rep* 18(4):918–932.
487. Shin J-H, et al. (2011) PARIS (ZNF746) repression of PGC-1 α contributes to neurodegeneration in Parkinson's disease. *Cell* 144(5):689–702.
488. Siddiqui A, Rane A, Rajagopalan S, Chinta SJ, Andersen JK (2016) Detrimental effects of oxidative losses in parkin activity in a model of sporadic Parkinson's disease are attenuated by restoration of PGC1alpha. *Neurobiol Dis* 93:115–120.
489. Siddiqui A, et al. (2015) Mitochondrial Quality Control via the PGC1 α -TFEB Signaling Pathway Is Compromised by Parkin Q311X Mutation But Independently Restored by Rapamycin. *J Neurosci* 35(37):12833–12844.
490. Ciron C, et al. (2015) PGC-1 α activity in nigral dopamine neurons determines vulnerability to α -synuclein. *Acta Neuropathol Commun* 3:16.
491. Zheng B, et al. (2010) PGC-1 α , a potential therapeutic target for early intervention in Parkinson's disease. *Sci Transl Med* 2(52):52ra73.
492. Scarpulla RC (2011) Metabolic control of mitochondrial biogenesis through the PGC-1 family regulatory network. *Biochim Biophys Acta* 1813(7):1269–1278.
493. Lin J, et al. (2004) Defects in adaptive energy metabolism with CNS-linked hyperactivity in PGC-1alpha null mice. *Cell* 119(1):121–135.
494. Johri A, Chandra A, Beal MF (2013) PGC-1 α , mitochondrial dysfunction, and Huntington's disease. *Free Radic Biol Med* 62:37–46.

495. Cui L, et al. (2006) Transcriptional repression of PGC-1alpha by mutant huntingtin leads to mitochondrial dysfunction and neurodegeneration. *Cell* 127(1):59–69.
496. Hering T, Birth N, Taanman J-W, Orth M (2015) Selective striatal mtDNA depletion in end-stage Huntington's disease R6/2 mice. *Exp Neurol* 266:22–29.
497. Yin X, Manczak M, Reddy PH (2016) Mitochondria-targeted molecules MitoQ and SS31 reduce mutant huntingtin-induced mitochondrial toxicity and synaptic damage in Huntington's disease. *Hum Mol Genet* 25(9):1739–1753.
498. Shiwaku H, Okazawa H (2015) Impaired DNA damage repair as a common feature of neurodegenerative diseases and psychiatric disorders. *Curr Mol Med* 15(2):119–128.
499. Madabhushi R, Pan L, Tsai L-H (2014) DNA damage and its links to neurodegeneration. *Neuron* 83(2):266–282.
500. Johri A, Beal MF (2012) Mitochondrial dysfunction in neurodegenerative diseases. *J Pharmacol Exp Ther* 342(3):619–630.
501. Fang EF, et al. (2016) Nuclear DNA damage signalling to mitochondria in ageing. *Nat Rev Mol Cell Biol* 17(5):308–321.